IMPORTANCE OF HEPATIC TRANSPORTERS, INCLUDING BASOLATERAL EFFLUX PROTEINS, IN DRUG DISPOSITION: IMPACT OF PHOSPHOLIPIDOSIS AND NON-ALCOHOLIC STEATOHEPATITIS

Brian C. Ferslew

A dissertation submitted to the faculty of the University of North Carolina at Chapel Hill in partial fulfillment of the requirements for the degree of Doctor of Philosophy in the Department of Pharmaceutical Sciences in the UNC Eshelman School of Pharmacy

Chapel Hill
2014

Approved by:

Dhiren Thakker

Mary F. Paine

A. Sidney Barritt

Kim L.R. Brouwer

Jo Ellen Rodgers

Wei Jia

ABSTRACT

Brian C. Ferslew: Importance of Hepatic Transporters, Including Basolateral Efflux Proteins, in Drug Disposition: Impact of Phospholipidosis and Non-Alcoholic Steatohepatitis
(Under the direction of Kim L.R. Brouwer)

The objective of this dissertation project was to develop preclinical and clinical tools to assess the impact of liver pathology on transporter-mediated systemic and hepatic exposure to medications. A translational approach utilizing established pre-clinical hepatic transport systems, mathematical modeling, and a pivotal *in vivo* human study was employed. A novel application of rat sandwich-cultured hepatocytes (SCH) was developed to evaluate the impact of drug-induced phospholipidosis on the vectorial transport of probe substrates for hepatic basolateral and canalicular transport proteins. Results indicated that rat SCH treated with prototypical hepatic phospholipidosis inducers are a sensitive and selective model for drug-induced phospholipidosis; both organic anion transporting polypeptide-mediated uptake and bile salt export pump-mediated biliary excretion were reduced after the onset of phospholipidosis. Enalapril currently is being investigated for its anti-fibrotic effects in the treatment of patients with non-alcoholic steatohepatitis (NASH). Although the basolateral uptake transporters responsible for enalapril entry into the hepatocyte are well characterized, less is known about translocation of enalaprilat (the active metabolite) across the basolateral membrane into the systemic circulation. Studies were conducted using membrane vesicles prepared from transporter-expressing cells and a novel human SCH efflux protocol to assess the involvement of two hepatic basolateral efflux transporters known to be up-regulated in inflammatory liver disease [i.e., multidrug resistance-associated protein (MRP)3 and MRP4]; enalaprilat is transported across the basolateral membrane, in part, by MRP4. A novel clinical protocol was developed using morphine glucuronides as a probe for MRP3 function to determine the impact of altered hepatic transporter expression on drug disposition in patients

with NASH. A physiologically-based mathematical model was constructed to inform study design. Systemic concentrations of morphine glucuronides were increased significantly in patients with NASH compared to healthy subjects, as predicted by the model. This work provides a mechanistic understanding of the impact that hepatic transporter function has on the disposition of drugs and endogenous compounds under normal conditions and in response to altered liver function due to drug-induced phospholipidosis or liver disease, specifically non-alcoholic steatohepatitis. This knowledge is fundamental to safe and efficacious dosing of medications that depend on these transporters for disposition and/or elimination.

To my family, who enabled and provided guidance.
Thank you for your unwavering support and encouragement.

ACKNOWLEDGEMENTS

I want to thank Kim Brouwer for the opportunities she helped me to realize during this research project. I also want to thank my committee members for their invaluable support and contributions, both scientific and personal, during my graduate tenure: Mary Paine, my early committee chair, who was always available for scientific discussion, but also demanded quarterly updates to keep me on track scientifically and personally; Dhiren Thakker for taking over as my committee chair without hesitation and providing critical and objective advice; Jo Ellen Rodgers for always advocating for my progression through the program; Wei Jia for his ability to provide excellent scientific insight from a different perspective and outstanding collaboration; and Sid Barritt for his ability to condense complex ideas and problems down to specific actionable steps and providing clinical expertise spanning my research project. The specific and generalized contributions from this diverse committee have guided my personal and scientific growth. Thank you for everything!

I would be amiss without acknowledging the help of my friends and colleagues, both past and present, who assisted in this research along the way. I want to thank Nathan Pfeifer for his friendship and support through my graduate studies. Thank you for everything you have done for me from spending countless hours at Weaver Street Market doing what people do there to being a scientific sounding board. I could not have asked for a better colleague and friend. I also want to sincerely thank Curtis Johnston. Curtis, I could not have done the work detailed herein without you. Your ability to calmly and systematically address issues is inspiring. Thank you for your unwavering and very timely help in all aspects. Many times I was struggling to keep up with you and feel this strengthened my research drastically. I hope that you were able to learn as much from me as I did from you. Additionally I would like to thank my late roommate, Ellie Exner. Your support through my tenure has been truly exceptional.

Selflessly helping me through the most trying times experimentally, professionally and personally are far more than I could have expected. Additionally I need to acknowledge many others that have taught me a great deal: Julie Dumond, Kathleen Köck, Arlo Brown, Kathy Maboll, Danny Gonzalez, Brandon Swift, Tracy Marion, Kevin Watt, and Eleftheria Tsakalozou. Finally, I would like to thank two inanimate objects (or maybe the people/animals behind them) for their ability to provide me a place devoid of distractions to clear my mind. Garland Pobletts thank you for allowing me to use the mountain house ad libitum. Many long weekends were spent doing the things I love without interruption. And to the bunny who kept my garden interesting. Although we had many standoffs, focusing on outsmarting you, a rabbit, was humbling. I have the utmost respect and sympathy for Elmer Fudd.

Lastly, I need to thank the people that helped me to get here and kept everything in perspective. Jayme Hostetter, thank you for your patience with me and listening ear throughout. You always found a way to calmly work through problems and obstacles. Long standing friends who have never judged or asked me to explain, but instead offered their support time and time again: David McGowan from 3rd grade, I have relied on you to remind me to have fun; George Francisco for being the impetus for getting myself into this mess, but also for being a solid sounding board; and Matt Felbringer for never a dull moment. Finally, to my family; the people that got me here and through, through my best and worst. The family you have built has enabled us so much! I cannot say thank you enough. Matthew, thank you for all the advice and help, whether you knew it or not. From not getting scolded for coming home late (yes, you bore the brunt of that) to how to handle tough situations to when best to wax my new car, learning from your lead has kept me on a relatively straight path. Just please don't swing the bat again when I'm walking by. Dad, thank you for your support. Thank you for listening and guiding, but allowing me to forge my own path. Grandpa seems to have influenced many generations with his saying, "What do you think?". Mom, I don't need to expand on you; I could not have finished this without you.

TABLE OF CONTENTS

LIST OF TABLES

LIST OF FIGURES

LIST OF ABBREVIATIONS

AUC	Area under the curve
BEI	Biliary excretion index
BSEP	Bile salt export pump
CAD	Cationic amphiphilic drug
$CL_{biliary}$	*In vitro* biliary clearance
C_{max}	Maximal concentration
CYP	Cytochrome P450
DDI	Drug-drug interaction
HOMA-IR	Homeostasis model for assessing insulin resistance
MRP	Multidrug resistance-associated protein
NAFLD	Non-alcoholic fatty liver disease
NAS	NAFLD activity score
NASH	Non-alcoholic steatohepatitis
NTCP	Sodium-taurocholate cotransporting polypeptide
OATP	Organic anion transporting polypeptide
PLD	Phospholipidosis
RSV	Rosuvastatin
SCH	Sandwich-cultured hepatocytes
TC	Taurocholate
UGT	Uridine 5’-diphosphate-glucuronosyltransferase

CHAPTER 1. Introduction: Drug Transport in the Liver

Hepatic Physiology: Liver Structure and Function

The liver is a major organ involved in drug metabolism and excretion. The hepatocyte, the predominant cell type in the liver, is responsible for selective uptake, metabolism via phase I enzymes (e.g. cytochrome P450 [CYP], flavin-containing monooxygenase [FMO], carboxylesterase [CES]) and/or phase II conjugation systems, and excretion of numerous drugs, xenobiotics and endogenous compounds. It is now appreciated that many compounds cannot cross cellular plasma membranes by simple diffusion, and that transport proteins may be required for clearance of drugs from hepatic sinusoidal blood or excretion of parent compound and/or metabolite(s) from the hepatocyte into bile. Hepatocytes are polarized cells that extend in chord-like arrays throughout the liver, and are characterized by plasma membrane domains with distinct physiological functions: the sinusoidal (basolateral) domain has specialized proteins responsible for the exchange of compounds with the sinusoidal plasma in the space of Disse, while the canalicular (apical) domain has distinct proteins responsible for excretion of compounds into the lumen of the bile canaliculi. (Figure 1.1) Several members of the solute carrier (SLC) and ATP-binding cassette (ABC) transport protein superfamilies are involved in the uptake and efflux across the basolateral and apical membranes of hepatocytes. Members of the SLC family are typically uptake transporters that use ion gradients resulting from secondary or tertiary active transport processes to drive translocation of drugs across membranes. Members of the ABC superfamily function primarily as active efflux pumps that are driven by energy provided by the direct hydrolysis of ATP to move compounds out

This work has been published in *Drug Transporters: Molecular Characterization and Role in Drug Disposition*, Second Edition and is presented in the style of that book. Edited by Guofeng You and Marilyn E. Morris.

of the hepatocyte. Human transport genes/proteins are identified by upper case letters (e.g *ABCC2*, MRP2), whereas genes/proteins from preclinical species are identified by lowercase letters (e.g. *Abcc2*, Mrp2).

In this chapter we will review the substrate specificity for uptake and efflux transporters expressed in the liver, and discuss the impact of driving force(s), as well as translational and posttranslational regulation on hepatic transport. In addition, an overview of methodology and approaches currently in use or under development to evaluate the function of hepatic transport proteins is provided. Finally, the clinical significance of altered hepatic transport with respect to disease states and/or drug interactions will be discussed. The major focus of this chapter is on human proteins and clinically relevant drug-drug interactions (DDIs).

Hepatic Uptake Transport Proteins

The liver is the interface between the intestine and the systemic circulation; hepatic basolateral uptake is the first step of hepatobiliary elimination. Members of the *SLC10*, *SLC22* and *SLCO* gene families represent the predominant transport proteins known to mediate uptake of xeno- and endobiotics across the basolateral membrane of the hepatocyte.

NTCP (*SLC10A1*) The sodium taurocholate cotransporting polypeptide (NTCP) is expressed exclusively in the liver. NTCP, which belongs to the SLC10 family, mediates Na^+-dependent bile acid uptake into human liver against a 5- to 10-fold concentration gradient and with a 2:1 sodium-taurocholate (TC) stoichiometry. The substrate specificity of NTCP primarily comprises bile acids such as taurocholate, as well as conjugated di- and trihydroxy-bile acids, but this protein also transports the cholephilic compounds bromosulfophthalein (BSP) and estrone-3-sulfate (E1S). Statins such as fluvastatin, rosuvastatin, and pitavastatin have been identified as substrates of NTCP. However, recent studies indicate that NTCP only contributes modestly to overall statin accumulation in human hepatocytes. [1,2] Interestingly, NTCP*2, a variant resulting in a protein with no ability to transport bile acids, demonstrated increased transport of rosuvastatin *in vitro*. [2] In addition to bile acid transport, NTCP is a functional

receptor for hepatitis B and hepatitis D virus, consistent with the liver tropism of hepatitis B and D virus and exclusive liver expression of NTCP. [3]

OATPs (*SLCOs*) Organic anion transporting polypeptides (OATPs) play an essential role in the hepatic uptake of many drugs, and it is now well established that these transport proteins can impact the pharmacokinetic and pharmacodynamic profile of drugs. The location of OATPs on the basolateral membrane of the hepatocyte often renders them the rate-limiting step in the hepatobiliary clearance of drugs, thus controlling the hepatic elimination and/or oral bioavailability of various compounds. In contrast to NTCP, OATPs operate in a Na^+-independent manner, possibly as electroneutral exchangers with intracellular bicarbonate, glutathione, or glutathione conjugates. [4] Human OATPs are not exact orthologs of rodent Oatps, which may explain some discrepancies in the hepatic disposition of substrates between preclinical species and humans. OATP1B1, OATP1B3, and OATP2B1 have been identified on the liver basolateral membrane domain. OATP1B1 is exclusively expressed in liver; OATP1B3 is predominantly expressed in the liver whereas OATP2B1 is widely expressed throughout the body. OATP1A2 also has been identified in liver tissue; however, expression appears to be exclusively localized in cholangiocytes, suggesting that OATP1A2 may be involved in reabsorption of compounds excreted into bile. [5] OATPs are characterized by a largely overlapping and broad substrate spectrum (see Table 1.1). The importance of OATPs in the hepatic uptake of statins, DDIs and Rotor syndrome has received considerable attention in recent years (see Rotor Syndrome and Drug Interactions in Hepatobiliary Transport sections)

OATs (*SLC22*) Organic anion transporters (OATs) are members of the *SLC22* family. OATs mediate the uptake of negatively charged endogenous and xenobiotic compounds in exchange for intracellular organic anions including dicarboxylate, lactate or short-chain fatty acids. The majority of data regarding OAT transport has been generated with respect to renal drug transport due to the substantial expression of OATs in the kidney. Of the six human members, OAT2 (*SLC22A7*) is predominantly expressed on the basolateral membrane of hepatocytes, but also has been found on the basolateral membrane of renal proximal tubule cells. Endogenous substrates of human OAT2 include nucleosides and nucleotides,

prostaglandins, dehydroepiandrosterone sulfate (DHEAS), E1S, L-ascorbate and urate. Certain anticancer drugs as well as H_2 receptor antagonists and antibiotics have been identified as substrates of this transporter (see Table 1.1). Human OAT2 has 79% sequence identity to its rat ortholog Oat2, but subtle differences in substrate specificity exist. OAT7 (*SLC22A9*) is expressed exclusively in the basolateral membrane of the liver and has been shown to transport sulfated hormones such as E1S and DHEAS with high affinity. [6] Unlike other OAT proteins, OAT7 does not transport para-aminohippurate, α-ketoglutarate, prostaglandins, cyclic nucleotides, or salicylic acid.

OCTs and OCTNs (*SLC22A*) Organic cation transporters (OCTs) and organic cation/carnitine transporters (OCTNs) are members of the *SLC22* family and are polyspecific transporters that mediate the electrogenic and Na^+-independent transport primarily of small (<400 Da) cations or neutral molecules. Human OCT1 (*SLC22A1*), OCT3, and OCTN2 (*SLC22A5*) are the isoforms expressed on the basolateral membrane of hepatocytes. While OCT1 is almost exclusively expressed in liver in humans, OCT3 and OCTN2 have a much broader tissue distribution including kidney, brain, skeletal muscle, and placenta. OCT1 exhibits a broad substrate spectrum that includes endogenous compounds (e.g., choline, acetylcholine and monoamine neurotransmitters) and drugs such as some antivirals, H_2-receptor antagonists, and the antidiabetic metformin. Substrates for OCT3 appear to be more limited to endogenous substances and neurotransmitters.

OSTα/β (*SLC51A/B*) The organic solute transporter (OST) α/β is a heteromeric transporter expressed in small intestine, kidney, testis, and adrenal gland. In the liver, OSTα/β is expressed on the basolateral membrane. Substrate transport is bidirectional depending on the electrochemical gradient of the substrate.[7] The expression of this protein in organs involved in bile acid homeostasis together with regulation by the bile acid sensing farnesoid X receptor (FXR), and inherent ability to transport bile acids, suggest that OSTα/β may be associated with bile acid malabsorption or cholestasis.

Hepatic Efflux Transport Proteins

Hepatic excretion of xeno- and endobiotics from the liver may occur across the basolateral membrane into sinusoidal blood, or across the canalicular (apical) membrane into the bile which flows

through fine tubular canals between adjacent liver cells (see Figure 1.1). A list of substrates for human hepatic export proteins is provided (see Table 1.2).

Canalicular Transport Proteins

Canalicular transporters responsible for the biliary excretion of drugs and metabolites primarily belong to the ATP-binding cassette (ABC) family of transport proteins, which mediate ATP-dependent transfer of solutes. In addition, multidrug and toxin extrusion 1 (MATE1) is a protein belonging to the solute carrier family involved in the transport of organic cations across the canalicular membrane.

MDR1 P-glycoprotein (*ABCB1*) Multidrug resistance protein 1 P-glycoprotein (P-gp) was first identified in multidrug-resistant (MDR) tumor cells. [8] P-gp represents the most widely studied ABC transport protein and is responsible for biliary excretion of bulky hydrophobic and cationic substrates including chemotherapeutic agents, cardiac glycosides, cyclosporin A and HIV protease inhibitors (PIs). P-gp modulators have been evaluated to increase oral bioavailability, tissue concentrations and drug sensitivity for a number of compounds, especially in cancer chemotherapy where overexpression of P-gp in the tumor is one reason for therapeutic failure. Unfortunately, this strategy has had limited success. [9]

MDR3 (*ABCB4*) Multidrug resistance protein 3 (MDR3) plays a crucial role in basic liver physiology in humans and rats. MDR3, a phospholipid flippase, is involved in the biliary secretion of phospholipids, cholesterol and cholephilic compounds, which are responsible for the formation of micelles that solubilize bile acids in the lumen of the bile canaliculi. [10] Mutations in the MDR3 gene lead to progressive familial intrahepatic cholestasis type 3 (PFIC3), a disease that is characterized by increased γ-glutamyltranspeptidase levels, ductular proliferation and inflammatory infiltration that can progress to biliary cirrhosis.

BSEP (*ABCB11*) The bile salt export pump (BSEP), mediates the biliary excretion of conjugated and unconjugated bile acids. Although bile acids appear to be the predominant substrates, BSEP also can transport the non-bile acid substrate pravastatin. [11] Patients with progressive familial intrahepatic cholestasis (PFIC) type 2 (PFIC2) have mutations in the *ABCB11* gene that result in proteosomal and

lysosomal degradation of the misfolded proteins and a complete absence or reduced expression of functional BSEP on the apical membrane. [12] Increased intracellular concentrations of detergent-like bile acids secondary to inhibition of BSEP has been suggested as one mechanism for drug-induced liver injury. [13]

MRP2 (*ABCC2*) Multidrug resistance-associated protein 2 (MRP2) is a major xenobiotic efflux pump on the canalicular membrane. MRP2 plays a key role in the biliary excretion of organic anions, including bilirubin-diglucuronide, glutathione conjugates, sulfated bile acids, and divalent bile acid conjugates, as well as numerous drugs, including indomethacin, methotrexate, telmisartan, many glucuronide and sulfate conjugates of drugs such as acetaminophen-glucuronide and -sulfate, and even metal complexes such as arsenic-glutathione conjugates. The absence of functional MRP2 leads to Dubin-Johnson syndrome, which is associated with defective biliary excretion of bilirubin. [14] Animals with hereditary conjugated hyperbilirubinemia [MRP2-deficient rats (GY/TR$^-$) and Eisai hyperbilirubinemic rats (EHBR)] exhibit increased expression of Mrp3, an efflux transporter on the basolateral membrane that provides a compensatory mechanism to enable excretion of Mrp2 substrates into the systemic circulation, thus helping to avoid excessive accumulation of organic anions in the hepatocyte (see Dubin-Johnson Syndrome section). [15,16]

BCRP (*ABCG2*) Breast cancer resistance protein (BCRP), a half-transport protein that forms a functional heterodimer, is expressed on the canalicular membrane of the hepatocyte and mediates the transport of E1S and various other sulfated steroidal compounds as well as many fluoroquinolone analogs, glyburide and rosuvastatin. Additionally, BCRP is involved in the development of resistance to a variety of anticancer agents, such as SN-38, mitoxantrone, and doxorubicin. [17,18]

MATEs (*SLC47A*) Multidrug and toxin extrusion protein 1 (MATE1), is expressed on the canalicular membrane of hepatocytes. In contrast to the other canalicular transporters discussed above, MATE1 belongs to the solute carrier family and is thought to function as a proton exchanger. MATE1 substrates include the organic cations guanidine and thiamine, as well as numerous drugs. [19]

Basolateral Efflux Transport Proteins

Members of the ATP-dependent MRP subfamily of transport proteins represent the major class of export proteins on the hepatic basolateral membrane. MRP 1, 3, 4, 5 and 6 are involved in the cellular transport of both hydrophobic uncharged molecules and hydrophilic anionic compounds (see Table 1.2). [20] In addition to these MRPs, other transport proteins on the basolateral membrane may play a role in hepatic basolateral excretion. For example, the OATPs and OSTα/β have been hypothesized to function as basolateral export proteins under certain conditions, although the *in vivo* role of these transport proteins in basolateral excretion of drugs from the hepatocyte remains to be elucidated. [21,22]

MRP1 (*ABCC1*) Multidrug resistance-associated protein 1 (MRP1) is responsible for efflux of various organic anions, including glucuronide, glutathione, and sulfate-conjugated drugs, doxorubicin, etoposide glucuronide, glutathione-conjugated chlorambucil and E1S. Although MRP1 expression is very low on the basolateral membrane in the healthy human liver, it is highly inducible during severe liver injury and up-regulated in dividing hepatocytes; therefore, MRP1 may play a role in liver protection. [23]

MRP3 (*ABCC3*) Multidrug resistance-associated protein 3 (MRP3) is involved in the hepatic excretion of glucuronide conjugates (e.g. acetaminophen-glucuronide, estradiol-17β-glucuronide and morphine-3 and 6-glucuronides) as well as bilirubin, methotrexate and some conjugated bile acids. Expression of MRP3 in normal liver is relatively low, but MRP3 expression is increased markedly in the absence of functional MRP2, such as in patients with Dubin-Johnson syndrome (see Dubin-Johnson Syndrome section). Excretion of glucuronide conjugates across the basolateral membrane in the absence of functional MRP2 may play a protective role by preventing the toxic accumulation of both endogenous and exogenous chemicals in the hepatocyte.

MRP4 (*ABCC4*) Multidrug resistance-associated protein 4 (MRP4) is involved in the transport of adefovir, bile acids (including glycine- and taurine-conjugated forms), prostaglandins and leukotrienes. MRP4 expression under normal conditions is relatively low, but is induced in inflammatory, cholestatic and necrotic hepatic states, as well as in critical illness. [24-25] MRP4 function recently was postulated to modulate efficacy and toxicity of anticancer drugs in HIV-infected patients treated with nelfinavir. [26]

Additional studies are required to fully elucidate the role of MRP4 in hepatic and systemic disposition of drugs and metabolites in healthy individuals and patients with hepatic disease.

MRP5 and MRP6 (*ABCC5* and *ABCC6*) Little is known about the physiologic relevance of multidrug resistance-associated proteins 5 and 6 (MRP5 and MRP6, respectively) in the hepatic disposition of drugs and metabolites in human liver. MRP5 transports adefovir, cyclic-AMP and -GMP, 6-mercaptopurine, folate and 6-thioguanine. In humans, inflammatory conditions secondary to acetaminophen overdose, resulted in induction of MRP5, as well as MRP1, MRP4, BCRP and P-gp. [27] MRP5 may play a crucial role in cellular protection, nucleotide homeostasis and signaling. MRP6 transports glutathione conjugates and the endothelin receptor antagonist, BQ-123, but its functional role in hepatic transport remains to be elucidated. [28]

Regulation of Hepatic Drug Transport Proteins

Transcriptional Regulation

Due to their role in cellular homeostasis of both endogenous and exogenous molecules, transport proteins are tightly regulated through multiple processes including translational and posttranslational mechanisms. Transcriptional regulation occurs through a large family of nuclear receptors (NRs) that are involved in developmental, physiological and pathophysiological responses. For example, bilirubin and bile acids have been shown to regulate transcription of transport proteins involved in their own disposition through binding to NRs. In addition to endogenous compounds, many xenobiotics interact with NRs and the resulting complexes bind to the regulatory region of genes, recruit co-regulators and regulate polymerase II binding and activity at the target promoters to modulate gene expression. The following sections give an overview of the general role of NRs with regard to regulation of hepatic drug transport proteins; Table 1.3 summarizes current knowledge about the regulation of transport proteins by specific NRs. At present, most of our knowledge is based on animal and *in vitro* models.

AhR Aryl hydrocarbon receptor (AhR) has a large number of known ligands, including environmental chemicals such as polyaromatic hydrocarbons and dioxins, as well as natural dietary compounds and endogenous metabolites. [29]

CAR Constitutive androstane receptor (CAR) is a nuclear hormone receptor that is constitutively active even in the absence of a ligand. However, CAR can be regulated by chemical agonists as well as inverse agonists. After a ligand binds, CAR translocates to the nucleus where it binds to retinoid X receptor (RXR) and activates genes containing a phenobarbital response element.

FXR Farnesoid-X receptor (FXR) is an intracellular bile acid sensor that plays an important role in bile acid and lipid homeostasis, fat and glucose metabolism, and inflammation. One of the main functions of FXR in the liver is the reduction of the hepatic bile acid burden. Activation of FXR by bile acids inhibits bile acid synthesis through small heterodimer partner (SHP)-mediated repression of transcription of CYP7A1, the rate-limiting enzyme for conversion of cholesterol to bile acids. Activation of FXR in the intestine results in induction of fibroblast growth factor (Fgf)-15, which translocates to the liver where it activates hepatic FGF receptor 4, which leads to inhibition of hepatic bile acid synthesis. [30] *In vivo* models confirm the complimentary roles of FXR and Fgf-15 in the liver and intestine, where activation of intestinal FXR protects mice from cholestatic liver injury after bile duct ligation. [31]

Nrf2 NFE2-related factor 2 (Nrf2) is a transcription factor that is a crucial regulator of cellular redox homeostasis, and plays an important role in protecting cells from oxidative stress. Nrf2 normally is retained in the cytoplasm by associating with the actin-kelch-like-ECH-associated protein 1 (Keap1). However, under oxidative stress, this interaction is disrupted and Nrf2 translocates into the nucleus to activate antioxidant-responsive elements in the promoter of target genes. [32] Typical Nrf2 target genes include genes involved in redox homeostasis such as superoxide dismutase, catalase, or glutathione peroxidase. [33] However, there is increased recognition that Nrf2 regulates drug metabolizing enzymes and drug transporters. [34]

PXR pregnane X receptor (PXR) is activated by a variety of endogenous and dietary compounds as well as pharmaceuticals. PXR is the key transcriptional regulator of CYP-3A isozymes, and it also is involved

in the regulation of a number of transport proteins. Upon binding of ligands, PXR translocates into the nucleus, heterodimerizes with RXR and binds to response elements in the promoter region of target genes. [35] In addition to its role in detoxification and transport, PXR may be involved in glucose and lipid metabolism and the pathogenesis of metabolic diseases. [36]

PPARs Peroxisome proliferator-activated receptors (PPARs) are a group of NRs that are key regulators of glucose and lipid homeostasis, cell proliferation, differentiation, and inflammatory response. The three main subtypes are PPARα, PPARγ and PPARδ. Endogenous ligands include fatty acids and eicosanoids, while some drugs (e.g., fibrates and thiazolindinediones) as well as environmental chemicals (e.g., phthalates [plasticizers] and perfluorinated fatty acids) act as exogenous ligands.

HNFs Hepatocyte nuclear factors (HNFs) are involved in regulation of the basal expression of many genes and are known as master transcription factors because they are able to regulate other NRs and transcription factors. HNFs are involved in organ development and important cellular functions such as metabolism of glucose, bile acids, fatty acids, and drugs. Members of the HNF family are ubiquitously expressed; HNF1α and 4α are liver-enriched transcription factors.

Post-Translational Regulation

In addition to transcriptional processes, post-translational regulation through phosphorylation, glycosylation, ubiquitination, SUMOylation and/or insertion/retrieval of transport proteins into/from the plasma membrane allows short-term regulation of membrane transport by altering the number or activity of transport proteins in the plasma membrane. Transport proteins stored in intracellular vesicles are targeted to, and fuse with, the correct plasma domain (i.e. apical or basolateral) in response to appropriate stimuli; when the stimulus is withdrawn or another opposing stimulus is applied, the transporters are removed from the membrane by endocytosis. After endocytosis, the transport proteins are degraded via the lysosomal or proteasomal pathway, or remain in intracellular storage vesicles until restimulation, when they are again expressed on the plasma membrane. In summary, the number of transport proteins on the cell surface is regulated by *de novo* synthesis, exocytotic insertion of proteins from cytoplasmatic

vesicles into the plasma membrane, endocytotic retrieval from the plasma membrane, and protein degradation.

Apical transport proteins Because of the central role of BSEP in bile acid transport and enterohepatic circulation of bile acids, trafficking of this transporter has been studied extensively. Short-term regulation resulting in rapid insertion and retrieval into and from the canalicular membrane has been observed in response to various stimuli including hormones, bile salts, or oxidative stress. [37-40] For example, treatment of rats with bile acids or cAMP resulted in a microtubule-dependent mobilization of intracellularly sequestered Bsep to the canalicular membrane within minutes. [41,42] In addition, activation of p38MAP kinase and subsequent translocation of Bsep to the canalicular membrane has been proposed as the underlying mechanism for the choleretic effect observed after administration of certain bile acids such as tauroursodeoxycholic acid (TUDCA). [43] In addition to exocytosis, internalization in response to various stimuli has been reported. For example, activation of Ca^{2+}-dependent PKC isoforms resulted in retrieval of Bsep from the canalicular membrane and induced cholestasis in the isolated perfused rat liver. [44]

Similar to BSEP, MRP2/Mrp2 internalization/insertion in the canalicular membrane has been demonstrated in response to various stimuli such as glutathione (GSH) depletion, lipopolysaccharide (LPS) administration, or cAMP treatment. [45,46] Infusion of taurochenodeoxycholic acid (TCDCA) in bile duct cannulated rats, a model of bile acid-induced cholestasis, resulted in reduced bile flow and Mrp2 internalization. [47] Taurolithocholic acid (TLCA) also resulted in intracellular retrieval of Mrp2, while TUDCA increased Mrp2 expression and function at the canalicular membrane and counteracted the effect of TLCA via a PKC-dependent mechanism. [48]

It is now well recognized that Mrp2 localization is dependent on the interaction with the anchoring protein radixin [49], a member of the ezrin-radixin-moesin family of proteins that cross-links actin filaments with integral membrane proteins and transitions between an active phosphorylated, membrane-anchoring (p-radixin) and an inactive dephosphorylated (radixin) form. Disruption of interaction between MRP2/Mrp2 and radixin results in MRP2/Mrp2 internalization, as demonstrated in

patients with primary biliary cirrhosis, in rodent experimental cholestatic models, or in rat liver after LPS treatment. [47,50,51]

For both MRP2/Mrp2 and BSEP/Bsep, osmolarity plays an important role in regulating localization. In perfused rat livers, hypo-osmotic solutions increased taurocholate biliary excretion due to the increased translocation of Bsep to the canalicular membrane, while hyperosmolarity resulted in endocytic retrieval and reduced biliary excretion. [52] Similarly, under hyper-osmotic conditions, Mrp2 resides intracellularly, whereas hypo-osmotic conditions result in Mrp2 translocation to the plasma membrane. [53]

Basolateral transport proteins Phosphorylation of human and rodent OATPs/Oatps affects membrane expression of these proteins. [54,55] Activation of protein kinase C (PKC) results in internalization and degradation of human OATP2B1. [56] Similarly, the phosphorylation state of Ntcp determines whether this protein is localized on the basolateral membrane or in an intracellular endosomal compartment. Cyclic AMP treatment stimulates PI3K and PKC resulting in dephosphorylation and translocation of Ntcp from the cytosol to the basolateral membrane. [57,58] In addition to cAMP, perfusion of TCDCA, but not TC or TUDCA, in isolated perfused rat liver studies resulted in Ntcp retrieval from the plasma membrane, which may be a protective mechanism to reduce the hepatic uptake of bile acids during periods of increased exposure to portal bile acids. [59] cAMP-mediated short-term regulation of MRP3/Mrp3, with increased plasma membrane expression and function of this protein, has been demonstrated in human and rat hepatocytes. [60]

Taken together, transcriptional and posttranslational regulation allows fine tuning of transport processes and adaptation to varying physiological and non-physiological conditions. Regulation processes vary depending on the transport protein, species, and even tissue. One challenge in interpreting the results of these studies is whether the data obtained *in vitro* can readily be translated to complex organ systems.

Disease State Alterations in Hepatic Transport Proteins

Genetic mutations of transport proteins can result in disease through dysfunctional excretion and accumulation of toxic endogenous and/or exogenous compounds. In addition, underlying disease

processes themselves can influence transport protein expression, localization, and function, and thus result in altered pharmacokinetics and/or pharmacodynamics.

Cholestasis

A major function of the liver is the synthesis of cholesterol and bile acids. In humans, the rate-limiting step in formation of bile after synthesis of bile acids is the efflux across the hepatic canalicular membrane via BSEP. PFIC is a heterogeneous group of autosomal recessive disorders with disrupted bile formation resulting in cholestasis early in childhood and adolescence. PFIC can be classified into three different types based on the underlying mechanism of disease. PFIC type 1 is caused by a mutation in the gene encoding the familiar intrahepatic cholestasis 1 protein (FIC1, *ATP8A1*). ATP8A1 plays a role in maintaining the enrichment of phosphatidylserine and -ethanolamine in the inner leaflet of the canalicular plasma membrane. Tight regulation of phospholipid and bile acid secretion into the bile canaliculi is postulated to be protective against high bile acid concentrations in the canalicular lumen. FXR-mediated downregulation of BSEP in patients with PFIC type 1 has been shown. PFIC2 and PFIC type 3 (PFIC3) are caused by mutations in the genes encoding BSEP and phospholipid translocase (MDR3), respectively. Mutations in BSEP that are associated with decreased bile acid secretion lead to reduced bile flow and accumulation of bile acids in the hepatocytes, resulting in hepatocellular damage secondary to cholestasis. Impaired function of BSEP due to altered gene coding or gene regulation also has been implicated in benign recurrent intrahepatic cholestasis type 2 (BRIC2), and intrahepatic cholestasis of pregnancy. [61,62] MDR3 is a phospholipid translocator expressed in the canalicular membrane of the hepatocyte. Phospholipids protect the endothelial cells lining the bile canaliculi from the detergent effects of secreted bile acids; decreased function of MDR3 results in continuous exposure to hydrophobic bile acids in patients with PFIC type 3 and subsequent liver damage.

In addition to genetic defects, many forms of acquired defects in bile acid transport that have been described involve direct inhibition of the function or expression of the bile acid transport proteins resulting in cholestasis, including drug-induced cholestasis, sepsis-associated cholestasis, and intrahepatic

cholestasis of pregnancy. Drug-induced cholestasis may involve BSEP inhibition, which can result in intracellular accumulation of bile acids and subsequent liver damage.

Endogenous compounds also have been implicated in cholestasis. Estrogen and C17-alkylated steroids can cause a type of cholestasis that is similar in clinical presentation to intrahepatic cholestasis of pregnancy (ICP). ICP usually occurs during the third trimester of pregnancy and resolves spontaneously after delivery. Cholestatic estrogen metabolites appear to play a major role in the pathogenesis of ICP. In animal models of cholestasis, $E_2$17G or the synthetic estrogen ethinylestradiol, causes internalization and intracellular retention of Bsep and Mrp2, which rapidly impairs the excretory function of these canalicular proteins. [37,63]

Dubin-Johnson Syndrome

Dubin-Johnson Syndrome (DJS) is a rare autosomal recessive disease with impaired secretion of organic anions, characterized by chronic conjugated hyperbilirubinemia and pigmented liver due to hepatic accumulation of bilirubin. Although a defect in canalicular secretion of bilirubin had long been assumed, the underlying mechanism was identified in the late 1990s, when an *ABCC2* gene mutation was linked to impaired expression and function of MRP2 in this disease. [64] Similar mutations have been found in the Mrp2 gene in TR$^-$/GY Wistar rats and EHBR (Esai hyperbilirubinemic) Sprague-Dawley rats. Both rat strains are deficient in the canalicular transport of anionic conjugates such as bilirubin glucuronide as well as glutathione and sulfate conjugates of various compounds. [65,66] Patients with DJS and Mrp2-deficient rats exhibit increased hepatic basolateral expression of MRP3/Mrp3, which is hypothesized as a compensatory mechanism for excretion of bilirubin conjugates. In EHBR rats, the contribution of Mrp2 to the DJS phenotype was proven by infection with adenovirus carrying *ABCC2*, which compensated for the genetic defect and corrected the transport deficiency. [67]

Rotor Syndrome

Rotor syndrome is a rare, benign autosomal recessive liver disease clinically similar to DJS. Rotor syndrome is characterized by conjugated hyperbilirubinemia, but in contrast to DJS, these patients

lack the hepatic pigment accumulation. Furthermore, in Rotor syndrome, delayed clearance of certain anionic drugs (e.g. BSP) and impaired hepatic uptake of diagnostic dyes (e.g. ^{99m}TC-HIDA) has been observed. Inactivating mutations of the *SLCO1B1* and *SLCO1B3* genes resulting in functional deficiency of OATP1B1 and OATP1B3, and hence disrupted hepatic reuptake of bilirubin glucuronide, were identified as the underlying mechanism for this liver disease. [68] Transporter knockout mouse models were used to show that Mrp3 secreted bilirubin conjugates into the blood while Oatp1a/1b mediated their hepatic reuptake. Expression of human OATP1B1 or OATP1B3 in Oatp1a/1b-deficient mice restored bilirubin glucuronide reuptake and detoxification mechanisms. It has been suggested that hepatic (re)uptake represents a detoxification strategy to shuttle bilirubin conjugates to downstream hepatocytes to prevent local saturation of detoxification processes. [68]

Non-Alcoholic Steatohepatitis (NASH)

Approximately one-third of the U.S. population suffers from non-alcoholic fatty liver disease; 10-20 percent of these individuals present with the more progressive inflammatory form, steatohepatitis (NASH). [69,70] Driven by the dual epidemics of diabetes and obesity, the incidence of these chronic liver diseases is increasing at an alarming rate. In addition to the risk of disease progression from simple fatty liver to NASH, cirrhosis, liver failure and hepatocellular carcinoma, there are risks inherent to patients with milder forms of the disease. Specifically, changes in the hepatic disposition of common medications may reduce drug efficacy or increase toxicity. Enzymes and transporters responsible for hepatic uptake and metabolism are down-regulated in NASH (e.g., OATPs; CYP2C8, CYP2C19, and CYP3A4), while proteins excreting drugs/toxins from the liver into the blood or bile are up-regulated (e.g., MRP3, MRP4, P-gp and BCRP). [71,72] Progression of inflammation and fibrosis ultimately results in cirrhosis, which impairs biliary excretion of both endogenous and exogenous compounds. The *in vivo* functional effect of NASH on hepatic handling of drugs in humans remains to be investigated. Preclinical data suggest that NASH may shift the excretion profile of medications, potentially leading to increased systemic toxicity or decreased hepatic efficacy of many drugs administered to patients with NASH. [73,74]

Inflammation and Inflammation-Induced Cholestasis

Inflammation often contributes to the development of liver injury during cholestasis. However, inflammatory processes themselves can be the cause for cholestasis due to reduction in bile flow associated with the release of bacterial endotoxins or inflammatory cytokines. Impaired basolateral and canalicular bile acid and organic anion transport has been observed in the isolated perfused rat liver after injection of LPS. [75] In a rodent model of endotoxin-induced cholestasis, LPS induced an early and selective, but reversible retrieval of Mrp2 from the apical membrane followed by down-regulation in Mrp2 mRNA. [76] Similarly, a decrease in both Bsep mRNA and protein accounted for the reduced canalicular secretion of bile acids in endotoxin-treated rats. [77,78]

Pro-inflammatory cytokines such as tumor necrosis factor α (TNFα), interleukin (IL)-1β and IL-6 regulate the expression of hepatic transporters in rodents and primary and sandwich-cultured human hepatocytes. [79-82] In general, bile acid transport proteins as well as basolateral uptake transport proteins are repressed, whereas drug efflux transporters may be unchanged, or up- or down-regulated at the mRNA, protein or activity level (for review see [83]). A recent study showing differential effects of BSEP/Bsep expression between sandwich-cultured human and rat hepatocytes after treatment with pro-inflammatory cytokines[79] demonstrated the potential for species differences in response to inflammatory mediators, and highlighted the need to carefully consider model selection and clinical inferences. Little information on the effect of inflammation on transport protein function is available in humans. In patients with primary biliary cirrhosis and primary sclerosing cholangitis, which are associated with inflammation, reduced expression of NTCP, OATPs, MRP2, and BSEP was reported, whereas MRP3 and OSTα/β expression was increased. [84,85] Furthermore, disrupted canalicular localization of MRP2 in patients with primary biliary cirrhosis was observed. [86] Although not directly correlated with inflammation, Vanwijngaerden et al. reported increased bile acid and bilirubin concentrations in patients in the intensive care unit. Liver biopsies taken from these patients immediately post mortem indicated that MRP2, MRP3 and MRP4 mRNA and protein were increased while OATP1B1 and OATP1B3 mRNA and protein were decreased. [25]

Human Immunodeficiency Virus Infection (HIV)

To our knowledge no studies have been published that directly compare hepatic transporter expression between HIV infected patients and healthy individuals. In 2008, Jung et al. reported that mRNA levels of OCT1 and OCT2 in lymph node tissue were markedly increased in patients infected with HIV compared to non-infected controls [87]. Although not investigated, direct viral- or indirect inflammatory-mediated activation of signaling cascades may alter normal expression and function of hepatic transport proteins and metabolic enzymes, thereby altering systemic clearance, efficacy or toxicity of drugs. Altered basolateral and/or canalicular transport protein expression may be of particular relevance in HIV pharmacotherapy; protease inhibitors (PIs) are often OATP and MRP2/P-gp substrates, whereas the nucleoside analog reverse transcriptase inhibitors (NRTIs), such as lamivudine and zalcitabine, are OCT1 and OCT2 substrates. [87,88] Furthermore, since many HIV drugs are substrates or inhibitors of transport proteins and metabolic enzymes, HIV patients have an increased risk for drug-drug interactions (DDIs). The most well-known DDI associated with HIV treatment is CYP3A4 inhibition by ritonavir. This interaction is used clinically to "boost" the concentrations of coadministered PIs. In addition, ritonavir also potently inhibits P-gp, MRP2 and other drug transporters. Ritonavir-mediated inhibition of P-gp was proposed as the mechanism for the significant decrease in the non-renal clearance of digoxin in healthy volunteers. [89] Although many PIs and NRTIs inhibit a multitude of transporters including P-gp, MRP2, OATP1B1, OATP1B3, and NTCP, clinically relevant interactions with MRP2 have not been established, potentially due to concentrations below the inhibitory level at the site of transport (i.e. intracellular for MRP2). [90,91] Certain antiretroviral agents are associated with an increased incidence of hepatotoxicity, which may be related, in part, to interactions with hepatic transporters. [88,91,92]

Chronic Hepatitis C Viral (HCV) Infection

Chronic HCV infection results in prolonged cellular oxidative stress and production of pro-inflammatory cytokines, which lead to progressive fibrosis. In rodent models and human derived cell lines, pro-inflammatory cytokines including IL-1β, TNF-α and IL-6 have been shown to modulate nuclear

receptor and transporter expression. [80,93] Multiple studies have investigated the effect of HCV and HCV-induced inflammation on hepatic transporter expression. Liver biopsies from patients with HCV exhibited increased P-gp, MRP1, MRP3 and MRP4, and decreased OATP1B1, OATP1B3, MRP2 and BCRP mRNA and/or protein compared to uninfected controls. [23,94,95] Additionally, increasing fibrosis stage in patients with HCV infection has been inversely correlated with mRNA expression of BSEP, MDR3, MRP2, NTCP, OAT2, OCT1, OATP2B1 and OATP1B1. [96] Although mRNA and protein do not always correlate directly for transport proteins, altered hepatic transporter expression may be linked to decreased expression and presumably transcriptional activation by the nuclear receptors AhR, PXR and PPARα. [95,96] Even though the clinical significance of altered transporter expression is unclear, the systemic clearance of the P-gp substrate, nelfinavir, was significantly reduced in HIV/HCV co-infected patients compared to HIV patients without HCV. [97] Further studies are needed to elucidate the pharmacokinetic and pharmacodynamic consequences of fibrosis, cirrhosis and altered transporter expression in the liver, as well as other clearance organs, due to HCV infection and treatment.

Model Systems for Studying Hepatobiliary Drug Transport

Several model systems have been applied successfully to the study of hepatobiliary drug transport, ranging from models mimicking the transporter-mediated transmembrane movement of drugs (e.g. membrane vesicles) to sophisticated *in vitro* and *in vivo* models (e.g. cultured hepatocytes and knockout animals). Significant species differences in transporter affinity and expression profiles [98,99] remain a key consideration in selecting the appropriate model. The relevance of a particular model to human hepatobiliary drug disposition will depend largely on whether the model is derived from human tissue (e.g. human hepatocytes) or whether human transport proteins are expressed. Furthermore, since the rate-limiting step in hepatobiliary disposition differs between drugs, the relative expression levels of drug-metabolizing enzymes and transport proteins must be considered for each model, and data must be interpreted cautiously and in conjunction with complementary model systems when such expression levels do not reflect the *in vivo* situation. Table 1.4 summarizes applications as well as advantages and disadvantages of various hepatobiliary drug transport models.

In Vitro Systems

Membrane Vesicle Systems Isolated purified canalicular (cLPM) and basolateral (bLPM) liver plasma membrane vesicles with functional transport properties have been used to assess the mechanisms of transport (driving forces, electrogenicity) and to identify substrates and inhibitors of transport proteins. [100,101] This classic method was used to characterize bile acid and bilirubin glucuronide transport across the canalicular membrane, leading to the discovery of BSEP and MRP2. [102,103] For efflux transporters, inside-out vesicles are required to permit access of ATP and the drug/inhibitor of interest to the catalytic site of the transporter and allow direct translocation of substrates into the vesicles. LPM vesicle preparations contain both inside-out and right-side-out vesicles at varying ratios. Since uptake transporters generally do not directly require ATP, data obtained from inside-out bLPM vesicles intended for investigation of basolateral efflux transporters may be confounded by uptake transporters pumping in the opposite direction. Finally, concurrent with the tissue of origin, vesicles made from cLPMs or bLPMs contain multiple ABC transport proteins making identification of specific substrates or inhibitors impossible.

With the evolution of cloning and transfection techniques allowing expression of individual (human) transport proteins, tissue-based LPM vesicle assays have largely been replaced by vesicles prepared from vector-transfected and virus-infected cell lines (over-) expressing a single transport protein. Initially, baculovirus-infected *Spodoptera frugiperda*, Sf9 cells, were widely used, but due to notable differences in glycosylation patterns and cholesterol content of the isolated membranes [104], more human relevant cell lines, such as human embryonic kidney (HEK) 293, Madin-Darby canine kidney (MDCK) II or porcine kidney epithelial (LLC-PK1) cells are now used more frequently. Vesicles prepared from single-transporter expressing cell lines are suitable for high-throughput screening of substrates or inhibitors, yielding kinetic parameters for the transporter of interest including the Michaelis-Menten constant (K_m), maximal transport rate (V_{max}) as well as the inhibition constant (K_i). This system is ideal for assessing the potential for DDIs *in vitro*, but fails to allow comparison of the relative contribution of individual transporters to the overall hepatic disposition of a compound.

Transfected Cell Systems Mammalian cell lines (predominantly HEK293, MDCK II and LLC-PK1) transfected with one or more transport proteins have evolved rapidly as one of the most widely used techniques to generate efficient and flexible *in vitro* tools for identification of substrates and inhibitors of hepatic transport proteins in humans. [105] Although expression of a single uptake transporter allows kinetic analysis of the substrate and inhibitor spectrum of individual transport proteins, researchers continue to examine ways to evaluate the interplay between uptake and efflux transport proteins. Expression of at least two transport proteins (one for uptake and one for excretion) in polarized cell lines such as MDCKII or LLC-PK1 mimic the *in vivo* expression of uptake and excretory transporters and are a valuable tool to study vectorial transport. Recently, Fahrmayr et al. developed a triple-transfected cell line expressing both influx and efflux transporters as well as the drug-metabolizing enzyme uridine diphosphate glucuronosyl transferase (UGT) 1A1 to study transporter-metabolism interactions. [106] Disadvantages of transfected cell systems include altered protein trafficking and localization due to species differences or the cell type used for transfection. Importantly, the relative expression levels of transport proteins and metabolizing enzymes remain difficult to assess and standardize, resulting in a rather artificial model exhibiting differences in the rate-limiting steps compared to *in vivo*. In addition, the actual functional activity of a given transport protein is likely to depend on the cellular environment, which is clearly different in a transfected system compared to normal hepatocytes. [107]

Primary Hepatocytes Freshly isolated hepatocytes are considered to be the most comprehensive cell-based model to study hepatic drug transport. Suspended hepatocytes remain a useful and convenient system to characterize hepatic drug uptake mechanisms. Unfortunately, hepatocytes rapidly lose cellular polarity upon isolation [108] and internalization of canalicular transport proteins has been observed [109]; thus, it is impossible to differentiate drug efflux across the basolateral versus canalicular membrane domains in suspended hepatocytes. Furthermore, suspended hepatocytes only remain viable for a few hours. Hepatocytes cultured on a single layer of an extracellular collagen matrix ("conventional configuration") have been used to study hepatotoxicity, metabolism and enzyme induction. However, hepatocytes in this conventional configuration continue to dedifferentiate rapidly with complete loss of cell polarity and

many hepatocyte-specific functions. [110] In contrast, hepatocytes cultured between two layers of gelled collagen ("sandwich configuration"; sandwich-cultured hepatocytes), maintain mature hepatocyte morphology and long-term expression of a differentiated phenotype. [110,111] This includes re-establishment of cell polarity, formation of functional canalicular networks in culture, and maintenance of drug transport proteins and metabolizing enzymes, thus allowing for the study of hepatobiliary drug metabolism and transport. [112] Hepatocyte-like cells derived from the human hepatoma cell line, HepaRG, are being tested as an alternative to human hepatocytes. HepaRG cells express relevant transport proteins, although mRNA and protein expression may differ compared to human hepatocytes. [113,114] Further studies are required to determine whether HepaRG cells could be used as an accurate alternative to primary cultured hepatocytes for *in vitro* hepatobiliary transport studies. Additionally, inducible pluripotent stem (iPS) cells have been differentiated successfully into hepatocyte-like cells. Although the transport characteristics of these cells remain to be characterized, other hepatocyte specific functions, such as CYP450 induction have been documented. Hepatocytes derived from a specific individual may serve as a powerful tool to understand the mechanisms behind idiosyncratic liver injury. [115] More recently, three-dimensional hepatocyte models (e.g. LiverChip®, Hμrel®) are being developed to more closely mimic *in vivo* hepatic physiology. Additional studies are needed to establish the utility of these highly complex, but physiologically relevant models for the study of drug disposition and transport.

Isolated Perfused Liver Models The isolated perfused liver (primarily rat) has been used widely to investigate hepatobiliary transport of drugs and xenobiotics. Although time- and animal-consuming, the main advantage of this model system is that the normal liver physiology (including bile flow) is maintained throughout the time of the experiment. Moreover, the ability to sample from both perfusate (blood compartment) and bile makes this model system particularly useful for mechanistic studies (including pharmacokinetic modeling) without potentially confounding factors from other tissues and clearance organs that exist *in vivo*. Perfused liver studies may be performed *in situ* or *ex vivo* using a single-pass or recirculating technique. In the single-pass technique, the outflow from the perfusion does

not re-enter the system, allowing steady-state conditions to be achieved rapidly. Data from single-pass liver perfusion allows calculation of the steady-state extraction of the parent compound as well as determination of basolateral and canalicular excretion of parent and formed metabolites. Large amounts of perfusate are required, making this technique less feasible when only a small quantity of drug is available. Alternatively, recirculating perfusions do not require as much perfusate; however, this method only allows calculation of total hepatic clearance because the parent and formed metabolites are continuously returned to the liver and clearance into bile is the only permanent elimination route from the system. Additionally, since metabolites are only cleared from the system through the bile, they may accumulate in the perfusate or liver tissue and potentially result in artificially magnified drug-metabolite transporter or metabolism interactions. An attractive feature of both perfusion techniques is the ability to assess the effects of *in vivo* pretreatments (e.g. with inducing agents or disease-inducing diets) on hepatobiliary transport and metabolism. [116] Livers obtained from transporter knockout or transporter-deficient (e.g. TR^- Wistar or EHBR Sprague-Dawley rats, which have a functionally relevant defect in the *Abcc2* gene) also can be used in perfusion experiments. [117,118]

In Vivo Systems

The gold standard for studying the role of hepatic transporters in the systemic disposition and elimination of xenobiotics is pharmacokinetic studies in humans. Evaluation of the whole integrative system provides the most robust information regarding the potential for DDIs, herb-drug or diet-drug interactions in the clinic by including compensatory elimination pathways. Although *in vivo* studies are the most relevant clinically, mechanistic evaluation of transporter-based interactions in humans is difficult because of the significant overlap of substrates and inhibitors for multiple transport proteins, and obvious limitations regarding the types of samples that can be collected.

Single Nucleotide Polymorphisms and Knockout Models Humans with single nucleotide polymorphisms (SNPs) that alter the expression and/or function of hepatic transport, and genetic knockout models in rodents, offer a unique opportunity to study the role of transport proteins in the

hepatic and systemic disposition of drugs and xenobiotics; however, the compensatory up-regulation of other transporters or species differences must be considered prior to direct translation of the findings into the clinic. SNPs have been identified in almost all human genes, including both uptake and efflux transport proteins. Ho et al. demonstrated that polymorphisms in *SLC10A1* (NTCP) resulted in decreased transport of prototypical bile acid substrates and paradoxically increased drug transport by NTCP *in vitro.* [2,119] Additionally, increased risk for statin induced myopathy and decreased efficacy have been well documented secondary to increased systemic and presumably lower hepatic concentrations in patients with polymorphisms in the genes encoding for OATP1B1. [120] Similarly, rodent models lacking Bcrp on the canalicular membrane exhibit decreased biliary clearance of rosuvastatin. Altered rosuvastatin pharmacokinetics has been confirmed in both Chinese and Finnish populations with polymorphisms in BCRP, which diminish its function, demonstrating the utility of knockout rodent models to predict altered pharmacokinetics in humans. [121-123] Studies to-date in knockout animals and humans with SNPs that alter transporter function have documented the importance of transport proteins in the systemic and hepatic disposition of some drugs and generated metabolites. Additional studies assessing the impact of altered hepatic transport function on the *in vivo* efficacy and toxicity of drugs, xenobiotics and endobiotics are needed to fully understand the pivotal role that transporters play.

***In Vivo* Biliary Excretion Studies** Biliary excretion is an important route of elimination for some drugs and represents a potential site of interactions that may alter hepatic and/or systemic drug exposure. Accurate measurement of biliary clearance and understanding the underlying mechanisms of biliary excretion are important in predicting clinical DDIs or proposing mechanisms of transporter-associated, drug-induced hepatobiliary toxicity.

One method, primarily utilized in rodents, to completely collect bile involves cannulation of the bile duct and exteriorization of bile flow. Proper study design, including pharmacokinetic sampling and complete bile collection, generates datasets containing information about the extent of biliary excretion and involvement of enterohepatic recirculation in the overall systemic exposure. In general, *in vivo* biliary clearance correlates well with *in vitro* biliary clearance estimated in sandwich-cultured hepatocytes.

[112,124,125] A second method, used primarily in humans, is direct aspiration of duodenal fluids using an oroenteric tube or absorbent sponge that can be placed distal to the sphincter of Oddi to collect recently excreted bile. These methods allow relatively non-invasive collection of bile from humans, but complete collection of bile for designated time intervals requires specialized techniques, making these methods largely qualitative. Incomplete and highly variable recovery of total bile excreted can be minimized by administration of cholecystokinin 8 (CCK-8) intravenously to stimulate gall bladder contraction. To generate quantitative data, correction for gall bladder ejection fraction and the portion of the dose lost during collection can be achieved with concurrent direct hepatic imaging by quantification of hepatic gamma-ray or positron emissions from administered radioactive agents.

Hepatobiliary Imaging Techniques Pharmacokinetic studies based on serum concentrations provide information on overall hepatic clearance, but do not allow determination of hepatic uptake, biliary clearance or liver concentrations/exposure. Quantification of the intrahepatic concentration of drugs may be especially relevant when the site of action or toxicity is in the liver. Therefore, several noninvasive imaging techniques such as gamma-ray quantification using ^{99m}Tc-labeled compounds, positron emission tomography (PET) using short-lived ^{11}C, ^{13}N, ^{15}O or ^{18}F- isotopes and magnetic-resonance imaging (MRI) have been employed to allow direct quantification of hepatic concentrations. A combination of these methods with the aforementioned oroenteric tube and pharmacokinetic sampling, allows direct quantification of all relevant clearance processes involved in the hepatic disposition of the imaging agent used.

Hendrikse et al. used the radiopharmaceuticals ^{99m}Tc-HIDA and ^{99m}Tc-MIBI to assess the function of the hepatic efflux proteins P-gp, Mrp1, and Mrp2 *in vivo*. [126] More recently, ^{99m}Tc-mebrofenin has been used to study the inhibitory effects of ritonavir on hepatic uptake and biliary efflux transport proteins in healthy volunteers. [90] Similarly, non-radioactive MRI contrast agents have been investigated to study hepatic transport. The gadolinium (Gd) derivatives Gd-BOPTA and Gd-EOB-DPTA allow liver imaging and facilitate the distinction between normal and pathological tissue. Hepatic uptake of Gd compounds is thought to be mediated by OATPs, while MRP2 mediates biliary excretion. [127,128] Studies

conducted in patients with hepatocellular carcinoma correlated the degree of expression and localization of OATP1B1/1B3 and MRP2 with hepatocyte-specific enhancement. [129,130] A combination approach of pharmacokinetic sampling and hepatic imaging techniques may emerge as a powerful tool to elucidate drug disposition and predict drug-transport interactions.

Drug Interactions in Hepatobiliary Transport

In recent years, the importance of transporter-related DDIs has become well recognized in the drug discovery and development arena. As screening programs have successfully filtered out chemical entities that display high affinities for CYP450 enzymes, the likelihood of selecting compounds during drug discovery that are transport inhibitors and/or that depend on transporters for their elimination/distribution has increased as a consequence. A DDI in hepatobiliary transport may occur when one drug interferes with the functional activity (e.g. inhibition) and/or expression levels (e.g. induction, altered regulation) of a hepatic transport protein that is critically involved in hepatobiliary elimination of another drug. In addition, since endogenous compounds often rely on hepatic transport proteins to maintain normal hepatic physiology (e.g. bile flow), administration of drugs that inhibit the function of key transport proteins may cause disturbances in physiological homeostasis. One example of this phenomenon is drug-induced liver injury (DILI) due to inhibition of bile acid transport.

A substantial number of DDIs in hepatobiliary transport reported in recent years occur at the level of hepatic uptake (see Table 1.5). Various clinical studies have revealed “perpetrator” drugs that inhibit the OATP family of transporters resulting in altered hepatic uptake of “victim” drugs such as HMG-CoA reductase inhibitors ("statins"). For example, concomitant treatment with the CYP3A4 inhibitor cyclosporin A (CsA) elevated cerivastatin plasma concentrations 3- to 5-fold, despite dual CYP2C8- and CYP3A4-mediated metabolism of cerivastatin; inhibition of OATP1B1-mediated uptake of cerivastatin was identified as a plausible mechanism. [131,132] Similarly, for atorvastatin, pravastatin, lovastatin, and rosuvastatin, 6-, 5-, 22-, and 7-fold increases in plasma concentrations, respectively, were observed upon coadministration with CsA compared to controls. [133-135] It should be noted, however, that for most clinically relevant drug interactions involving statins, the relative importance of CYP3A4 (or other CYPs)

[136] versus OATP1B1 [137] inhibition remains to be elucidated. At least for rosuvastatin, where metabolism is a minor route of elimination, OATP1B1 inhibition appears to play the key role in this clinically observed DDI. [136] Transporter-mediated drug interactions elicited by CsA clearly are not limited to statins; CsA coadministration increased the plasma area under the curve (AUC) of the endothelin receptor antagonist bosentan (30-fold), the antidiabetic repaglinide (4-fold) as well as the antigout medication colchicine (3-fold). [138-140] *In vivo* data generated in the rat with bosentan strongly suggest that inhibition of hepatocellular uptake plays an important role in this severe drug interaction. The important role of OATP1B1 in the hepatic uptake of repaglinide has been demonstrated in a separate study. [141] Inhibition of OATP1B1, in addition to CYP2C8 by the fibric acid derivative gemfibrozil may contribute to the DDI between gemfibrozil and repaglinide. Gemfibrozil also has been reported to alter the pharmacokinetics of statins, possibly due in part to inhibition of hepatic OATP1B1. The use of gemfibrozil as a comedication during cerivastatin therapy resulted in more than a 5-fold increase in cerivastatin exposure (plasma AUC). [142] Shitara et al. conducted *in vitro* studies to assess the relative importance of the inhibitory effects of gemfibrozil and gemfibrozil glucuronide on CYP2C8-mediated metabolism and on OATP1B1-mediated hepatic uptake of cerivastatin. [143] Both gemfibrozil and gemfibrozil glucuronide were more potent inhibitors of CYP2C8 than OATP1B1, suggesting a major role for CYP2C8 and possibly minor involvement of OATP1B1 in this DDI. A less pronounced interaction was reported between gemfibrozil and simvastatin, resulting in a ~1.9-fold increase in simvastatin acid AUC values. [144] Since no inhibition of CYP3A4, the major enzyme involved in simvastatin metabolism, by gemfibrozil was observed *in vitro*, the possible role for OATP inhibition in this DDI remains to be elucidated. The same conclusion can be drawn for DDIs following coadministration of gemfibrozil with pravastatin or lovastatin. [145,146] Interestingly, recent *in vitro* data indicate that gemfibrozil stands out among other fibric acid derivatives tested for its potency to inhibit OATP1B1. [147]

Recently telaprevir, a first in class hepatitis C viral protease inhibitor, was approved as add-on therapy in the treatment of chronic hepatitis C. Early *in vitro* studies demonstrated that telaprevir is a potent inhibitor of CYP3A and P-gp. In two well-designed cross-over clinical studies, the AUC values of

CsA, tacrolimus and atorvastatin were increased by 4.6-, 70- and 7.9-fold when coadministered with telaprevir compared to control. [148,149] This interaction was attributed primarily to CYP inhibition, although telaprevir also inhibits P-gp. Subsequent data revealed that telaprevir potently inhibits OATP1B1, OATP1B3 and OCT2, with IC_{50} values between 2.15 and 6.77 μM. With steady-state plasma concentrations of telaprevir reported to reach 5.1 μM (2.1 μM unbound), inhibition of OATP-mediated hepatic uptake of CsA, tacrolimus and atorvastatin is likely, in addition to metabolism interactions with CYP3A. [150] This example highlights the importance of both hepatic metabolism and vectorial transport in understanding and predicting the mechanisms underlying DDIs.

For some hepatic drug interactions, the use of animal models to elucidate the underlying mechanism(s) of interaction may be justified, despite considerable species differences in transporter affinity profiles and the fact that human transporters might not be orthologs of rat proteins (e.g. OATPs). For instance, for OATPs, the pharmacokinetic interaction between the antiarrhythmic drug amiodarone and digoxin has been observed in both humans and rats. [151,152] *In vitro* data suggest that inhibition of Oatp1a4-mediated hepatic uptake of digoxin by amiodarone probably plays a predominant role in this drug interaction. [153] Data generated in OAT2 expressing oocytes strongly support a role for OAT2 in the well-known drug interaction between theophylline and erythromycin in human liver. [154] Additional *in vitro* data have demonstrated substantial inhibition of OAT2-mediated tetracycline uptake in oocytes by acetaminophen, erythromycin, chloramphenicol, ibuprofen, bumetanide and furosemide; therefore, it is likely that DDIs may involve OAT2-mediated transport. [154] Numerous drugs (including H_2 antagonists cimetidine and famotidine [155] and several HIV PIs [156]) have been identified as potent inhibitors of OCT1 and/or OCT3. Although numerous DDIs have been reported involving inhibition of OCT1/3-mediated tubular secretion in the kidney, clinically relevant drug interactions involving hepatic transport have not been reported.

In addition to hepatic uptake proteins, inhibition of canalicular transport also has resulted in clinically relevant DDIs, including a reduction in digoxin biliary clearance (by about 40%) in patients who were coadministered the P-gp inhibitors quinidine or verapamil. [157,158] Inhibition of P-gp was

proposed as the mechanism behind the significant decrease in the non-renal clearance of digoxin in healthy volunteers who were coadministered the HIV PI ritonavir. [89] Although, P-gp inhibition would result in a decrease in non-renal clearance of digoxin, based on clinically relevant concentrations of ritonavir, this interaction may be attributed to inhibition of hepatic OATP–mediated uptake of digoxin. [90,159] Apart from the DDIs in hepatobiliary transport discussed above, various drugs interfere with the hepatic handling of endogenous compounds, including bilirubin, bile acids and thyroid hormones. For instance, Campbell et al. demonstrated that the *in vitro* potency of several OATP inhibitors (including CsA, rifamycin SV, and the PIs saquinavir and ritonavir) is directly correlated to the incidence of hyperbilirubinemia in humans. [160] These observations are consistent with the predominant role of OATP1B1 and OATP1B3 compared to other *SLCO* gene products in hepatic bilirubin uptake. [68] Numerous drugs also interact with BSEP-mediated bile acid transport, thus causing alterations in the hepatobiliary handling of bile acids, which may lead to hepatotoxicity (see Hepatic Transport Proteins as Determinants of Drug Toxicity section).

In addition to direct inhibition of transporter activity, altered transporter expression following drug-mediated transporter induction is another important mechanism underlying DDIs in hepatobiliary transport. Indeed, as discussed in the Regulation of Hepatic Drug Transport Proteins section, transporters are under regulatory control of nuclear receptors such as PXR and CAR. Therefore, administration of drugs that are ligands for these orphan nuclear receptors may lead to altered transporter expression and activity (induction/up-regulation or down-regulation). This may cause substantial changes in the hepatobiliary elimination kinetics of drugs that are substrates for these transporters. Clinically relevant induction of P-gp has been observed at the intestinal level [161], and induction of hepatic P-gp in animals has been reported. For instance, rifampicin treatment resulted in a 4- to 13-fold increase in hepatic P-gp in monkeys. [162] Similarly, treatment of rats with the P-gp inducer tamoxifen resulted in about a 12-fold increase in hepatic Mdr1b mRNA accompanied by increased biliary excretion of tamoxifen and its metabolites. [163]

In recent years, there has been an increasing number of reports concerning clinically relevant interactions in hepatobiliary drug transport. These findings illustrate the unmet need for sophisticated and representative model systems allowing the early prediction of hepatobiliary drug interaction potential in drug discovery programs.

Interplay Between Drug Metabolism and Transport

Drug elimination is mediated by the concerted action of multiple interacting processes including influx, metabolism, and efflux. An understanding of the interdependence of these processes is important to predict how alterations in one pathway affect alternative or compensatory pathways, and the overall impact of DDIs. Many *in vivo* studies in preclinical species have been conducted to provide mechanistic insight into the functional interplay between drug-metabolizing enzymes and transporters. [164]

Because of the intracellular localization of metabolizing enzymes, uptake across the plasma membrane is an important prerequisite for metabolism. Therefore, it is not surprising that altered function of uptake transport proteins can affect drug metabolism. For example, co-administration of digoxin with the Oatp2 inhibitor rifampicin reduced digoxin metabolism. [165] Interestingly, polymorphisms in OATP1B1 (e.g., OATP1B1*5) are associated with reduced erythromycin metabolism, independent of changes in CYP3A4 activity; these findings call into question the use of erythromycin as a probe to phenotype an individual's CYP3A4 activity. [166]

Due to the substantial overlap in substrate and inhibitor specificity, along with the shared response to prototypical inducers, the interaction between CYP3A4 and P-gp has received considerable attention and numerous studies have demonstrated hepatic interplay between CYP3A4-mediated drug metabolism and P-gp-mediated biliary excretion. [167] For instance, the extent of hepatic metabolism of the dual CYP3a/P-gp substrate tacrolimus was increased due to P-gp inhibition during isolated rat liver perfusion. [168,169] Similarly, enhanced metabolism of the CYP3a/P-gp substrate digoxin upon coadministration with the P-gp inhibitor quinidine was observed. [165] The frequently observed reciprocal relationship between metabolism and drug transport (the "seesaw" phenomenon), with apparent increases in the amount excreted by one pathway when the other elimination pathway is inhibited, is typically the

result of increased drug concentrations due to inhibition of one elimination pathway rather than a mechanistic link between metabolism- and transporter-mediated processes. [170] Endres et al. cautioned that the erroneous conclusion of induction or activation of alternate metabolizing enzymes could be drawn, if basic pharmacokinetic principles are disregarded. [170]

In addition to CYP-mediated elimination, phase II metabolic pathways such as glucuronidation and sulfation are interlinked with hepatic transport processes. Highly polar, conjugated metabolites are dependent on the function of efflux transport proteins such as BCRP or MRPs for elimination. The excretion of conjugates correlates inversely with the intracellular conjugate concentrations because transporter-mediated excretion controls the elimination of conjugates from the cell. [171] Some conjugated metabolites may undergo deconjugation to reform the precursor molecule, a process called futile cycling or reversible metabolism. In addition, interconversion between parent drug and metabolite also exists for some phase I metabolites. Modeling and simulation studies have demonstrated that inhibition of biliary excretion of the conjugate can affect the disposition of the precursor in the presence of futile cycling. [171,172]

In addition to direct interactions through inhibition of uptake or efflux mechanisms, indirect mechanisms of interaction with transport proteins and metabolizing enzymes exist. The coordinate regulation of hepatic drug metabolizing enzymes and transport protein expression on the transcriptional level through NRs (see Regulation of Hepatic Drug Transport Proteins section) is thought to protect the hepatocyte from intracellular accumulation of toxic xenobiotics and formed metabolites. [173] It is interesting to note, that uptake transporters regulate access of drugs to NR proteins (e.g., PXR, CAR), thereby influencing the intracellular concentrations of drugs that act as NR inducers. For example, OATP1B1 expression is a major determinant of the extent of PXR activation by rifampin. [174] Following chronic administration of rifampin with at least a 12-hour washout period, the PXR-mediated induction of OATP1B1 and CYP3A4 resulted in decreased systemic concentrations of the OATP substrates atorvastatin and glyburide. [175,176] Alternatively, acute intravenous dosing of rifampin was associated with increased systemic concentrations of atorvastatin [177], likely due to acute inhibition of OATP transport.

Glyburide concentrations returned to baseline with chronic oral rifampin administration (6 day pretreatment) followed by an acute intravenous rifampin dose immediately prior to glyburide administration. This study design highlighted that inhibition of OATP1B1 and CYP3A4 can counteract the inductive effects for this substrate. [176]

Hepatic Transport Proteins as Determinants of Drug Toxicity

Altered function of hepatic transport proteins may have far reaching consequences for drug toxicity. One of the best documented cases exemplifying the contribution of hepatic uptake transporters to toxicity is the increased risk of myopathy after statin treatment in patients with genetic OATP1B1 polymorphisms. Myopathy is a side effect that presents as muscle pain and fatigue, which can progress from mild myalgia to life-threatening rhabdomyolysis. Numerous studies have demonstrated that genetic variants linked to low activity of OATP1B1 (i.e., *5 and *15 haplotypes) are associated with an increased risk of statin-induced myopathy. (see comprehensive review in [120]) Physiologically-based modeling of statin disposition predicted increased systemic concentrations but only moderate effects on liver exposure with reduced OATP1B1 function. [178]

Transporter-mediated biliary excretion of irinotecan, mycophenolic acid, and nonsteroidal anti-inflammatory drugs is associated with a high incidence of diarrhea due to drug-induced injury to the small intestine. [179] In many cases, hepatically-derived metabolites are responsible for intestinal injury and dose-limiting toxicity. In addition to efflux transporters, hepatic uptake transporters might also contribute to gastrointestinal side effects. A genome-wide association study in children with acute lymphoblastic leukemia detected an association between certain OATP1B1 variants, which associated with enhanced clearance of methotrexate, and increased risk of gastrointestinal toxicity, which might be due to increased hepatic uptake and biliary clearance and subsequently higher intestinal concentrations. [180]

Another type of toxicity that may be associated with hepatic transport proteins is DILI. DILI may be mediated by the direct transport of hepatotoxic compounds, including metabolites, or the interaction of drugs/metabolites with the hepatic transport of endogenous substrates such as bile acids, which are cytotoxic at higher concentrations. [181] Drugs that are potent BSEP inhibitors are likely to be associated

with DILI including bosentan, cyclosporin A, glibenclamide, rifamycin, sulindac and troglitazone. [182-185] Two recent systematic screening approaches that compared the potency of BSEP inhibition and cholestatic potential of drugs revealed a markedly higher incidence and potency of BSEP inhibition among drugs that caused cholestatic DILI compared to non-cholestatic drugs. [13,182]

The Future of Hepatic Drug Transport

Although our knowledge of hepatic drug transport has increased tremendously during the past decade, considerable effort is still needed to understand the coordinated role of hepatic transport proteins in determining the systemic and hepatic exposure of drugs and metabolites. This is particularly important when the target site for drug efficacy and/or toxicity is the liver. Specifically, we have a rudimentary understanding of hepatic basolateral efflux proteins, how these proteins influence drug disposition, and the impact of disease, genetic variability, and DDIs on these proteins. In general, alterations in hepatic drug transport associated with disease remain to be elucidated. The structural features of a molecule that enhance the probability of interactions (e.g., transport, inhibition) with specific hepatic transport proteins remains to be defined. Molecular modeling approaches hold great promise in answering some of these fundamental questions. Additionally, a more sophisticated understanding of intracellular drug disposition is needed to fully understand indirect mechanisms of drug-transport interactions, such as altered trafficking and localization of transport proteins. The role of transport proteins other than those that reside on the basolateral and apical hepatocyte membranes (e.g., intracellular trafficking proteins, proteins on the endoplasmic reticulum), and the influence of these transport proteins on drug/metabolite disposition, efficacy, and toxicity, await exploration. More information about the hepatic disposition of endogenous substrates of hepatic transport proteins (e.g., bile acids) is urgently needed. This basic knowledge is prerequisite to accurate predictions of hepatic transporter-mediated DDIs and hepatotoxicity. The development of new techniques, tools, and/or model systems that address specific concerns with existing approaches (e.g., species-dependent differences, sample throughput, physiologic relevance, assessment of intracellular concentrations), and that can be used to answer both mechanistic and applied questions regarding hepatobiliary transport, is needed. Such tools will be useful in enhancing our understanding of

how drugs and metabolites move through the human liver to sites of action, biotransformation, and/or excretion. This knowledge is fundamental to the optimization of drug therapy to achieve desirable therapeutic outcomes, and to minimize the incidence of unwanted effects, including undesirable DDIs and DILI.

REFERENCES

1. Greupink R, Dillen L, Monshouwer M, Huisman MT, Russel FG. 2011. Interaction of fluvastatin with the liver-specific Na+ -dependent taurocholate cotransporting polypeptide (NTCP). European journal of pharmaceutical sciences : official journal of the European Federation for Pharmaceutical Sciences 44(4):487-496.

2. Ho RH, Tirona RG, Leake BF, Glaeser H, Lee W, Lemke CJ, Wang Y, Kim RB. 2006. Drug and bile acid transporters in rosuvastatin hepatic uptake: function, expression, and pharmacogenetics. Gastroenterology 130(6):1793-1806.

3. Yan H, Zhong G, Xu G, He W, Jing Z, Gao Z, Huang Y, Qi Y, Peng B, Wang H, Fu L, Song M, Chen P, Gao W, Ren B, Sun Y, Cai T, Feng X, Sui J, Li W. 2012. Sodium taurocholate cotransporting polypeptide is a functional receptor for human hepatitis B and D virus. eLife 1:e00049.

4. Roth M, Obaidat A, Hagenbuch B. 2012. OATPs, OATs and OCTs: the organic anion and cation transporters of the SLCO and SLC22A gene superfamilies. British journal of pharmacology 165(5):1260-1287.

5. Lee W, Glaeser H, Smith LH, Roberts RL, Moeckel GW, Gervasini G, Leake BF, Kim RB. 2005. Polymorphisms in human organic anion-transporting polypeptide 1A2 (OATP1A2): implications for altered drug disposition and central nervous system drug entry. The Journal of biological chemistry 280(10):9610-9617.

6. Shin HJ, Anzai N, Enomoto A, He X, Kim do K, Endou H, Kanai Y. 2007. Novel liver-specific organic anion transporter OAT7 that operates the exchange of sulfate conjugates for short chain fatty acid butyrate. Hepatology (Baltimore, Md) 45(4):1046-1055.

7. Ballatori N. 2005. Biology of a novel organic solute and steroid transporter, OSTalpha-OSTbeta. Experimental biology and medicine (Maywood, NJ) 230(10):689-698.

8. Juliano RL, Ling V. 1976. A surface glycoprotein modulating drug permeability in Chinese hamster ovary cell mutants. Biochimica et biophysica acta 455(1):152-162.

9. Oza AM. 2002. Clinical development of P glycoprotein modulators in oncology. Novartis Foundation symposium 243:103-115; discussion 115-108, 180-105.

10. Carrella M, Roda E. 1999. Evolving concepts in the pathophysiology of biliary lipid secretion. Italian journal of gastroenterology and hepatology 31(7):643-648.

11. Hirano M, Maeda K, Hayashi H, Kusuhara H, Sugiyama Y. 2005. Bile salt export pump (BSEP/ABCB11) can transport a nonbile acid substrate, pravastatin. The Journal of pharmacology and experimental therapeutics 314(2):876-882.

12. Kubitz R, Droge C, Stindt J, Weissenberger K, Haussinger D. 2012. The bile salt export pump (BSEP) in health and disease. Clinics and research in hepatology and gastroenterology 36(6):536-553.

13. Dawson S, Stahl S, Paul N, Barber J, Kenna JG. 2012. In vitro inhibition of the bile salt export pump correlates with risk of cholestatic drug-induced liver injury in humans. Drug metabolism and disposition: the biological fate of chemicals 40(1):130-138.

14. Tsujii H, Konig J, Rost D, Stockel B, Leuschner U, Keppler D. 1999. Exon-intron organization of the human multidrug-resistance protein 2 (MRP2) gene mutated in Dubin-Johnson syndrome. Gastroenterology 117(3):653-660.

15. Konig J, Rost D, Cui Y, Keppler D. 1999. Characterization of the human multidrug resistance protein isoform MRP3 localized to the basolateral hepatocyte membrane. Hepatology 29(4):1156-1163.

16. Kuroda M, Kobayashi Y, Tanaka Y, Itani T, Mifuji R, Araki J, Kaito M, Adachi Y. 2004. Increased hepatic and renal expressions of multidrug resistance-associated protein 3 in Eisai hyperbilirubinuria rats. Journal of gastroenterology and hepatology 19(2):146-153.

17. Kawabata S, Oka M, Shiozawa K, Tsukamoto K, Nakatomi K, Soda H, Fukuda M, Ikegami Y, Sugahara K, Yamada Y, Kamihira S, Doyle LA, Ross DD, Kohno S. 2001. Breast cancer resistance protein directly confers SN-38 resistance of lung cancer cells. Biochemical and biophysical research communications 280(5):1216-1223.

18. Maliepaard M, van Gastelen MA, de Jong LA, Pluim D, van Waardenburg RC, Ruevekamp-Helmers MC, Floot BG, Schellens JH. 1999. Overexpression of the BCRP/MXR/ABCP gene in a topotecan-selected ovarian tumor cell line. Cancer research 59(18):4559-4563.

19. Nies AT, Koepsell H, Damme K, Schwab M. 2011. Organic cation transporters (OCTs, MATEs), in vitro and in vivo evidence for the importance in drug therapy. Handbook of experimental pharmacology (201):105-167.

20. Köck K, Brouwer KL. 2012. A perspective on efflux transport proteins in the liver. Clinical pharmacology and therapeutics 92(5):599-612.

21. Soroka CJ, Ballatori N, Boyer JL. 2010. Organic solute transporter, OSTalpha-OSTbeta: its role in bile acid transport and cholestasis. Seminars in liver disease 30(2):178-185.

22. Li L, Meier PJ, Ballatori N. 2000. Oatp2 mediates bidirectional organic solute transport: a role for intracellular glutathione. Molecular pharmacology 58(2):335-340.

23. Ros JE, Libbrecht L, Geuken M, Jansen PL, Roskams TA. 2003. High expression of MDR1, MRP1, and MRP3 in the hepatic progenitor cell compartment and hepatocytes in severe human liver disease. The Journal of pathology 200(5):553-560.

24. Campion SN, Johnson R, Aleksunes LM, Goedken MJ, van Rooijen N, Scheffer GL, Cherrington NJ, Manautou JE. 2008. Hepatic Mrp4 induction following acetaminophen exposure is dependent on Kupffer cell function. American journal of physiology Gastrointestinal and liver physiology 295(2):294-304.

25. Vanwijngaerden YM, Wauters J, Langouche L, Vander Perre S, Liddle C, Coulter S, Vanderborght S, Roskams T, Wilmer A, Van den Berghe G, Mesotten D. 2011. Critical illness evokes elevated circulating bile acids related to altered hepatic transporter and nuclear receptor expression. Hepatology (Baltimore, Md) 54(5):1741-1752.

26. Fukuda Y, Takenaka K, Sparreboom A, Cheepala SB, Wu CP, Ekins S, Ambudkar SV, Schuetz JD. 2013. Human immunodeficiency virus protease inhibitors interact with ATP binding cassette transporter 4/multidrug resistance protein 4: a basis for unanticipated enhanced cytotoxicity. Molecular pharmacology 84(3):361-371.

27. Barnes SN, Aleksunes LM, Augustine L, Scheffer GL, Goedken MJ, Jakowski AB, Pruimboom-Brees IM, Cherrington NJ, Manautou JE. 2007. Induction of hepatobiliary efflux transporters in acetaminophen-induced acute liver failure cases. Drug metabolism and disposition: the biological fate of chemicals 35(10):1963-1969.

28. Madon J, Hagenbuch B, Landmann L, Meier PJ, Stieger B. 2000. Transport function and hepatocellular localization of mrp6 in rat liver. Molecular pharmacology 57(3):634-641.

29. Barouki R, Aggerbeck M, Aggerbeck L, Coumoul X. 2012. The aryl hydrocarbon receptor system. Drug metabolism and drug interactions 27(1):3-8.

30. Inagaki T, Choi M, Moschetta A, Peng L, Cummins CL, McDonald JG, Luo G, Jones SA, Goodwin B, Richardson JA, Gerard RD, Repa JJ, Mangelsdorf DJ, Kliewer SA. 2005. Fibroblast growth factor 15 functions as an enterohepatic signal to regulate bile acid homeostasis. Cell metabolism 2(4):217-225.

31. Modica S, Petruzzelli M, Bellafante E, Murzilli S, Salvatore L, Celli N, Di Tullio G, Palasciano G, Moustafa T, Halilbasic E, Trauner M, Moschetta A. 2012. Selective activation of nuclear bile acid receptor FXR in the intestine protects mice against cholestasis. Gastroenterology 142(2):355-365 e351-354.

32. Cullinan SB, Gordan JD, Jin J, Harper JW, Diehl JA. 2004. The Keap1-BTB protein is an adaptor that bridges Nrf2 to a Cul3-based E3 ligase: oxidative stress sensing by a Cul3-Keap1 ligase. Molecular and cellular biology 24(19):8477-8486.

33. Kensler TW, Wakabayashi N, Biswal S. 2007. Cell survival responses to environmental stresses via the Keap1-Nrf2-ARE pathway. Annual review of pharmacology and toxicology 47:89-116.

34. Shen G, Kong AN. 2009. Nrf2 plays an important role in coordinated regulation of Phase II drug metabolism enzymes and Phase III drug transporters. Biopharmaceutics & drug disposition 30(7):345-355.

35. Staudinger J, Liu Y, Madan A, Habeebu S, Klaassen CD. 2001. Coordinate regulation of xenobiotic and bile acid homeostasis by pregnane X receptor. Drug metabolism and disposition: the biological fate of chemicals 29(11):1467-1472.

36. Gao J, Xie W. 2012. Targeting xenobiotic receptors PXR and CAR for metabolic diseases. Trends in pharmacological sciences 33(10):552-558.

37. Crocenzi FA, Mottino AD, Cao J, Veggi LM, Pozzi EJ, Vore M, Coleman R, Roma MG. 2003. Estradiol-17beta-D-glucuronide induces endocytic internalization of Bsep in rats. American journal of physiology Gastrointestinal and liver physiology 285(2):G449-459.

38. Cantore M, Reinehr R, Sommerfeld A, Becker M, Haussinger D. 2011. The Src family kinase Fyn mediates hyperosmolarity-induced Mrp2 and Bsep retrieval from canalicular membrane. The Journal of biological chemistry 286(52):45014-45029.

39. Perez LM, Milkiewicz P, Elias E, Coleman R, Sanchez Pozzi EJ, Roma MG. 2006. Oxidative stress induces internalization of the bile salt export pump, Bsep, and bile salt secretory failure in isolated rat hepatocyte couplets: a role for protein kinase C and prevention by protein kinase A. Toxicological sciences : an official journal of the Society of Toxicology 91(1):150-158.

40. Dombrowski F, Stieger B, Beuers U. 2006. Tauroursodeoxycholic acid inserts the bile salt export pump into canalicular membranes of cholestatic rat liver. Laboratory investigation; a journal of technical methods and pathology 86(2):166-174.

41. Wakabayashi Y, Kipp H, Arias IM. 2006. Transporters on demand: intracellular reservoirs and cycling of bile canalicular ABC transporters. The Journal of biological chemistry 281(38):27669-27673.

42. Gatmaitan ZC, Nies AT, Arias IM. 1997. Regulation and translocation of ATP-dependent apical membrane proteins in rat liver. The American journal of physiology 272(5 Pt 1):G1041-1049.

43. Kurz AK, Graf D, Schmitt M, Vom Dahl S, Haussinger D. 2001. Tauroursodesoxycholate-induced choleresis involves p38(MAPK) activation and translocation of the bile salt export pump in rats. Gastroenterology 121(2):407-419.

44. Kubitz R, Saha N, Kuhlkamp T, Dutta S, vom Dahl S, Wettstein M, Haussinger D. 2004. Ca2+-dependent protein kinase C isoforms induce cholestasis in rat liver. The Journal of biological chemistry 279(11):10323-10330.

45. Roelofsen H, Soroka CJ, Keppler D, Boyer JL. 1998. Cyclic AMP stimulates sorting of the canalicular organic anion transporter (Mrp2/cMoat) to the apical domain in hepatocyte couplets. Journal of cell science 111 (Pt 8):1137-1145.

46. Sekine S, Mitsuki K, Ito K, Kugioka S, Horie T. 2012. Sustained intrahepatic glutathione depletion causes proteasomal degradation of multidrug resistance-associated protein 2 in rat liver. Biochimica et biophysica acta 1822(6):980-987.

47. Rost D, Kloeters-Plachky P, Stiehl A. 2008. Retrieval of the rat canalicular conjugate export pump Mrp2 is associated with a rearrangement of actin filaments and radixin in bile salt-induced cholestasis. European journal of medical research 13(7):314-318.

48. Beuers U, Bilzer M, Chittattu A, Kullak-Ublick GA, Keppler D, Paumgartner G, Dombrowski F. 2001. Tauroursodeoxycholic acid inserts the apical conjugate export pump, Mrp2, into canalicular membranes and stimulates organic anion secretion by protein kinase C-dependent mechanisms in cholestatic rat liver. Hepatology (Baltimore, Md) 33(5):1206-1216.

49. Kikuchi S, Hata M, Fukumoto K, Yamane Y, Matsui T, Tamura A, Yonemura S, Yamagishi H, Keppler D, Tsukita S. 2002. Radixin deficiency causes conjugated hyperbilirubinemia with loss of Mrp2 from bile canalicular membranes. Nature genetics 31(3):320-325.

50. Kojima H, Sakurai S, Uemura M, Kitamura K, Kanno H, Nakai Y, Fukui H. 2008. Disturbed colocalization of multidrug resistance protein 2 and radixin in human cholestatic liver diseases. Journal of gastroenterology and hepatology 23(7 Pt 2):e120-128.

51. Saeki J, Sekine S, Horie T. 2011. LPS-induced dissociation of multidrug resistance-associated protein 2 (Mrp2) and radixin is associated with Mrp2 selective internalization in rats. Biochemical pharmacology 81(1):178-184.

52. Haussinger D, Schmitt M, Weiergraber O, Kubitz R. 2000. Short-term regulation of canalicular transport. Seminars in liver disease 20(3):307-321.

53. Kubitz R, D'Urso D, Keppler D, Haussinger D. 1997. Osmodependent dynamic localization of the multidrug resistance protein 2 in the rat hepatocyte canalicular membrane. Gastroenterology 113(5):1438-1442.

54. Choi JH, Murray JW, Wolkoff AW. 2011. PDZK1 binding and serine phosphorylation regulate subcellular trafficking of organic anion transport protein 1a1. American journal of physiology Gastrointestinal and liver physiology 300(3):G384-393.

55. Glavy JS, Wu SM, Wang PJ, Orr GA, Wolkoff AW. 2000. Down-regulation by extracellular ATP of rat hepatocyte organic anion transport is mediated by serine phosphorylation of oatp1. The Journal of biological chemistry 275(2):1479-1484.

56. Köck K, Koenen A, Giese B, Fraunholz M, May K, Siegmund W, Hammer E, Volker U, Jedlitschky G, Kroemer HK, Grube M. 2010. Rapid modulation of the organic anion transporting polypeptide 2B1 (OATP2B1, SLCO2B1) function by protein kinase C-mediated internalization. The Journal of biological chemistry 285(15):11336-11347.

57. Anwer MS, Gillin H, Mukhopadhyay S, Balasubramaniyan N, Suchy FJ, Ananthanarayanan M. 2005. Dephosphorylation of Ser-226 facilitates plasma membrane retention of Ntcp. The Journal of biological chemistry 280(39):33687-33692.

58. Mukhopadhayay S, Ananthanarayanan M, Stieger B, Meier PJ, Suchy FJ, Anwer MS. 1997. cAMP increases liver Na+-taurocholate cotransport by translocating transporter to plasma membranes. The American journal of physiology 273(4 Pt 1):G842-848.

59. Muhlfeld S, Domanova O, Berlage T, Stross C, Helmer A, Keitel V, Haussinger D, Kubitz R. 2012. Short-term feedback regulation of bile salt uptake by bile salts in rodent liver. Hepatology (Baltimore, Md) 56(6):2387-2397.

60. Chandra P, Zhang P, Brouwer KL. 2005. Short-term regulation of multidrug resistance-associated protein 3 in rat and human hepatocytes. American journal of physiology Gastrointestinal and liver physiology 288(6):G1252-1258.

61. Dixon PH, van Mil SW, Chambers J, Strautnieks S, Thompson RJ, Lammert F, Kubitz R, Keitel V, Glantz A, Mattsson LA, Marschall HU, Molokhia M, Moore GE, Linton KJ, Williamson C. 2009. Contribution of variant alleles of ABCB11 to susceptibility to intrahepatic cholestasis of pregnancy. Gut 58(4):537-544.

62. Davit-Spraul A, Gonzales E, Baussan C, Jacquemin E. 2009. Progressive familial intrahepatic cholestasis. Orphanet journal of rare diseases 4:1.

63. Mottino AD, Crocenzi FA, Pozzi EJ, Veggi LM, Roma MG, Vore M. 2005. Role of microtubules in estradiol-17beta-D-glucuronide-induced alteration of canalicular Mrp2 localization and activity. American journal of physiology Gastrointestinal and liver physiology 288(2):G327-336.

64. Paulusma CC, Kool M, Bosma PJ, Scheffer GL, ter Borg F, Scheper RJ, Tytgat GN, Borst P, Baas F, Oude Elferink RP. 1997. A mutation in the human canalicular multispecific organic anion transporter gene causes the Dubin-Johnson syndrome. Hepatology (Baltimore, Md) 25(6):1539-1542.

65. Mikami T, Nozaki T, Tagaya O, Hosokawa S, Nakura T, Mori H, Kondou S. 1986. The characters of a new mutant in rats with hyperbilirubinuria syndrome. Congenital Anom 26:250-251.

66. Jansen PL, Peters WH, Lamers WH. 1985. Hereditary chronic conjugated hyperbilirubinemia in mutant rats caused by defective hepatic anion transport. Hepatology (Baltimore, Md) 5(4):573-579.

67. Hirouchi M, Suzuki H, Sugiyama Y. 2005. Treatment of hyperbilirubinemia in Eisai hyperbilirubinemic rat by transfecting human MRP2/ABCC2 gene. Pharmaceutical research 22(4):661-666.

68. van de Steeg E, Stranecky V, Hartmannova H, Noskova L, Hrebicek M, Wagenaar E, van Esch A, de Waart DR, Oude Elferink RP, Kenworthy KE, Sticova E, al-Edreesi M, Knisely AS, Kmoch S, Jirsa M, Schinkel AH. 2012. Complete OATP1B1 and OATP1B3 deficiency causes human Rotor syndrome by interrupting conjugated bilirubin reuptake into the liver. The Journal of clinical investigation 122(2):519-528.

69. Williams CD, Stengel J, Asike MI, Torres DM, Shaw J, Contreras M, Landt CL, Harrison SA. 2011. Prevalence of nonalcoholic fatty liver disease and nonalcoholic steatohepatitis among a largely middle-aged population utilizing ultrasound and liver biopsy: a prospective study. Gastroenterology 140(1):124-131.

70. Chalasani N, Younossi Z, Lavine JE, Diehl AM, Brunt EM, Cusi K, Charlton M, Sanyal AJ. 2012. The diagnosis and management of non-alcoholic fatty liver disease: practice guideline by the American Gastroenterological Association, American Association for the Study of Liver Diseases, and American College of Gastroenterology. Gastroenterology 142(7):1592-1609.

71. Fisher CD, Lickteig AJ, Augustine LM, Ranger-Moore J, Jackson JP, Ferguson SS, Cherrington NJ. 2009. Hepatic cytochrome P450 enzyme alterations in humans with progressive stages of nonalcoholic fatty liver disease. Drug metabolism and disposition: the biological fate of chemicals 37(10):2087-2094.

72. Hardwick RN, Fisher CD, Canet MJ, Scheffer GL, Cherrington NJ. 2011. Variations in ATP-binding cassette transporter regulation during the progression of human nonalcoholic fatty liver disease. Drug metabolism and disposition: the biological fate of chemicals 39(12):2395-2402.

73. Torres DM, Jones FJ, Shaw JC, Williams CD, Ward JA, Harrison SA. 2011. Rosiglitazone versus rosiglitazone and metformin versus rosiglitazone and losartan in the treatment of nonalcoholic steatohepatitis in humans: a 12-month randomized, prospective, open- label trial. Hepatology 54(5):1631-1639.

74. Sanyal AJ, Chalasani N, Kowdley KV, McCullough A, Diehl AM, Bass NM, Neuschwander-Tetri BA, Lavine JE, Tonascia J, Unalp A, Van Natta M, Clark J, Brunt EM, Kleiner DE, Hoofnagle JH, Robuck PR. 2010. Pioglitazone, vitamin E, or placebo for nonalcoholic steatohepatitis. The New England journal of medicine 362(18):1675-1685.

75. Bolder U, Ton-Nu HT, Schteingart CD, Frick E, Hofmann AF. 1997. Hepatocyte transport of bile acids and organic anions in endotoxemic rats: impaired uptake and secretion. Gastroenterology 112(1):214-225.

76. Kubitz R, Wettstein M, Warskulat U, Haussinger D. 1999. Regulation of the multidrug resistance protein 2 in the rat liver by lipopolysaccharide and dexamethasone. Gastroenterology 116(2):401-410.

77. Green RM, Beier D, Gollan JL. 1996. Regulation of hepatocyte bile salt transporters by endotoxin and inflammatory cytokines in rodents. Gastroenterology 111(1):193-198.

78. Vos TA, Hooiveld GJ, Koning H, Childs S, Meijer DK, Moshage H, Jansen PL, Muller M. 1998. Up-regulation of the multidrug resistance genes, Mrp1 and Mdr1b, and down-regulation of the organic anion transporter, Mrp2, and the bile salt transporter, Spgp, in endotoxemic rat liver. Hepatology (Baltimore, Md) 28(6):1637-1644.

79. Diao L, Li N, Brayman TG, Hotz KJ, Lai Y. 2010. Regulation of MRP2/ABCC2 and BSEP/ABCB11 expression in sandwich cultured human and rat hepatocytes exposed to inflammatory cytokines TNF-{alpha}, IL-6, and IL-1{beta}. The Journal of biological chemistry 285(41):31185-31192.

80. Hartmann G, Cheung AK, Piquette-Miller M. 2002. Inflammatory cytokines, but not bile acids, regulate expression of murine hepatic anion transporters in endotoxemia. The Journal of pharmacology and experimental therapeutics 303(1):273-281.

81. Siewert E, Dietrich CG, Lammert F, Heinrich PC, Matern S, Gartung C, Geier A. 2004. Interleukin-6 regulates hepatic transporters during acute-phase response. Biochemical and biophysical research communications 322(1):232-238.

82. Donner MG, Schumacher S, Warskulat U, Heinemann J, Haussinger D. 2007. Obstructive cholestasis induces TNF-alpha- and IL-1 -mediated periportal downregulation of Bsep and zonal regulation of Ntcp, Oatp1a4, and Oatp1b2. American journal of physiology Gastrointestinal and liver physiology 293(6):1134-1146.

83. Fardel O, Le Vee M. 2009. Regulation of human hepatic drug transporter expression by pro-inflammatory cytokines. Expert opinion on drug metabolism & toxicology 5(12):1469-1481.

84. Boyer JL, Trauner M, Mennone A, Soroka CJ, Cai SY, Moustafa T, Zollner G, Lee JY, Ballatori N. 2006. Upregulation of a basolateral FXR-dependent bile acid efflux transporter OSTalpha-OSTbeta in cholestasis in humans and rodents. American journal of physiology Gastrointestinal and liver physiology 290(6):1124-1130.

85. Zollner G, Fickert P, Zenz R, Fuchsbichler A, Stumptner C, Kenner L, Ferenci P, Stauber RE, Krejs GJ, Denk H, Zatloukal K, Trauner M. 2001. Hepatobiliary transporter expression in

percutaneous liver biopsies of patients with cholestatic liver diseases. Hepatology (Baltimore, Md) 33(3):633-646.

86. Kojima H, Nies AT, Konig J, Hagmann W, Spring H, Uemura M, Fukui H, Keppler D. 2003. Changes in the expression and localization of hepatocellular transporters and radixin in primary biliary cirrhosis. Journal of hepatology 39(5):693-702.

87. Jung N, Lehmann C, Rubbert A, Knispel M, Hartmann P, van Lunzen J, Stellbrink HJ, Faetkenheuer G, Taubert D. 2008. Relevance of the organic cation transporters 1 and 2 for antiretroviral drug therapy in human immunodeficiency virus infection. Drug metabolism and disposition: the biological fate of chemicals 36(8):1616-1623.

88. Hartkoorn RC, Kwan WS, Shallcross V, Chaikan A, Liptrott N, Egan D, Sora ES, James CE, Gibbons S, Bray PG, Back DJ, Khoo SH, Owen A. 2010. HIV protease inhibitors are substrates for OATP1A2, OATP1B1 and OATP1B3 and lopinavir plasma concentrations are influenced by SLCO1B1 polymorphisms. Pharmacogenetics and genomics 20(2):112-120.

89. Ding R, Tayrouz Y, Riedel KD, Burhenne J, Weiss J, Mikus G, Haefeli WE. 2004. Substantial pharmacokinetic interaction between digoxin and ritonavir in healthy volunteers. Clinical pharmacology and therapeutics 76(1):73-84.

90. Pfeifer ND, Goss SL, Swift B, Ghibellini G, Ivanovic M, Heizer WD, Gangarosa LM, Brouwer KLR. 2013. Effect of Ritonavir on 99mTechnetium-Mebrofenin Disposition in Humans: A Semi-PBPK Modeling and In Vitro Approach to Predict Transporter-Mediated DDIs. CPT: pharmacometrics and systems pharmacology 2:e20.

91. Ye ZW, Camus S, Augustijns P, Annaert P. 2010. Interaction of eight HIV protease inhibitors with the canalicular efflux transporter ABCC2 (MRP2) in sandwich-cultured rat and human hepatocytes. Biopharmaceutics & drug disposition 31(2-3):178-188.

92. McRae MP, Lowe CM, Tian X, Bourdet DL, Ho RH, Leake BF, Kim RB, Brouwer KL, Kashuba AD. 2006. Ritonavir, saquinavir, and efavirenz, but not nevirapine, inhibit bile acid transport in human and rat hepatocytes. The Journal of pharmacology and experimental therapeutics 318(3):1068-1075.

93. Hinoshita E, Taguchi K, Inokuchi A, Uchiumi T, Kinukawa N, Shimada M, Tsuneyoshi M, Sugimachi K, Kuwano M. 2001. Decreased expression of an ATP-binding cassette transporter, MRP2, in human livers with hepatitis C virus infection. Journal of hepatology 35(6):765-773.

94. Ogasawara K, Terada T, Katsura T, Hatano E, Ikai I, Yamaoka Y, Inui K. 2010. Hepatitis C virus-related cirrhosis is a major determinant of the expression levels of hepatic drug transporters. Drug metabolism and pharmacokinetics 25(2):190-199.

95. Kurzawski M, Dziedziejko V, Post M, Wojcicki M, Urasinska E, Mietkiewski J, Drozdzik M. 2012. Expression of genes involved in xenobiotic metabolism and transport in end-stage liver disease: up-regulation of ABCC4 and CYP1B1. Pharmacological reports : PR 64(4):927-939.

96. Hanada K, Nakai K, Tanaka H, Suzuki F, Kumada H, Ohno Y, Ozawa S, Ogata H. 2012. Effect of nuclear receptor downregulation on hepatic expression of cytochrome P450 and transporters in chronic hepatitis C in association with fibrosis development. Drug metabolism and pharmacokinetics 27(3):301-306.

97. Regazzi M, Maserati R, Villani P, Cusato M, Zucchi P, Briganti E, Roda R, Sacchelli L, Gatti F, Delle Foglie P, Nardini G, Fabris P, Mori F, Castelli P, Testa L. 2005. Clinical pharmacokinetics of nelfinavir and its metabolite M8 in human immunodeficiency virus (HIV)-positive and HIV-hepatitis C virus-coinfected subjects. Antimicrobial agents and chemotherapy 49(2):643-649.

98. Ninomiya M, Ito K, Horie T. 2005. Functional analysis of dog multidrug resistance-associated protein 2 (Mrp2) in comparison with rat Mrp2. Drug metabolism and disposition: the biological fate of chemicals 33(2):225-232.

99. Niinuma K, Kato Y, Suzuki H, Tyson CA, Weizer V, Dabbs JE, Froehlich R, Green CE, Sugiyama Y. 1999. Primary active transport of organic anions on bile canalicular membrane in humans. The American journal of physiology 276(5 Pt 1):1153-1164.

100. Boyer JL, Meier PJ. 1990. Characterizing mechanisms of hepatic bile acid transport utilizing isolated membrane vesicles. Methods in enzymology 192:517-533.

101. Wolters H, Spiering M, Gerding A, Slooff MJ, Kuipers F, Hardonk MJ, Vonk RJ. 1991. Isolation and characterization of canalicular and basolateral plasma membrane fractions from human liver. Biochimica et biophysica acta 1069(1):61-69.

102. Blitzer BL, Donovan CB. 1984. A new method for the rapid isolation of basolateral plasma membrane vesicles from rat liver. Characterization, validation, and bile acid transport studies. The Journal of biological chemistry 259(14):9295-9301.

103. Jedlitschky G, Leier I, Buchholz U, Hummel-Eisenbeiss J, Burchell B, Keppler D. 1997. ATP-dependent transport of bilirubin glucuronides by the multidrug resistance protein MRP1 and its hepatocyte canalicular isoform MRP2. The Biochemical journal 327 (Pt 1):305-310.

104. Pal A, Mehn D, Molnar E, Gedey S, Meszaros P, Nagy T, Glavinas H, Janaky T, von Richter O, Bathori G, Szente L, Krajcsi P. 2007. Cholesterol potentiates ABCG2 activity in a heterologous expression system: improved in vitro model to study function of human ABCG2. The Journal of pharmacology and experimental therapeutics 321(3):1085-1094.

105. Brouwer KL, Keppler D, Hoffmaster KA, Bow DA, Cheng Y, Lai Y, Palm JE, Stieger B, Evers R. 2013. In vitro methods to support transporter evaluation in drug discovery and development. Clinical pharmacology and therapeutics 94(1):95-112.

106. Fahrmayr C, Konig J, Auge D, Mieth M, Fromm MF. 2012. Identification of drugs and drug metabolites as substrates of multidrug resistance protein 2 (MRP2) using triple-transfected MDCK-OATP1B1-UGT1A1-MRP2 cells. British journal of pharmacology 165(6):1836-1847.

107. Wagner CA, Friedrich B, Setiawan I, Lang F, Broer S. 2000. The use of Xenopus laevis oocytes for the functional characterization of heterologously expressed membrane proteins. Cellular physiology and biochemistry : international journal of experimental cellular physiology, biochemistry, and pharmacology 10(1-2):1-12.

108. Groothuis GM, Hulstaert CE, Kalicharan D, Hardonk MJ. 1981. Plasma membrane specialization and intracellular polarity of freshly isolated rat hepatocytes. European journal of cell biology 26(1):43-51.

109. Bow DA, Perry JL, Miller DS, Pritchard JB, Brouwer KL. 2008. Localization of P-gp (Abcb1) and Mrp2 (Abcc2) in freshly isolated rat hepatocytes. Drug metabolism and disposition: the biological fate of chemicals 36(1):198-202.

110. LeCluyse EL, Bullock PL, Parkinson A, Hochman JH. 1996. Cultured rat hepatocytes. Pharmaceutical biotechnology 8:121-159.

111. Dunn JC, Yarmush ML, Koebe HG, Tompkins RG. 1989. Hepatocyte function and extracellular matrix geometry: long-term culture in a sandwich configuration. FASEB journal : official publication of the Federation of American Societies for Experimental Biology 3(2):174-177.

112. Liu X, Chism JP, LeCluyse EL, Brouwer KR, Brouwer KL. 1999. Correlation of biliary excretion in sandwich-cultured rat hepatocytes and in vivo in rats. Drug metabolism and disposition: the biological fate of chemicals 27(6):637-644.

113. Le Vee M, Noel G, Jouan E, Stieger B, Fardel O. 2013. Polarized expression of drug transporters in differentiated human hepatoma HepaRG cells. Toxicology in vitro : an international journal published in association with BIBRA.

114. Kotani N, Maeda K, Debori Y, Camus S, Li R, Chesne C, Sugiyama Y. 2012. Expression and Transport Function of Drug Uptake Transporters in Differentiated HepaRG Cells. Molecular pharmaceutics.

115. Song Z, Cai J, Liu Y, Zhao D, Yong J, Duo S, Song X, Guo Y, Zhao Y, Qin H, Yin X, Wu C, Che J, Lu S, Ding M, Deng H. 2009. Efficient generation of hepatocyte-like cells from human induced pluripotent stem cells. Cell research 19(11):1233-1242.

116. Patel NJ, Zamek-Gliszczynski MJ, Zhang P, Han YH, Jansen PL, Meier PJ, Stieger B, Brouwer KL. 2003. Phenobarbital alters hepatic Mrp2 function by direct and indirect interactions. Molecular pharmacology 64(1):154-159.

117. Maher JM, Dieter MZ, Aleksunes LM, Slitt AL, Guo G, Tanaka Y, Scheffer GL, Chan JY, Manautou JE, Chen Y, Dalton TP, Yamamoto M, Klaassen CD. 2007. Oxidative and electrophilic stress induces multidrug resistance-associated protein transporters via the nuclear factor-E2-related factor-2 transcriptional pathway. Hepatology (Baltimore, Md) 46(5):1597-1610.

118. Nezasa K, Tian X, Zamek-Gliszczynski MJ, Patel NJ, Raub TJ, Brouwer KL. 2006. Altered hepatobiliary disposition of 5 (and 6)-carboxy-2',7'-dichlorofluorescein in Abcg2 (Bcrp1) and Abcc2 (Mrp2) knockout mice. Drug metabolism and disposition: the biological fate of chemicals 34(4):718-723.

119. Ho RH, Leake BF, Roberts RL, Lee W, Kim RB. 2004. Ethnicity-dependent polymorphism in Na+-taurocholate cotransporting polypeptide (SLC10A1) reveals a domain critical for bile acid substrate recognition. The Journal of biological chemistry 279(8):7213-7222.

120. Niemi M, Pasanen MK, Neuvonen PJ. 2011. Organic anion transporting polypeptide 1B1: a genetically polymorphic transporter of major importance for hepatic drug uptake. Pharmacological reviews 63(1):157-181.

121. Kitamura S, Maeda K, Wang Y, Sugiyama Y. 2008. Involvement of multiple transporters in the hepatobiliary transport of rosuvastatin. Drug metabolism and disposition: the biological fate of chemicals 36(10):2014-2023.

122. Zhang W, Yu BN, He YJ, Fan L, Li Q, Liu ZQ, Wang A, Liu YL, Tan ZR, Fen J, Huang YF, Zhou HH. 2006. Role of BCRP 421C>A polymorphism on rosuvastatin pharmacokinetics in healthy Chinese males. Clinica chimica acta; international journal of clinical chemistry 373(1-2):99-103.

123. Keskitalo JE, Zolk O, Fromm MF, Kurkinen KJ, Neuvonen PJ, Niemi M. 2009. ABCG2 polymorphism markedly affects the pharmacokinetics of atorvastatin and rosuvastatin. Clinical pharmacology and therapeutics 86(2):197-203.

124. Li N, Singh P, Mandrell KM, Lai Y. 2010. Improved extrapolation of hepatobiliary clearance from in vitro sandwich cultured rat hepatocytes through absolute quantification of hepatobiliary transporters. Molecular pharmaceutics 7(3):630-641.

125. Nakakariya M, Ono M, Amano N, Moriwaki T, Maeda K, Sugiyama Y. 2012. In vivo biliary clearance should be predicted by intrinsic biliary clearance in sandwich-cultured hepatocytes. Drug metabolism and disposition: the biological fate of chemicals 40(3):602-609.

126. Hendrikse NH, Kuipers F, Meijer C, Havinga R, Bijleveld CM, van der Graaf WT, Vaalburg W, de Vries EG. 2004. In vivo imaging of hepatobiliary transport function mediated by multidrug resistance associated protein and P-glycoprotein. Cancer chemotherapy and pharmacology 54(2):131-138.

127. Leonhardt M, Keiser M, Oswald S, Kuhn J, Jia J, Grube M, Kroemer HK, Siegmund W, Weitschies W. 2010. Hepatic uptake of the magnetic resonance imaging contrast agent Gd-EOB-DTPA: role of human organic anion transporters. Drug metabolism and disposition: the biological fate of chemicals 38(7):1024-1028.

128. Pascolo L, Petrovic S, Cupelli F, Bruschi CV, Anelli PL, Lorusso V, Visigalli M, Uggeri F, Tiribelli C. 2001. Abc protein transport of MRI contrast agents in canalicular rat liver plasma vesicles and yeast vacuoles. Biochemical and biophysical research communications 282(1):60-66.

129. Narita M, Hatano E, Arizono S, Miyagawa-Hayashino A, Isoda H, Kitamura K, Taura K, Yasuchika K, Nitta T, Ikai I, Uemoto S. 2009. Expression of OATP1B3 determines uptake of Gd-EOB-DTPA in hepatocellular carcinoma. Journal of gastroenterology 44(7):793-798.

130. Tsuboyama T, Onishi H, Kim T, Akita H, Hori M, Tatsumi M, Nakamoto A, Nagano H, Matsuura N, Wakasa K, Tomoda K. 2010. Hepatocellular carcinoma: hepatocyte-selective enhancement at gadoxetic acid-enhanced MR imaging--correlation with expression of sinusoidal and canalicular transporters and bile accumulation. Radiology 255(3):824-833.

131. Shitara Y, Itoh T, Sato H, Li AP, Sugiyama Y. 2003. Inhibition of transporter-mediated hepatic uptake as a mechanism for drug-drug interaction between cerivastatin and cyclosporin A. The Journal of pharmacology and experimental therapeutics 304(2):610-616.

132. Muck W, Mai I, Fritsche L, Ochmann K, Rohde G, Unger S, Johne A, Bauer S, Budde K, Roots I, Neumayer HH, Kuhlmann J. 1999. Increase in cerivastatin systemic exposure after single and

multiple dosing in cyclosporine-treated kidney transplant recipients. Clinical pharmacology and therapeutics 65(3):251-261.

133. Asberg A, Hartmann A, Fjeldsa E, Bergan S, Holdaas H. 2001. Bilateral pharmacokinetic interaction between cyclosporine A and atorvastatin in renal transplant recipients. American journal of transplantation : official journal of the American Society of Transplantation and the American Society of Transplant Surgeons 1(4):382-386.

134. Olbricht C, Wanner C, Eisenhauer T, Kliem V, Doll R, Boddaert M, O'Grady P, Krekler M, Mangold B, Christians U. 1997. Accumulation of lovastatin, but not pravastatin, in the blood of cyclosporine-treated kidney graft patients after multiple doses. Clinical pharmacology and therapeutics 62(3):311-321.

135. Simonson SG, Raza A, Martin PD, Mitchell PD, Jarcho JA, Brown CD, Windass AS, Schneck DW. 2004. Rosuvastatin pharmacokinetics in heart transplant recipients administered an antirejection regimen including cyclosporine. Clinical pharmacology and therapeutics 76(2):167-177.

136. Martin J, Krum H. 2003. Cytochrome P450 drug interactions within the HMG-CoA reductase inhibitor class: are they clinically relevant? Drug safety : an international journal of medical toxicology and drug experience 26(1):13-21.

137. Kim RB. 2004. 3-Hydroxy-3-methylglutaryl-coenzyme A reductase inhibitors (statins) and genetic variability (single nucleotide polymorphisms) in a hepatic drug uptake transporter: what's it all about? Clinical pharmacology and therapeutics 75(5):381-385.

138. Kajosaari LI, Niemi M, Neuvonen M, Laitila J, Neuvonen PJ, Backman JT. 2005. Cyclosporine markedly raises the plasma concentrations of repaglinide. Clinical pharmacology and therapeutics 78(4):388-399.

139. Treiber A, Schneiter R, Delahaye S, Clozel M. 2004. Inhibition of organic anion transporting polypeptide-mediated hepatic uptake is the major determinant in the pharmacokinetic interaction between bosentan and cyclosporin A in the rat. The Journal of pharmacology and experimental therapeutics 308(3):1121-1129.

140. Terkeltaub RA, Furst DE, Digiacinto JL, Kook KA, Davis MW. 2011. Novel evidence-based colchicine dose-reduction algorithm to predict and prevent colchicine toxicity in the presence of cytochrome P450 3A4/P-glycoprotein inhibitors. Arthritis and rheumatism 63(8):2226-2237.

141. Niemi M, Backman JT, Kajosaari LI, Leathart JB, Neuvonen M, Daly AK, Eichelbaum M, Kivisto KT, Neuvonen PJ. 2005. Polymorphic organic anion transporting polypeptide 1B1 is a major determinant of repaglinide pharmacokinetics. Clinical pharmacology and therapeutics 77(6):468-478.

142. Backman JT, Kyrklund C, Neuvonen M, Neuvonen PJ. 2002. Gemfibrozil greatly increases plasma concentrations of cerivastatin. Clinical pharmacology and therapeutics 72(6):685-691.

143. Shitara Y, Hirano M, Sato H, Sugiyama Y. 2004. Gemfibrozil and its glucuronide inhibit the organic anion transporting polypeptide 2 (OATP2/OATP1B1:SLC21A6)-mediated hepatic uptake and CYP2C8-mediated metabolism of cerivastatin: analysis of the mechanism of the clinically

relevant drug-drug interaction between cerivastatin and gemfibrozil. The Journal of pharmacology and experimental therapeutics 311(1):228-236.

144. Backman JT, Kyrklund C, Kivisto KT, Wang JS, Neuvonen PJ. 2000. Plasma concentrations of active simvastatin acid are increased by gemfibrozil. Clinical pharmacology and therapeutics 68(2):122-129.

145. Kyrklund C, Backman JT, Kivisto KT, Neuvonen M, Laitila J, Neuvonen PJ. 2001. Plasma concentrations of active lovastatin acid are markedly increased by gemfibrozil but not by bezafibrate. Clinical pharmacology and therapeutics 69(5):340-345.

146. Kyrklund C, Backman JT, Neuvonen M, Neuvonen PJ. 2003. Gemfibrozil increases plasma pravastatin concentrations and reduces pravastatin renal clearance. Clinical pharmacology and therapeutics 73(6):538-544.

147. Yamazaki M, Li B, Louie SW, Pudvah NT, Stocco R, Wong W, Abramovitz M, Demartis A, Laufer R, Hochman JH, Prueksaritanont T, Lin JH. 2005. Effects of fibrates on human organic anion-transporting polypeptide 1B1-, multidrug resistance protein 2- and P-glycoprotein-mediated transport. Xenobiotica; the fate of foreign compounds in biological systems 35(7):737-753.

148. Lee JE, van Heeswijk R, Alves K, Smith F, Garg V. 2011. Effect of the hepatitis C virus protease inhibitor telaprevir on the pharmacokinetics of amlodipine and atorvastatin. Antimicrobial agents and chemotherapy 55(10):4569-4574.

149. Garg V, van Heeswijk R, Lee JE, Alves K, Nadkarni P, Luo X. 2011. Effect of telaprevir on the pharmacokinetics of cyclosporine and tacrolimus. Hepatology (Baltimore, Md) 54(1):20-27.

150. Kunze A, Huwyler J, Camenisch G, Gutmann H. 2012. Interaction of the antiviral drug telaprevir with renal and hepatic drug transporters. Biochemical pharmacology 84(8):1096-1102.

151. Nademanee K, Kannan R, Hendrickson J, Ookhtens M, Kay I, Singh BN. 1984. Amiodarone-digoxin interaction: clinical significance, time course of development, potential pharmacokinetic mechanisms and therapeutic implications. Journal of the American College of Cardiology 4(1):111-116.

152. Lambert C, Lamontagne D, Hottlet H, du Souich P. 1989. Amiodarone-digoxin interaction in rats. A reduction in hepatic uptake. Drug metabolism and disposition: the biological fate of chemicals 17(6):704-708.

153. Kodawara T, Masuda S, Wakasugi H, Uwai Y, Futami T, Saito H, Abe T, Inu K. 2002. Organic anion transporter oatp2-mediated interaction between digoxin and amiodarone in the rat liver. Pharmaceutical research 19(6):738-743.

154. Kobayashi Y, Sakai R, Ohshiro N, Ohbayashi M, Kohyama N, Yamamoto T. 2005. Possible involvement of organic anion transporter 2 on the interaction of theophylline with erythromycin in the human liver. Drug metabolism and disposition: the biological fate of chemicals 33(5):619-622.

155. Bourdet DL, Pritchard JB, Thakker DR. 2005. Differential substrate and inhibitory activities of ranitidine and famotidine toward human organic cation transporter 1 (hOCT1; SLC22A1),

hOCT2 (SLC22A2), and hOCT3 (SLC22A3). The Journal of pharmacology and experimental therapeutics 315(3):1288-1297.

156. Zhang L, Gorset W, Washington CB, Blaschke TF, Kroetz DL, Giacomini KM. 2000. Interactions of HIV protease inhibitors with a human organic cation transporter in a mammalian expression system. Drug metabolism and disposition: the biological fate of chemicals 28(3):329-334.

157. Angelin B, Arvidsson A, Dahlqvist R, Hedman A, Schenck-Gustafsson K. 1987. Quinidine reduces biliary clearance of digoxin in man. European journal of clinical investigation 17(3):262-265.

158. Hedman A, Angelin B, Arvidsson A, Beck O, Dahlqvist R, Nilsson B, Olsson M, Schenck-Gustafsson K. 1991. Digoxin-verapamil interaction: reduction of biliary but not renal digoxin clearance in humans. Clinical pharmacology and therapeutics 49(3):256-262.

159. Chu X, Korzekwa K, Elsby R, Fenner K, Galetin A, Lai Y, Matsson P, Moss A, Nagar S, Rosania GR, Bai JP, Polli JW, Sugiyama Y, Brouwer KL. 2013. Intracellular drug concentrations and transporters: measurement, modeling, and implications for the liver. Clinical pharmacology and therapeutics 94(1):126-141.

160. Campbell SD, de Morais SM, Xu JJ. 2004. Inhibition of human organic anion transporting polypeptide OATP 1B1 as a mechanism of drug-induced hyperbilirubinemia. Chemico-biological interactions 150(2):179-187.

161. Westphal K, Weinbrenner A, Zschiesche M, Franke G, Knoke M, Oertel R, Fritz P, von Richter O, Warzok R, Hachenberg T, Kauffmann HM, Schrenk D, Terhaag B, Kroemer HK, Siegmund W. 2000. Induction of P-glycoprotein by rifampin increases intestinal secretion of talinolol in human beings: a new type of drug/drug interaction. Clinical pharmacology and therapeutics 68(4):345-355.

162. Gant TW, O'Connor CK, Corbitt R, Thorgeirsson U, Thorgeirsson SS. 1995. In vivo induction of liver P-glycoprotein expression by xenobiotics in monkeys. Toxicology and applied pharmacology 133(2):269-276.

163. Riley J, Styles J, Verschoyle RD, Stanley LA, White IN, Gant TW. 2000. Association of tamoxifen biliary excretion rate with prior tamoxifen exposure and increased mdr1b expression. Biochemical pharmacology 60(2):233-239.

164. Pang KS, Maeng HJ, Fan J. 2009. Interplay of transporters and enzymes in drug and metabolite processing. Molecular pharmaceutics 6(6):1734-1755.

165. Lau YY, Wu CY, Okochi H, Benet LZ. 2004. Ex situ inhibition of hepatic uptake and efflux significantly changes metabolism: hepatic enzyme-transporter interplay. The Journal of pharmacology and experimental therapeutics 308(3):1040-1045.

166. Lancaster CS, Bruun GH, Peer CJ, Mikkelsen TS, Corydon TJ, Gibson AA, Hu S, Orwick SJ, Mathijssen RH, Figg WD, Baker SD, Sparreboom A. 2012. OATP1B1 polymorphism as a determinant of erythromycin disposition. Clinical pharmacology and therapeutics 92(5):642-650.

167. Mudra DR, Desino KE, Desai PV. 2011. In silico, in vitro and in situ models to assess interplay between CYP3A and P-gp. Current drug metabolism 12(8):750-773.

168. Wu CY, Benet LZ. 2003. Disposition of tacrolimus in isolated perfused rat liver: influence of troleandomycin, cyclosporine, and gg918. Drug metabolism and disposition: the biological fate of chemicals 31(11):1292-1295.

169. Jeong H, Chiou WL. 2006. Role of P-glycoprotein in the hepatic metabolism of tacrolimus. Xenobiotica; the fate of foreign compounds in biological systems 36(1):1-13.

170. Endres CJ, Endres MG, Unadkat JD. 2009. Interplay of drug metabolism and transport: a real phenomenon or an artifact of the site of measurement? Molecular pharmaceutics 6(6):1756-1765.

171. Wu B. 2012. Pharmacokinetic interplay of phase II metabolism and transport: a theoretical study. Journal of pharmaceutical sciences 101(1):381-393.

172. Pang KS, Durk MR. 2010. Physiologically-based pharmacokinetic modeling for absorption, transport, metabolism and excretion. Journal of pharmacokinetics and pharmacodynamics 37(6):591-615.

173. Eloranta JJ, Meier PJ, Kullak-Ublick GA. 2005. Coordinate transcriptional regulation of transport and metabolism. Methods in enzymology 400:511-530.

174. Lau YY, Okochi H, Huang Y, Benet LZ. 2006. Multiple transporters affect the disposition of atorvastatin and its two active hydroxy metabolites: application of in vitro and ex situ systems. The Journal of pharmacology and experimental therapeutics 316(2):762-771.

175. Backman JT, Luurila H, Neuvonen M, Neuvonen PJ. 2005. Rifampin markedly decreases and gemfibrozil increases the plasma concentrations of atorvastatin and its metabolites. Clinical pharmacology and therapeutics 78(2):154-167.

176. Zheng HX, Huang Y, Frassetto LA, Benet LZ. 2009. Elucidating rifampin's inducing and inhibiting effects on glyburide pharmacokinetics and blood glucose in healthy volunteers: unmasking the differential effects of enzyme induction and transporter inhibition for a drug and its primary metabolite. Clinical pharmacology and therapeutics 85(1):78-85.

177. Lau YY, Huang Y, Frassetto L, Benet LZ. 2007. Effect of OATP1B transporter inhibition on the pharmacokinetics of atorvastatin in healthy volunteers. Clinical pharmacology and therapeutics 81(2):194-204.

178. Watanabe T, Kusuhara H, Maeda K, Shitara Y, Sugiyama Y. 2009. Physiologically based pharmacokinetic modeling to predict transporter-mediated clearance and distribution of pravastatin in humans. The Journal of pharmacology and experimental therapeutics 328(2):652-662.

179. DeGorter MK, Xia CQ, Yang JJ, Kim RB. 2012. Drug transporters in drug efficacy and toxicity. Annual review of pharmacology and toxicology 52:249-273.

180. Trevino LR, Shimasaki N, Yang W, Panetta JC, Cheng C, Pei D, Chan D, Sparreboom A, Giacomini KM, Pui CH, Evans WE, Relling MV. 2009. Germline genetic variation in an organic

anion transporter polypeptide associated with methotrexate pharmacokinetics and clinical effects. J Clin Oncol 27(35):5972-5978.

181. Jonker JW, Liddle C, Downes M. 2012. FXR and PXR: potential therapeutic targets in cholestasis. The Journal of steroid biochemistry and molecular biology 130(3-5):147-158.

182. Morgan RE, Trauner M, van Staden CJ, Lee PH, Ramachandran B, Eschenberg M, Afshari CA, Qualls CW, Jr., Lightfoot-Dunn R, Hamadeh HK. 2010. Interference with bile salt export pump function is a susceptibility factor for human liver injury in drug development. Toxicological sciences : an official journal of the Society of Toxicology 118(2):485-500.

183. Fattinger K, Funk C, Pantze M, Weber C, Reichen J, Stieger B, Meier PJ. 2001. The endothelin antagonist bosentan inhibits the canalicular bile salt export pump: a potential mechanism for hepatic adverse reactions. Clinical pharmacology and therapeutics 69(4):223-231.

184. Funk C, Pantze M, Jehle L, Ponelle C, Scheuermann G, Lazendic M, Gasser R. 2001. Troglitazone-induced intrahepatic cholestasis by an interference with the hepatobiliary export of bile acids in male and female rats. Correlation with the gender difference in troglitazone sulfate formation and the inhibition of the canalicular bile salt export pump (Bsep) by troglitazone and troglitazone sulfate. Toxicology 167(1):83-98.

185. Lee JK, Paine MF, Brouwer KL. 2010. Sulindac and its metabolites inhibit multiple transport proteins in rat and human hepatocytes. The Journal of pharmacology and experimental therapeutics 334(2):410-418.

Table 1.1: Uptake transporter substrates

Protein	Gene Symbol	Substrate
NTCP	*SCL10A1*	Bile acids, BSP, E1S, fluvastatin, pitavastatin, rosuvastatin
OATP1B1	*SLCO1B1*	Arsenic, atorvastatin, atrasentan, benzylpenicillin, bilirubin, bile acids, bosentan, BQ-123, BSP, caspofungin, cefazolin, cefditoren, cefoperazone, cerivastatin, darunavir, DHEAS, demethylphalloin, eltrombopag, enalapril, $E_2$17G, E1S, ezetimibe glucuronide, fluorescein, fluvastatin, gimatecan, hydroxyurea, LTC_4, LTE_4, lopinavir, mesalazine, MTX, microcystin, mycophenolic acid-7-O-glucuronide, nafcillin, olmesartan, phalloidin, pitavastatin, pravastatin, PGE_2, rifampicin, rosuvastatin, saquinavir, simvastatin acid, SN-38, temocapril, thromboxane B2, thyroxine, torsemide, triiodothyronine, troglitazone sulfate, valsartan
OATP1B3	*SLCO1B3*	Amanitin, atrasentan, benzylpenicillin, bilirubin, bile acids, bosentan, BSP, cefadroxil, cefazolin, cefditoren, cefmetazole, cefoperazone, cephalexin, cholecystokinin 8, DHEAS, deltorphin II, demethylphalloin, diclofenac, digoxin, docetaxel, enalapril, epicatechin gallate, epigallocatechin gallate, erythromycin, $E_2$17G, E1S, fexofenadine, fluorescein, Fluo-3, fluvastatin, glutathione, hydroxyurea, imatinib, LTC_4, mesalazine, MTX, microcystin, mycophenolic acid-7-O-glucuronide, nafcillin, olmesartan, quabain, paclitaxel, phalloidin, pitavastatin, rifampicin, rosuvastatin, saquinavir, telmisartan, thyroxine, triiodthyronine, valsartan
OATP2B1	*SLCO2B1*	Aliskiren, atorvastatin, benzylpenicillin, bile acids, bosentan, BSP,

		DHEAS, eltrombopag, E1S, ezetimibe glucuronide, fexofenadine, fluvastatin, glibenclamide, latanoprost acid, mesalazine, montelukast, pravastatin, pitavastatin, pregnenolone sulfate, PGE_2, rosuvastatin, talinolol, tebipenem pivoxil, thyroxine
OAT2	*SLC22A5*	5-fluorouracil, acyclovir, allopurinol, paclitaxel, p-aminohippurate, alpha-ketoglutarate, bumetanide, cAMP, cGMP, DHEAS, erythromycin, E1S, ganciclovir, glutamate, glutarate, L-ascorbic acid, MTX, orotic acid, penciclovir, PGE_2, ranitidine, tetracycline, theophylline
OAT7	*SLC22A9*	Butyrate, DHEAS, E1S
OCT1	*SLC22A1*	1-methyl-4-phenylpyridinium, acyclovir, choline, famotidine, ganciclovir, imatinib, metformin, n-methylnicotinamide, n-methylquinidine, n-methylquinine, PGE_2, $PGF_{2\alpha}$, ranitidine, tetraethylammonium, tributylmethylammonium
OSTα/β	*SLC51a/b*	Bile acids, E1S, DHEAS

BQ-123, cyclo(D-Trp-D-Asp-L-Pro-D-Val-L-Leu); BSP, bromosulfophthalein; cAMP, cyclic AMP; CCK-8, cholecystokinin; cGMP, cyclic GMP; DHEAS, dehydroepiandrosterone sulfate; $E_2$17G, estradiol-17β-D-glucuronide; E1S, estrone-3-sulfate; GSH, glutathione; PG, prostaglandin; LT, leukotriene; MTX, methotrexate

Table 1.2: Efflux transporter substrates

Protein	Gene Symbol	Substrates
	Apical Membrane	
MDR1/P-gp	*ABCB1*	Aldosterone, amprenavir, berberine, colchicine, corticosterone, cyclosporin A, debrisoquine, dexamethasone, digoxin, doxorubicin, erythromycin, etoposide, fexofenadine, grepafloxacin, indinavir, irinotecan, levofloxacin, loperamide, lovastatin, losartan, nelfinavir, mitoxantrone, nicardipine, norverapamil, paclitaxel, quinidine, rhodamine 123, ritonavir, saquinavir, tacrolimus, talinolol, terfenadine, topotecan, valinomycin, verapamil, vinblastine
MDR3	*ABCB4*	Phospholipids , digoxin, paclitaxel, verapamil, vinblastine
BSEP	*ABCB11*	Conjugated and unconjugated bile acids, pravastatin
MRP2	*ABCC2*	Carboxydichlorofluorescein, camptothecin, cerivastatin, cisplatin, cholecystokinin , DHEAS, doxorubicin, $E_2$17G, E1S, etoposide, glibenclamide, indomethacin, irinotecan, LTC_4, MTX, ochratoxin A, olmesartan, para-aminohippurate, pravastatin, rifampin, SN-38, valsartan, vinblastine, vincristine, numerous glucuronide, glutathione and sulfate conjugates
BCRP	*ABCG2*	4-methylumbelliferone sulfate, 9-(2-phosphomethoxyethyl) adenine, acyclovir, aflatoxin B1, chlorothiazide, ciprofloxacin, dasatinib, daunorubicin, dipyridamole, doxorubicin, $E_2$17G, E1S, estradiol, etoposide, furosemide, ganciclovir, genistein, glyburide, harmol sulfate, hematoporphyrin, imatinib, irinotecan, lapatinib,

		MTX, mitoxantrone, nitrofurantoin, ofloxacin, pitavastatin, prazosin, rhodamine 123, rosuvastatin, SN-38, sulfasalazine, tamoxifen, taurocholate, teniposide, testosterone, topotecan, urate
MATE1	*SLC47A1*	1-methyl-4-phenylpyridinium, acyclovir, cimetidine, creatinine, E1S, fexofenadine, guanidine, metformin, oxaliplatin, procainamide, tetraethylammonium, thiamine, topotecan
Basolateral Membrane		
MRP1	*ABCC1*	Aflatoxin B1, bilirubin, daunorubicin, difloxacin, doxorubicin, etoposide, flutamide, folic acid, glutathione, grepafloxacin, irinotecan, leucovorin, MTX, paclitaxel, saquinavir, ritonavir, vinblastine, vincristine, and numerous glutathione, glucuronide, and sulfate conjugates
MRP3	*ABCC3*	Acetaminophen glucuronide, DHEAS, $E_2$17G, ethinylestradiol glucuronide, etoposide, fexofenadine, folic acid, leucovorin, LTC_4, MTX, monovalent and sulfated bile salts
MRP4	*ABCC4*	9-(2-phosphomethoxyethyl) adenine, adefovir, ADP, azidothymidine, chenodeoxycholylglycine, cholate, taurocholate, cAMP, cGMP, DHEAS, $E_2$17G, folic acid, MTX, nelfinavir, olmesartan, para-aminohippurate, PGE_1, PGE_2, rosuvastatin, tenofovir, topotecan, urate, ADP,
MRP5	*ABCC5*	Adefovir, cAMP, cGMP
MRP6	*ABCC6*	BQ-123, LTC_4-glutathione, dinitrophenol glucuronide

ADP, adenosine diphosphate; cAMP, cyclic AMP; cGMP, cyclic GMP; CSA, cyclosporin; DHEAS, dehydroepiandrosterone sulfate; $E_2$17G, estradiol-17β-D-glucuronide; E1S, estrone-3-sulfate; MTX, methotrexate; PG, prostaglandin; LT, leukotriene; TC, taurocholate

Table 1.3: Nuclear receptors (NRs) and transporter regulation

Nuclear Receptor	Transport Protein	Change	RNA/Protein	Ligand	Test System[a]
	NTCP	↓	mRNA	TCDD	HH
	Oatp1a1 (m)	↓	mRNA	TCDD, BNF	*In vivo*
	Oatp1a4 (r)	↓	mRNA, protein	TCDD, BNF, PCB126	*In vivo*
	OATP1B3	↓	mRNA	TCDD	HH
	OATP2B1	↓	mRNA	TCDD	HH
	OAT2	↓	mRNA	TCDD	HH
AhR	OCT1	↓	mRNA	TCDD	HH
	MDR1	↑	mRNA	TCDD	HH
	BSEP	↓	mRNA	TCDD	HH
	Mrp2 (m)	↑	mRNA	3-MC, TCDD, PCB126, BNF	*In vivo*
	BCRP	↑	mRNA	TCDD	HepG2, HH
	Bcrp (m)	↔	mRNA	TCDD, 3-MC	*In vivo*
	Mrp3 (m)	↑	mRNA	TCDD, PCB126, BNF	*In vivo*
	MRP4	↑	mRNA, protein	TCDD, 3-MC	HepG2, HH

	Mrp5 (m)	↑	mRNA	TCDD, PCB126, BNF	*In vivo*
CAR	NTCP	↓,↑	mRNA	PB	HH, HLS
	OATP1B3	↓	mRNA	PB	HH
	OATP2B1	↓	mRNA	PB	HH
	Oatp1a1 (m)	↓	mRNA	PB,TCPOBOP, DAS	*In vivo*
	Oatp1a4 (m)	↑	mRNA	PB,TCPOBOP	*In vivo*
	Oatp1a4 (r)	↑	mRNA, protein	PB, DAS, PCB99	*In vivo*
	Oatp1a5 (m)	↓	mRNA	PB,TCPOBOP, DAS	*In vivo*
	OCT1	↓	mRNA	PB	HH
	MDR1	↑	mRNA	PB	HH
	MDR1	↑	mRNA	PB	HLS
	BSEP	↓	mRNA	PB	HH
	BSEP	↑	mRNA	PB	HLS
	BCRP	↑	mRNA	PB	HH
	MRP2	↑	mRNA	PB	HH, HLS
	Mrp2 (m)	↑	mRNA	TCPOBOP	*In vivo*
	Mrp2 (r)	↑	mRNA	PB	RH
	Mrp3 (r)	↑	mRNA	PB, PCB99, DAS, PB	In vivo, HepG2

	Mrp3 (m)	↑	mRNA	TCPOBOP, DAS, PB	*In vivo*
	Mrp4 (m)	↑	mRNA, protein	TCPOBOP, PB	*In vivo*
	Mrp5 (m)	↑	mRNA	TCPOBOP, DAS	*In vivo*
FXR	Ntcp (m)	↓	mRNA	Bile duct ligation, CA	*In vivo*
	OATP1B3	↓	mRNA	CDCA	HLS
	BSEP	↑	mRNA	CDCA	HLS
	MRP2	↑	mRNA	CDCA, GW4064	HepG2
	Mrp2 (r)	↑	mRNA	CDCA, GW4064	HH, FAO
Nrf2	NTCP	↓	mRNA	OPZ	HH
	OATP1B3	↓	mRNA	OPZ	HH
	Oatp1a1 (m)	↓	mRNA	BHA, EXQ	*In vivo*
	Oatp2b1 (m)	↑	mRNA	BHA, EXQ	*In vivo*
	OAT2	↓	mRNA	OPZ	HH
	MDR1	↑	mRNA	OPZ	HH
	BSEP	↓	mRNA	OPZ	HH
	BCRP	↑	mRNA	OPZ	HH
	MRP2	↑	mRNA	OPZ	HH
	Mrp2 (m)	↑	mRNA	OPZ, BHA, EXQ	*In vivo*

	Mrp2 (r)	↑	protein	OPZ, EXQ	*In vivo*
	MRP3	↑	mRNA	OPZ	HH
	Mrp3 (m)	↑	mRNA	OPZ, BHA	*In vivo*
	Mrp3 (r)	↑	mRNA	OPZ, BHA, EXQ	*In vivo*
	MRP4	↑	mRNA, protein	OPZ	HepG2, HH
	Mrp4 (m)	↑	mRNA	OPZ, BHA, EXQ	*In vivo*
	Mrp5 (m)	↑	mRNA	BHA, OPZ, EXQ	*In vivo*
	Ntcp (m)	↓	protein	CPFB	*In vivo*
	Oatp1a1 (m)	↓	mRNA, protein	CLFB, DEHP, CPFB	*In vivo*
	Oatp1a6 (m)	↓	mRNA	CLFB	*In vivo*
	Oatp2b1 (m)	↓	mRNA	CLFB, DEHP	*In vivo*
	Mdr1 (m)	↑	protein	CPFB	*In vivo*
PPARα	Bsep (m)	↓	protein	CPFB	*In vivo*
	Mrp2 (r)	↔ (protein), ↓(mRNA)	mRNA, protein	CLFB, DEHP, PFDA	*In vivo*
	Bcrp (m)	↑	mRNA, protein	CLFB	*In vivo*
	Mrp3 (m)	↑	mRNA, protein	CLFB, CPFB, DEHP	*In vivo*
	Mrp4 (m)	↑	mRNA, protein	CLFB	*In vivo*

	NTCP	↓	mRNA	RIF	HH
	OATP1B1	↑	mRNA	RIF	HH
	Oatp1a1 (m)	↓	mRNA	PCN, SPR, DEX	*In vivo*
	Oatp1a4 (m)	↑	mRNA	PCN, SPR	*In vivo*
	Oatp1a4 (r)	↑	mRNA, protein	PCN, SPR, DEX	*In vivo*
	Oatp1a5 (m)	↓	mRNA	SPR, DEX	*In vivo*
	OCT1	↓	mRNA	RIF	HH
PXR	BSEP	↓	mRNA	RIF	HH
	BSEP	↑	mRNA	RIF	HLS
	Mrp2 (m)	↑	mRNA	PCN, SPR	*In vivo*
	Mrp2 (r)	↑	mRNA, protein	DEX, PCN, SPR	RH, *in vivo*
	MRP2	↑	mRNA	RIF	HH, HLS
	BCRP	↑	mRNA	RIF	HH
	Bcrp (m)		mRNA	PCN	*In vivo*

[a] FAO, rat hepatoma cell line; HLS, human liver slices; HH, human hepatocytes; HepG2, human-derived liver cell line, m, mouse; r, rat; RH, rat hepatocytes

3-MC, 3-methylcholanthrene; BHA, butylated hydroxyanisole; BNF, β-naphthoflavone; CA, cholic acid; CDCA, chenodeoxycholic acid; CLFB, clofibric acid; CPFB, ciprofibrate; DAS, diallyl sulfide; DEX, dexamethasone; DEHP, di-(2-ethylhexyl)phthalate; EXQ, ethoxyquin; GW4064, 3-

(2,6-Dichlorophenyl)-4-(3’-carboxy-2-chlorostilben-4-yl)oxymethyl-5-isopropylisoxazole; OPZ, oltipraz; PB, phenobarbital; PCN, pregenolone-16α-carbonitrile; PCB99, 2,2'4,4',6-pentachlorobiphenyl ;PCB126, 3,3’,4,4’,5-pentachlorobiphenyl; PFDA, perfluorodecanoic acid; RIF, rifampicin; SPR, spironolactone; TCDD, 2,3,7,8-tetrachlorodibenzo-p-dioxin; TCPOBOP, 1,4-Bis-[2-(3,5-dichloropyridyloxy)]benzene, 3,3’,5,5’-Tetrachloro-1,4-bis(pyridyloxy)benzene

Table 1.4: Model systems for studying hepatic drug transport: Summary of major applications and advantages/disadvantages

Model System	Major Applications	Advantages/Disadvantages
In Vitro		
Membrane vesicles prepared from transfected systems	Screening for substrates and inhibitors of efflux transporters	+ High throughput + High transporter expression can be achieved + Preparation of large batches and cryopreservation possible - Interplay of multiple transport proteins cannot be assessed - Endogenous transport proteins may affect data interpretation - Parental cell differences might alter transport function (e.g. due to differences in cholesterol content or glycosylation)
Purified membrane vesicles from liver tissue	Mechanistic studies of substrate transport at a particular membrane domain	+ All relevant transporters expressed, no interference from metabolism - Preparation of high-purity vesicles is technically challenging and labor-intensive - Contribution of a single transporter is difficult to assess
Non-polarized transfected cells	High-throughput screening for substrates and	+ High-throughput cell-based model + Stable transfection allows for multiple

	inhibitors; evaluation of drug interactions		passages
		-	Endogenous transport proteins may affect data interpretation
		-	Transporter expression levels difficult to standardize
		-	Not optimal to study efflux transport proteins
Polarized transfected cells	Investigation of vectorial transport and qualitative interplay between uptake and efflux transporters	+	Polarized phenotype mimics hepatocyte polarity
		+	Active transport vs. diffusion can be assessed
		+	Multiple transfections with transport proteins and/or metabolizing enzymes can be conducted
		-	Transporter expression levels difficult to standardize
		-	Complicated assay design
Suspended hepatocytes	Investigation of hepatic uptake; identification of uptake inhibitors; characterization of substrate uptake kinetics	+	Expression of uptake transporters may be closer to *in vivo*
		+	Easily transferable to species of interest
		-	Rapid loss of viability
		-	Not suitable to study canalicular efflux transporters
Sandwich-cultured hepatocytes	Evaluation of hepatobiliary disposition, hepatic drug interactions, transporter interplay and regulation;	+	Expression of hepatic transporters, drug-metabolizing enzymes and regulatory proteins resembles *in vivo*
		+	Can be established from cryopreserved or

	assessment of intracellular concentrations and subcellular distribution		freshly isolated hepatocytes from the species of interest
		+	Identification of inhibitors and inducers of transport proteins possible
		-	Formation of polarized phenotype requires time
		-	Expression of transporters and metabolizing enzymes may be altered by culture conditions
Liver slices	Mechanistic studies on interplay of hepatic metabolism and transport	+	*In vivo* architecture maintained at cellular level
		-	Viability limited to a few hours
Isolated perfused liver	Mechanistic studies of hepatic uptake, metabolism and biliary excretion	+	Intact organ physiology and bile flow maintained
		+	No interference with non-hepatic transport and/or non-hepatic metabolism
		+	Animals can be pre-treated to assess the effects of inhibitors and inducers on transport protein expression
		-	Low throughput, labor- and animal-intensive
		-	Viability limited to ~3 hours after liver isolation
		-	Limited to rodents due to technical/practical issues
In Vivo			

Human genetic polymorphism or rodent knockout	Investigation of the impact of transporter loss-of-function on whole body disposition	+	Non-invasive assessment of impact of a single transporter on systemic disposition of drugs/metabolites
		+	Ability to evaluate impact of basolateral (uptake and efflux) and canalicular transporters
		-	Depending on frequency, identification of human subjects with nonfunctional polymorphism may be rate-limiting
		-	Alteration in compensatory pathways may confound data interpretation
		-	Very low throughput
Magnetic resonance imaging	Investigation of liver and biliary tree anatomy and function of hepatic uptake and efflux transporters	+	Non-invasive 3D image of liver and biliary tree with inherent ability to quantify total intracellular drug concentrations
		+	Safer compared to radiation-based imaging
		-	Probes are limited to existing MRI imaging agents
		-	Parent agent and metabolites cannot be differentiated
		-	Low throughput/expensive
Single-photon emission computed tomography (SPECT) and positron emission	Investigate the function of hepatic uptake and efflux transporters	+	Non-invasive 3D image of liver and biliary tree with inherent ability to quantify total intracellular drug concentration
		-	Use of short half-life radionuclides limits the

tomography (PET)			potential number of substrates that can be synthesized (PET) - Use of technetium-chelated ligands limits useful probes to those currently used in clinical practice (SPECT) - Parent drug and metabolites cannot be differentiated - Low throughput/expensive
Bile duct cannulation/ CHOL-ect® multi-lumen catheter	Direct measurement of biliary excretion	+	Studies may be conducted in humans/freely moving animals - Very low throughput/expensive - Technically challenging - Long-term cannulation might affect normal physiology (e.g. changes in bile acid pool)

Table 1.5: Examples of clinically relevant transporter-mediated DDIs

Inhibiting Drug	Transporter Substrate Affected	Effect, Protein(s) Involved, Proposed Mechanism(s)
Amiodarone	Digoxin	Digoxin concentrations 2-fold ↑ in humans and rats; *in vitro* data support inhibition of Oatp2-mediated digoxin uptake in rats
Atorvastatin	Repaglinide	Repaglinide AUC and Cmax ↑ 43% and 18%, respectively; likely OATP1B1 inhibition
Cyclosporin A	Bosentan	30-fold ↑ bosentan plasma concentrations in humans; inhibition of OATP-mediated hepatic uptake of bosentan in rat
	Cerivastatin	Cerivastatin AUC 4-fold ↑; OATP1B1 inhibition (K_i = 0.2 µM)
	Colchicine	Colchicine AUC and C_{max} ~3-fold ↑; inhibition of P-gp and CYP3A4
	Pravastatin	Pravastatin AUC and C_{max} ~10-fold higher than historic controls; OATP inhibition by CsA
	Repaglinide	Repaglinide AUC 4-fold ↑; inhibition of CYP3A4 and OATP1B1
	Rosuvastatin	Rosuvastatin AUC 7.1-fold ↑; OATP1B1 inhibition (IC_{50} = 2.2 µM at 5 µM rosuvastatin)
Erythromycin	Theophylline	25% erythromycin dose reduction advised; inhibition of OAT2-mediated theophylline transport, enzyme inhibition also may be involved

Gemfibrozil	Atorvastatin	Atorvastatin and metabolites AUC and C_{max} ↑
	Cerivastatin	Cerivastatin AUC 5.6-fold ↑; inhibition of CYP2C8 (major) and possibly OATP1B1 (minor)
	Lovastatin	Lovastatin acid AUC 2.8-fold ↑; mechanism(s) not elucidated
	Pravastatin	Pravastatin AUC 2-fold ↑ and CL_{renal} ↓; possibly in part hepatic OATP1B1 inhibition
	Repaglinide	Repaglinide AUC 8.1-fold ↑; CYP2C8 inhibition by gemfibrozil glucuronide, possibly OATP1B1 inhibition
	Rosuvastatin	Rosuvastatin AUC 1.9-fold ↑; OATP1B1 inhibition
	Simvastatin	Simvastatin acid AUC 1.9-fold ↑; mechanism(s) not confirmed, contribution of OATP1B1 to hepatic uptake may be limited
Quinine/Quinidine	Digoxin	Digoxin $CL_{biliary}$ ↓ by 35-42%; Pgp inhibition
Rifampicin	Atorvastatin	Atorvastatin acid AUC ~7-fold ↑; 2-hydroxy- and 4-hydroxy-atorvastatin acid AUC ~7- and 4-fold ↑; inhibition of OATP1B1B1/1B3
	Fimasartan	Fimasartan C_{max} ~10-fold ↑; OATP1B1 inhibition
	Pravastatin	Pravastatin AUC and C_{max} ~2.5-fold ↑
Rifampin	Atorvastatin	AUC and C_{max} of atorvastatin and metabolites ↓ by 43-93%
	Digoxin	Digoxin AUC and C_{max} ↓; $CL_{nonrenal}$ ↑
	Talinolol	Talinolol AUC, C_{max} and $t_{1/2}$ ↓, $CL_{nonrenal}$ and V_d ↑; likely hepatic and intestinal P-gp induction
St John's Wort	Talinolol	Talinolol $CL_{nonrenal}$ ↑ by ~40%; likely combination of hepatic and intestinal P-gp induction

Telaprevir	Atorvastatin	Atorvastatin AUC ~8-fold ↑; inhibition of OATP1B1/1B3 and CYP 3A4
	Cyclosporin A	Cyclosporin A AUC ~5-fold ↑
	Tacrolimus	Tacrolimus AUC ~70-fold ↑; inhibition of hepatic uptake and CYP3A4
Tipranavir/Ritonavir	Atorvastatin	Steady-state tipranavir/RTV ↑ atorvastatin AUC and C_{max} ~9-fold
	Rosuvastatin	Steady-state tipranavir/RTV ↑ rosuvastatin AUC and C_{max} ~2-fold
Verapamil	Digoxin	Digoxin $CL_{biliary}$ ↓ by 43%; Pgp inhibition

Figure 1.1: In vivo architecture of the liver (A), reproduced with permission from Chu et al.[20], and localization of transport proteins in hepatocytes (B), reproduced with permission from Köck and Brouwer.[164] Hepatocytes are polarized cells with two separate membrane domains facing blood and bile.

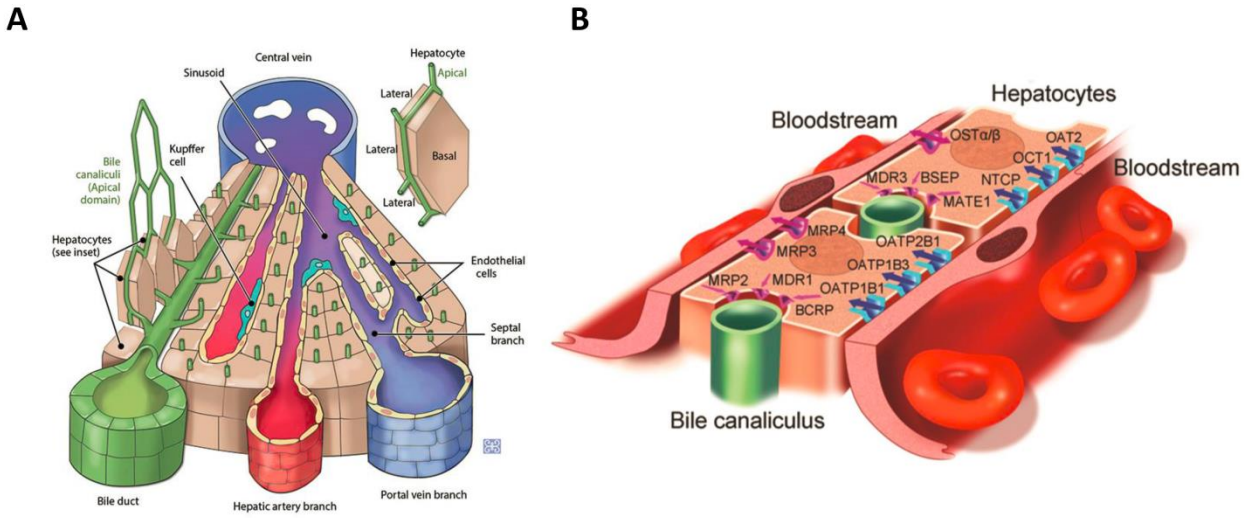

Project Rationale and Specific Aims

The objective of this dissertation research was to develop preclinical and clinical tools to assess the impact of liver pathology on transporter-mediated systemic and hepatic exposure to medications. The research strategy utilized preclinical models (including membrane vesicles from transporter-expressing cells and sandwich-cultured hepatocytes), mathematical modeling, and a novel clinical study to evaluate transporter function. This work provides a mechanistic understanding of the impact that hepatic transporter function has on the disposition of drugs and endogenous compounds under normal conditions and in response to altered liver function due to drug-induced phospholipidosis or liver disease, specifically non-alcoholic steatohepatitis.

Phospholipidosis (PLD) is a lysosomal storage disorder where phospholipids accumulate resulting in concentric lamellar bodies within the lysosome. Drug-induced PLD can occur in any tissue. Certain adverse or undesired effects (i.e. hepatic fibrosis, hERG channel inhibition and renal tubular toxicity) positively associate with known PLD inducers[1-3], but little is known about the impact of PLD on hepatic transport. Significant attention by industrial and regulatory scientists has been devoted to developing sensitive and specific models to detect PLD during pre-clinical drug development. Although *in silico* and *in vitro* models exist, unfortunately these models may not accurately predict PLD induced by metabolites, or which tissue(s) will be affected. Therefore, the first aim of this research was to develop a novel method using rat SCH to investigate whether SCH can serve as a sensitive and selective model to evaluate hepatic drug-induced PLD and determine whether PLD alters hepatic transporter-mediated uptake and biliary excretion processes.

The second aim of this project was to determine the involvement of two hepatic basolateral efflux transporters known to be up-regulated in inflammatory liver disease (i.e., MRP3 and MRP4) on enalaprilat transport from the hepatocyte to blood. The transport proteins responsible for the hepatic uptake and biliary excretion of enalapril and enalaprilat have been well described[4-7], but the processes involved in basolateral efflux of enalaprilat have not been well-characterized. Following oral administration, enalapril enters the hepatocyte and is hydrolyzed to the active form, enalaprilat, by hepatic

carboxylesterases. Enalaprilat must undergo excretion from the hepatocyte across the basolateral membrane into the systemic circulation to exert its systemic pharmacologic effect.[8] Additionally, enalapril is being investigated as an anti-fibrotic agent in patients with NASH.[9] Therefore, given the postulated intra-hepatocyte mechanism of action[10], understanding the mechanisms responsible for the hepatic disposition of enalaprilat following transformation from enalapril may have important therapeutic implications in liver disease where alterations in efflux function may impact both systemic as well as hepatic efficacy.

NASH is an intermediate pathologic state on the pathway from simple steatosis to cirrhosis that is characterized by hepatocyte steatosis, ballooning, inflammation and fibrosis. Multiple therapeutics have been used to improve insulin resistance in an effort to revert the inflammation associated with non-alcoholic fatty liver disease (NAFLD) and prevent fibrosis, including metformin, pioglitazone, rosiglitazone and rosuvastatin.[11-14] Unfortunately, the progression of fibrosis was not prevented reliably, or did not regress, for any tested pharmacologic intervention. Recently, expression of many uptake and efflux transporters and drug metabolizing enzymes was evaluated in liver samples from patients with NASH compared to healthy controls. In general, transport proteins responsible for hepatic drug uptake were down-regulated (*e.g.*, OATPs, NTCP), while excretory proteins were up-regulated (*e.g.*, MRP3, MRP4, BCRP) in NASH.[15-18] Since the major site of action for biguanides, glitazones and statins is within hepatocytes, diminished pharmacologic activity may be due, in part, to decreased intracellular hepatocyte concentrations as a consequence of altered hepatic transport. Therefore, the objective of the third aim of this dissertation research was to determine the functional impact of increased MRP3 protein expression on basolateral efflux of a probe substrate in patients with biopsy-confirmed NASH compared to healthy subjects. Following intravenous administration of morphine, the pharmacokinetics of morphine glucuronides, MRP3 substrates, were compared between healthy subjects and patients with NASH to determine the impact of altered basolateral efflux transporter expression.

In summary, this work follows a translational continuum ranging from identification of altered hepatic transport in response to drug-induced liver pathology (Aim #1, phospholipidosis) to identification

of hepatic transport proteins involved in the disposition of hepatically-derived active metabolites *in vitro* (Aim #2, enalaprilat), to developing *in vivo* methods to assess the impact of altered expression of basolateral efflux transporters secondary to liver disease (Aim #3, NASH).

Aim #1. Develop a novel screening tool to assess drug-induced hepatic phospholipidosis (PLD) and evaluate the impact of PLD on the hepatobiliary disposition of two probe substrates of hepatic basolateral and canalicular transport proteins.

Hypothesis: *Rat SCH can be used as a sensitive and selective model for hepatic PLD. Pathologic enlargement of lysosomes impairs hepatic transport of organic anions, as assessed using taurocholate and rosuvastatin.*

1.a. Develop a protocol to induce PLD in rat SCH using prototypic PLD-inducing compounds; confirm PLD by lysosomal visualization and transmission electron microscopy.

1.b. Evaluate the impact of PLD on hepatic basolateral and canalicular transport of organic anions using two probe substrates, taurocholate and rosuvastatin.

Aim #2. Elucidate the hepatic basolateral efflux proteins involved in the active transport of enalaprilat.

Hypothesis: *Enalaprilat undergoes efflux by MRP3 and/or MRP4 across the hepatic basolateral membrane; enalaprilat transport is inhibited by rosuvastatin.*

2.a. Identify basolateral efflux protein(s) involved in the hepatic basolateral excretion of enalaprilat using isolated expression systems in the presence and absence of rosuvastatin and the prototypic pan-MRP inhibitor MK-571.

2.b. Quantify the impact of basolateral transport protein inhibition with rosuvastatin and MK-571 on the excretion of enalaprilat *in vitro* using human SCH.

Aim #3. Quantify the functional consequences of altered hepatic transport protein expression in patients with non-alcoholic steatohepatitis (NASH) on the systemic disposition of morphine and its hepatically-derived glucuronide metabolites.

Hypothesis: *Altered hepatic excretory transport function in NASH patients will increase maximal plasma concentrations of morphine glucuronides following intravenous morphine administration compared to healthy subjects*

3.a. Develop a physiologically-based mathematical model to predict morphine and morphine glucuronides disposition in healthy subjects and patients with NASH to inform design of a clinical study.

3.b. Quantify the effect of altered hepatic excretory transport function in patients with NASH compared to healthy subjects on the pharmacokinetics of morphine glucuronide conjugates.

3.c. Evaluate the impact of NASH severity on morphine glucuronides pharmacokinetic metrics.

REFERENCES

1. Agoston, M., Orsi, F., Feher, E., Hagymasi, K., Orosz, Z., Blazovics, A., Feher, J.Vereckei, A. 2003. Silymarin and vitamin E reduce amiodarone-induced lysosomal phospholipidosis in rats. Toxicology 190(3);231-41.

2. Kaloyanides, G. J.Pastoriza-Munoz, E. 1980. Aminoglycoside nephrotoxicity. Kidney international 18(5);571-82.

3. Oikawa, H., Maesawa, C., Sato, R., Oikawa, K., Yamada, H., Oriso, S., Ono, S., Yashima-Abo, A., Kotani, K., Suzuki, K.Masuda, T. 2005. Liver cirrhosis induced by long-term administration of a daily low dose of amiodarone: a case report. World journal of gastroenterology : WJG 11(34);5394-7.

4. de Lannoy, I. A.Pang, K. S. 1986. Presence of a diffusional barrier on metabolite kinetics: enalaprilat as a generated versus preformed metabolite. Drug metabolism and disposition: the biological fate of chemicals 14(5);513-20.

5. Pang, K. S., Cherry, W. F., Terrell, J. A.Ulm, E. H. 1984. Disposition of enalapril and its diacid metabolite, enalaprilat, in a perfused rat liver preparation. Presence of a diffusional barrier for enalaprilat into hepatocytes. Drug metabolism and disposition: the biological fate of chemicals 12(3);309-13.

6. Pang, K. S., Wang, P. J., Chung, A. Y.Wolkoff, A. W. 1998. The modified dipeptide, enalapril, an angiotensin-converting enzyme inhibitor, is transported by the rat liver organic anion transport protein. Hepatology (Baltimore, Md.) 28(5);1341-6.

7. Schwab, A. J., Barker, F., 3rd, Goresky, C. A.Pang, K. S. 1990. Transfer of enalaprilat across rat liver cell membranes is barrier limited. The American journal of physiology 258(3 Pt 1);G461-75.

8. Ulm, E. H. 1983. Enalapril maleate (MK-421), a potent, nonsulfhydryl angiotensin-converting enzyme inhibitor: absorption, disposition, and metabolism in man. Drug metabolism reviews 14(1);99-110.

9. Sookoian, S., Gianotti, T. F., Rosselli, M. S., Burgueno, A. L., Castano, G. O.Pirola, C. J. 2011. Liver transcriptional profile of atherosclerosis-related genes in human nonalcoholic fatty liver disease. Atherosclerosis 218(2);378-85.

10. Mannisto, T. K., Karvonen, K. E., Kerola, T. V.Ryhanen, L. J. 2001. Inhibitory effect of the angiotensin converting enzyme inhibitors captopril and enalapril on the conversion of procollagen to collagen. Journal of hypertension 19(10);1835-9.

11. Torres, D. M., Jones, F. J., Shaw, J. C., Williams, C. D., Ward, J. A.Harrison, S. A. 2011. Rosiglitazone versus rosiglitazone and metformin versus rosiglitazone and losartan in the treatment of nonalcoholic steatohepatitis in humans: a 12-month randomized, prospective, open-label trial. Hepatology 54(5);1631-9.

12. Tikkanen, M. J., Fayyad, R., Faergeman, O., Olsson, A. G., Wun, C. C., Laskey, R., Kastelein, J. J., Holme, I.Pedersen, T. R. 2013. Effect of intensive lipid lowering with atorvastatin on cardiovascular outcomes in coronary heart disease patients with mild-to-moderate baseline elevations in alanine aminotransferase levels. International journal of cardiology.

13. Sanyal, A. J., Chalasani, N., Kowdley, K. V., McCullough, A., Diehl, A. M., Bass, N. M., Neuschwander-Tetri, B. A., Lavine, J. E., Tonascia, J., Unalp, A., Van Natta, M., Clark, J., Brunt, E. M., Kleiner, D. E., Hoofnagle, J. H.Robuck, P. R. 2010. Pioglitazone, vitamin E, or placebo for nonalcoholic steatohepatitis. The New England journal of medicine 362(18);1675-85.

14. Nakahara, T., Hyogo, H., Kimura, Y., Ishitobi, T., Arihiro, K., Aikata, H., Takahashi, S.Chayama, K. 2012. Efficacy of rosuvastatin for the treatment of non-alcoholic steatohepatitis with dyslipidemia: An open-label, pilot study. Hepatology research : the official journal of the Japan Society of Hepatology 42(11);1065-72.

15. Fisher, C. D., Lickteig, A. J., Augustine, L. M., Ranger-Moore, J., Jackson, J. P., Ferguson, S. S.Cherrington, N. J. 2009. Hepatic cytochrome P450 enzyme alterations in humans with progressive stages of nonalcoholic fatty liver disease. Drug metabolism and disposition: the biological fate of chemicals 37(10);2087-94.

16. Hardwick, R. N., Fisher, C. D., Canet, M. J., Scheffer, G. L.Cherrington, N. J. 2011. Variations in ATP-binding cassette transporter regulation during the progression of human nonalcoholic fatty liver disease. Drug metabolism and disposition: the biological fate of chemicals 39(12);2395-402.

17. Hardwick, R. N., Ferreira, D. W., More, V. R., Lake, A. D., Lu, Z., Manautou, J. E., Slitt, A. L.Cherrington, N. J. 2013. Altered UDP-glucuronosyltransferase and sulfotransferase expression and function during progressive stages of human nonalcoholic fatty liver disease. Drug metabolism and disposition: the biological fate of chemicals 41(3);554-61.

18. Lake, A. D., Novak, P., Fisher, C. D., Jackson, J. P., Hardwick, R. N., Billheimer, D. D., Klimecki, W. T.Cherrington, N. J. 2011. Analysis of global and absorption, distribution, metabolism, and elimination gene expression in the progressive stages of human nonalcoholic fatty liver disease. Drug metabolism and disposition: the biological fate of chemicals 39(10);1954-60.

CHAPTER 2. Identification of Hepatic Phospholipidosis Inducers in Sandwich-Cultured Rat Hepatocytes, a Physiologically Relevant Model, Reveals Altered Basolateral Uptake and Biliary Excretion of Anionic Probe Substrates

Introduction

Drug-induced phospholipidosis (PLD) manifests as lysosomal accumulation of phospholipids, resulting in development of concentric lamellar bodies visible via the gold standard method, electron microscopy[1]. Predictive computer models of PLD potential have suggested that most precipitant drugs are weakly basic and have amphiphilic features. These cationic amphiphilic drugs (CADs), including antiarrhythmics, antidepressants, and anti-infectives, are able to cross the lysosomal membrane where they become protonated at low physiologic pH (pH 3-5) and trapped due to an inability to exit the lysosomal compartment following protonation. Lysosomal trapping and PLD have been observed in many different tissue/cell types including lung, nerve, kidney, and liver cells[2-8]. Several mechanisms have been proposed for CAD-induced PLD, including inhibition of lysosomal phospholipases, inhibition of H^+-ATPases and direct binding to the phospholipids, resulting in inert phospholipid-drug complexes[9,10].

PLD has been associated with hepatic/alveolar fibrosis (amiodarone), renal tubular toxicity (gentamicin), and QT-wave prolongation secondary to inhibition of hERG channels in the heart (tamoxifen)[5,6,11-13]. Accordingly, significant industrial and regulatory attention, including the formation of the FDA sponsored PLD Working group in 2004, has been devoted to developing sensitive and specific

---

This work has been presented, in part, at the SOT Annual Meeting, San Antonio, TX, March 10-14, 2013 and has been published as Ferslew BC and Brouwer KL, Identification of Hepatic Phospholipidosis Inducers in Sandwich-Cultured Rat Hepatocytes, a Physiologically Relevant Model, Reveals Altered Basolateral Uptake and Biliary Excretion of Anionic Probe Substrates, *Toxicological Sciences,* 2014, 139 (1): 99-107, reprinted by permission of Oxford University Press and is presented in the style of that journal.

models to detect PLD during pre-clinical drug development. In response, multiple computer, non-cell, and cell-based models have been evaluated. Computer models utilizing molecular structure, as well as non-cell-based and cell-based models focusing on altered gene expression or lysosomal uptake and retention of fluorescent probes (e.g., Nile red, LysoTracker Red®), have shown modest sensitivity and specificity[8,14-17]. Unfortunately, computer or non-cell based models may not be predictive of PLD induced by metabolites, and often fail to predict which tissue(s) will be affected due to the absence of metabolizing enzymes and transport processes. Methods to visualize lysosomal compartments within the cell to screen for PLD potential are of particular interest to reduce the burden of confirmatory studies with electron microscopy.

Although most PLD-inducing drugs contain a cationic amphiphilic moiety, metabolically-deficient models may not accurately predict PLD liability of metabolites. Sandwich-cultured hepatocytes (SCH) are fully differentiated, express relevant metabolizing enzymes and hepatic transporters, and can be used to assess hepatic transport processes involved in the clearance of endogenous and exogenous substrates [18-22]. Therefore, this established system was selected for subsequent investigations to test the hypothesis that SCH represent a sensitive and selective model to screen for drug-induced hepatic PLD. Lysosomal dysfunction secondary to PLD may alter the cycling of transporters to and from the relevant membranes (basolateral or canalicular), resulting in altered hepatic transporter-mediated clearance of susceptible compounds.

The goal of the present study was to determine whether primary rat SCH can serve as a sensitive and selective model to evaluate hepatic drug-induced PLD and determine if PLD alters hepatic transport processes. Structurally diverse drugs that cause PLD to varying degrees by distinct mechanisms were selected for investigation. First, lysosomal localization was determined using LysoTracker Red®. Second, the presence or absence of PLD was confirmed using transmission electron microscopy. Third, hepatic uptake by sodium-taurocholate cotransporting polypeptide (Ntcp) and organic anion-transporting polypeptides (Oatps), and biliary excretion by the bile salt export pump (Bsep), multidrug resistance-associated protein 2 (Mrp2), and breast cancer resistance protein (Bcrp) were evaluated using taurocholate

(TC) and rosuvastatin (RSV) as probes for Ntcp/Bsep and Oatps/Mrp2/Bcrp, respectively. Results demonstrated that rat SCH are a promising screening tool for drug-induced PLD.

Methods

Chemicals and Reagents.

Dexamethasone, TC, amiodarone (AMD), chloroquine (CHQ), desipramine (DES), azithromycin (AZI), gentamicin (GTM), Hanks' balanced salt solution (HBSS; standard buffer), Ca^{2+}/Mg^{2+}-free HBSS (Ca^{2+}-free buffer), and thiazolyl blue tetrazolium bromide were purchased from Sigma-Aldrich (St. Louis, MO). Rosuvastatin (RSV) was purchased from Toronto Research Chemicals (Toronto, Ontario, Canada). [^{3}H]TC (1 mCi/mL; >97% purity) and [^{3}H]RSV (1 mCi/mL; >97% purity) were purchased from PerkinElmer (Waltham, MA) and American Radiolabeled Chemicals (St. Louis, MO), respectively. Dulbecco's Modified Eagle's Medium (DMEM), fetal bovine serum, penicillin/streptomycin and insulin were purchased from Gibco (Grand Island, NY). Minimum essential medium, nonessential amino acids, and LysoTracker Red® were purchased from Invitrogen (Carlsbad, CA). BioCoat™ culture plates, BioCoat™ glass inserts, Matrigel™ extracellular matrix, and insulin/transferrin/selenium culture supplement were purchased from BD Biosciences (Bedford, MA). All other chemicals and reagents were of analytical grade and readily available from commercial sources.

Animals

Male Wistar wild-type (WT) rats (250-350 g) from Charles River Labs (Wilmington, MA) were used as hepatocyte donors. Rats were allowed free access to water and food and were acclimated for a minimum of one week prior to experimentation. All animal procedures complied with the guidelines of the Institutional Animal Care and Use Committee at the University of North Carolina at Chapel Hill (Chapel Hill, NC). All procedures were performed while rats were under full anesthesia with ketamine/xylazine (140/8 mg/kg i.p.).

Culture of Primary Rat Hepatocytes in Sandwich Configuration.

Primary rat hepatocytes were isolated and cultured as described previously[22]. Briefly, hepatocytes were seeded at a density of 1.75 x 10^6 cells/well onto six-well BioCoat™ plates. Approximately 24 h

later, hepatocytes were overlaid with 2 ml of 0.25 mg/ml BD Matrigel™ basement membrane matrix in DMEM. Hepatocytes were cultured for 4 days to allow formation of canalicular networks before experimentation; medium was changed daily. For single ('acute') administration experiments, the 2-4 day feeding medium was not supplemented with DMSO or PLD-inducing drugs. For multiple ('chronic') administration experiments, the feeding medium used on days 2-4 (48 h) of culture was supplemented with 0.1% DMSO (vehicle control, used to solubilize PLD-inducing drugs), AMD (1, 10, or 50 µM), CHQ (1 or 10 µM), DES (1, 10, or 50 µM), AZI (1, 10, or 50 µM), or GTM (1 mM). The concentrations of the PLD-inducing drugs selected for investigation were based on in vivo plasma concentrations and estimated hepatic concentrations[23].

MTT Assay

Following incubation of rat SCH with the PLD inducers or vehicle control at 37°C for 48 h, the medium was aspirated, and 2 mL of 0.5 mg/mL thiazolyl blue tetrazolium bromide solution in plain DMEM was added. After 30 min, the medium was aspirated, and 1 mL of 0.04 M HCL in isopropanol was added to solubilize the cells. Lysates were analyzed by absorbance at 570 nm and 650 nm. SCH treated for 48 h with 100 µM CHQ and 0.1% DMSO served as positive and negative/vehicle controls, respectively.

LysoTracker Red® Localization in Rat Sandwich-Cultured Hepatocytes

On day 4, the medium from SCH treated with PLD-inducing drugs or vehicle control was aspirated and replaced with fresh medium containing 100 nM LysoTracker Red®. After 30 min at 37°C, wells were washed rapidly twice with warm Dulbecco's phosphate buffered saline, and both light and fluorescent (excitation/emission wavelengths of 577/590 nm) digital images were captured using a Zeiss Axiovert 200TV (Thornwood, NY) inverted phase contrast microscope. Images were analyzed using ImageJ software (free online at rsbweb.nih.gov).

Electron Microscopy of Rat Sandwich-Cultured Hepatocytes

BioCoat™ glass inserts were placed in the BioCoat™ plates, and hepatocytes were cultured as described above. The medium was aspirated on day 4, when SCH were fixed for 1 h with 2 mL of 2.5%

gluteraldehyde/1% tannic acid in 0.1 M sodium cacodylate (pH 7.3). The fixation solution was aspirated, and SCH were washed with 0.1 M cacodylate solution 3 times for 5 min each. SCH were post-fixed with 1% osmium tetroxide in 0.1 M cacodylate for 20 min, then rinsed 3 times with distilled water and 2 times with 50% ethanol for 5 min each. SCH were stained further with 2% uranyl acetate in 50% ethanol for 30 min. Finally, the SCH were dehydrated with increasing concentrations of ethanol (2 times with 70, 80, 90 and 95%, and then 3 times with 100%, for 5 min each), infiltrated with propylene oxide [1:1, 2:1, and 3:1 ratios of Epon 812 (Hatfield, PA) to propylene oxide for 1 h each], and finished with pure Epon for 1 h. The glass inserts were removed from the BioCoat™ plates, embedded in Epon 812, and allowed to cure at 60°C for at least 18 h. The glass inserts were dissolved with concentrated hydrofluoric acid and thinly sectioned on a Leica Ultracut ultramicrotome (Leica Microsystems, Buffalo Grove, IL). Sections were placed on copper grids and restained with uranyl acetate and lead citrate, after which digital images were captured using a Tecnai 12 electron microscope (Hillsboro, OR). Multiple SCH sections from each treatment were imaged using a Gatan Multiscan digital camera (Pleasanton, CA).

Probe Substrate Transport in Rat Sandwich-Cultured Hepatocytes

Determination of the uptake and biliary excretion of the probe substrates TC (Ntcp/Bsep) and RSV (Oatp/Mrp2/Bcrp) in rat SCH was described previously[24]. Prior studies have established that these probes are metabolically stable in rat SCH[25,26]. Briefly, day 4 SCH were washed twice with 2 ml of warm Ca^{2+}-containing HBSS (standard; cells + bile) or Ca^{2+}-free HBSS (cells) and then incubated with the same buffer for 10 min at 37°C. Subsequently, SCH were incubated with 1.5 ml of standard HBSS containing [^{3}H]TC (1 μM; 100 nCi/ml) or [^{3}H]RSV (1 μM; 100 nCi/ml) for 10 min. For acute dosing studies, PLD-inducing drugs (AMD 50 μM, CHQ 10 μM, DES 50 μM, AZI 50 μM, or GTM 1 mM) or vehicle control (0.1% DMSO) also were added to the incubation medium along with the probe substrates. After 10 min, SCH were washed 3 times with ice-cold standard HBSS and lysed with 0.5% Triton X-100 in phosphate-buffered saline. Radioactivity in cell lysates was quantified by liquid scintillation spectroscopy (Packard Tricarb; PerkinElmer, Waltham, MA). Accumulation of TC and RSV was normalized to hepatocyte total protein using a BCA protein assay (Pierce Chemical, Rockford, IL). The biliary excretion index (BEI) and

in vitro biliary clearance ($CL_{biliary}$; ml/min/kg) were calculated using B-CLEAR® technology (Qualyst Transporter Solutions, LCC, Durham, NC) based on the following equations:

Equation 1: $$BEI = \frac{Accumulation_{cells+bile} - Accumulation_{cells}}{Accumulation_{cells+bile}}$$

Equation 2: $$CL_{biliary} = \frac{Accumulation_{cells+bile} - Accumulation_{cells}}{AUC_{medium\ 0\text{-}T}}$$

where $AUC_{medium\ 0\text{-}T}$ represents the product of the incubation time (T) and the initial TC or RSV concentration in the medium[22,24,26]. $CL_{biliary}$ units were converted to ml/min/kg body weight based on previously reported values for protein content in liver tissue (200 mg/g liver weight) and liver weight (40 g/kg body weight)[27].

Data Analysis

The impact of chronic or acute incubation with PLD-inducing drugs on total (cells + bile) and cellular accumulation, BEI and $CL_{biliary}$ was determined using one-way ANOVA with Dunnett's *post-hoc* test. A p-value of <0.05 was considered significant for all tests. All data are presented as mean ± standard error of the mean (SEM) unless otherwise indicated.

Results

Rat Sandwich-Cultured Hepatocyte Toxicity

Initial pilot experiments showed that SCH incubated for 48 h with medium supplemented with 50-100 µM CHQ exhibited complete toxicity based on the MTT assay. Thus, SCH incubated for 48 h with DMEM containing 100 µM CHQ or 0.1% DMSO were selected as positive and negative (vehicle) controls, respectively. SCH treated with PLD-inducing drugs exhibited minimal to moderate toxicity (Fig 2.1): 8-43% for AMD, 17-29% for CHQ, 2-55% for DES, 19-43% for AZI, and 26% for GTM. Toxicity increased as the dosing concentration increased for AMD, CHQ, DES, and AZI.

LysoTracker® Red Localization

LysoTracker Red® localization was used to assess qualitatively the size and number of lysosomes in SCH treated with PLD-inducing drugs. Under standard conditions, LysoTracker Red® (depicted as green fluorescence for contrast, Figure 2.2) localized in vesicles close to the canalicular membrane. Exposure for 48 h to AMD, CHQ, DES, and AZI resulted in notably increased lysosomal size and/or number relative to control (Figure 2.2), suggestive of PLD. Increased background fluorescence was observed only with CHQ treatment. Interestingly, GTM-treated SCH did not exhibit increased lysosomal number or size.

Transmission Electron Microscopy

All major cellular organelles including the nucleus, rough/smooth endoplasmic reticulum, Golgi apparatus, and tight junctions between hepatocytes were visualized in each SCH preparation. Inspection of SCH treated with 0.1% DMSO and 1 mM GTM by electron microscopy showed a large number of mitochondria, glycogen granules, and small lysosomes; no pathologic lysosomes and only a few lipid droplets were observed. Inspection of SCH treated with AMD (50 µM), CHQ (10 µM), DES (50 µM), and AZI (50 µM) showed increased lipid droplet formation and enlarged lysosomal compartments with electron-dense deposits and membranous structures resembling laminar body inclusions, indicative of PLD (Figure 2.3).

Accumulation and Excretion of Taurocholate and Rosuvastatin in Rat SCH Following Acute (10-min) Exposure to PLD-Inducing Drugs

Total and cellular accumulation, BEI, and *in vitro* $CL_{biliary}$ of TC and RSV were compared in SCH after acute exposure to PLD-inducing drugs. Following a 10-min incubation of 1 µM [^{3}H]TC or [^{3}H]RSV with vehicle control (0.1% DMSO), AMD (50 µM), CHQ (10 µM), DES (50 µM), AZI (50 µM), or GTM (1 mM), no significant differences in total accumulation (cells + bile) or cellular accumulation of TC or RSV were observed. Likewise, no statistically significant differences were observed for BEI or *in vitro* $CL_{biliary}$ of either TC or RSV (Figure 2.4).

Accumulation and Excretion of Taurocholate and Rosuvastatin in Rat SCH Following Chronic (48-h) Exposure to PLD-Inducing Drugs

Accumulation of [^{3}H]TC and [^{3}H]RSV in cells + bile and cells, as well as the *in vitro* $CL_{biliary}$, were compared between SCH treated for 48 h with vehicle control or PLD-inducing drugs following a 10-min incubation with 1 µM [^{3}H]TC or [^{3}H]RSV. Total accumulation of TC (cells + bile) significantly decreased with increasing concentrations of AMD, CHQ, DES, and AZI (Figure 2.5, left panel). At the highest concentrations tested, TC total (cells + bile) accumulation decreased by 87.2% ± 1.8%, 71.8% ± 3.2%, 73.4% ± 0.9, and 75.3% ± 3.6% compared to control for AMD, CHQ, DES, and AZI, respectively. TC BEI significantly decreased at the highest tested concentrations of AMD, DES, and AZI (Table 2.1). At the highest concentrations tested, the TC $CL_{biliary}$ decreased by 92.3% ± 1.4%, 76.7% ± 3.4%, 81.0% ± 1.2%, and 89.3% ± 5.1% compared to control for AMD, CHQ, DES, and AZI, respectively. In contrast, TC cellular accumulation was not affected by any treatment (Figure 2.5, left panel).

Similarly, total (cells + bile) accumulation of RSV significantly decreased with increasing concentrations of AMD, CHQ, DES, and AZI (Figure 2.5, right panel). At the highest concentrations tested, RSV total (cells + bile) accumulation decreased by 89.2% ± 0.4%, 58.8% ± 2.2%, 85.2% ± 2.5%, and 77.1% ± 0.7% compared with control for AMD, CHQ, DES, and AZI, respectively. In contrast to TC, cellular RSV accumulation decreased with increasing concentrations of AMD, CHQ, DES, and AZI (Figure 2.5, right panel). At the highest concentrations tested, RSV cellular accumulation significantly decreased by 89.5 ± 1.8%, 68.9 ± 4.3%, 76.8 ± 1.3%, and 69.4 ± 2.5% compared with control for AMD, CHQ, DES and AZI, respectively. $CL_{biliary}$ of RSV decreased whereas BEI was unaffected by increasing concentrations of AMD, CHQ, DES, and AZI (Table 2.1). At the highest concentrations tested, RSV $CL_{biliary}$ decreased by 88.6% ± 2.8%, 50.5% ± 6.1%, 89.7% ± 2.5% and 81.4% ± 2.2%, compared with control for AMD, CHQ, DES and AZI, respectively. The kidney-specific PLD-inducer, GTM, had no effect on total accumulation, cellular accumulation, BEI or *in vitro* $CL_{biliary}$ of TC or RSV (Figure 2.5, Table 2.1).

Discussion

The primary goal of this study was to determine whether rat SCH could be used to detect hepatic drug-induced PLD. In addition, studies were designed to assess whether lysosomal dysfunction altered vectorial transport of two metabolically stable probe compounds[25,28], TC and RSV. Five structurally different prototypic PLD-inducing drugs with distinct mechanisms were selected: AMD, CHQ, DES, AZI, and GTM. All of these drugs are known to cause hepatic PLD, with the exception of GTM, which induces PLD in kidney at human-relevant physiologic concentrations. Maximal plasma concentrations (C_{max}) following a standard does of AMD (~4.3 μM), CHQ (~3.7 μM), DES (~1.9 μM), AZI (~1.1 μM) and GTM (~12 μM) were considered in selection of the lowest concentration of PLD-inducing drugs (1 μM) for investigation in the SCH system[23]. Concentrations that approximated 10- and 50-fold above the C_{max} values also were examined because these drugs accumulate in hepatocytes. The high concentration of GTM was selected as a negative control to demonstrate that hepatic PLD would not be detected, and no changes in transport of anionic substrates would be observed. Experiments with the well-established lysosomal imaging probe, LysoTracker Red®, demonstrated that a 48-h exposure of rat SCH to each of the four hepatic PLD inducers resulted in a qualitative increase in the number and/or size of lysosomal compartments, indicative of PLD (Figure 2.2). The increased background noted in SCH treated with CHQ likely was due to an increase in lysosomal pH associated with CHQ's distinct mechanism of action (inhibition of H^+-ATPase)[29,30]. Nonetheless, distinct and enlarged lysosomal compartments could be visualized in SCH treated with CHQ. As anticipated, GTM had no effect on either lysosomal number or size (Figure 2.2).

Transmission electron microscopy of rat SCH exposed for 48 h to PLD-inducing drugs enabled visualization of all major organelles; enlarged lysosomal compartments with laminar figures diagnostic of PLD were observed in SCH treated with all PLD-inducing drugs except for GTM, which had no effect (Figure 2.3). In agreement with previous publications, these results suggest that LysoTracker Red® may be a useful tool for screening novel drug candidates in SCH with hepatic PLD potential[16] (Figures 2.2 and 2.3). Transmission electron microscopy also showed that both the cellular and organelle membranes were

grossly intact. Membrane disruption has been reported in rats treated with high doses of AMD (150 mg/kg body weight per day) for three weeks[11]. However, at the concentrations investigated for all PLD-inducing drugs, there was no evidence of membrane disruption. Therefore, the mitochondrial toxicity observed in the current work, as measured by MTT formazan formation, does not appear to be due to membrane disruption.

An additional benefit of the rat SCH model is the ability to assess transporter-mediated vectorial flux of compounds through the hepatocyte into bile. Two probe substrates were selected to evaluate distinct transporters on the sinusoidal (blood side) and canalicular (bile side) membranes of hepatocytes. TC is a metabolically stable bile acid that is transported efficiently into the hepatocyte via Ntcp, and excreted into bile via Bsep; RSV is taken up by Oatps and possibly by Ntcp, and excreted into bile by Mrp2 and Bcrp[24,31-35]. Changes in cellular accumulation and biliary excretion of probe compounds were examined to determine potential transporter-mediated alterations due to 'acute' (10-min exposure with no pre-treatment) and 'chronic' (48-h pre-treatment) administration of PLD inducers (Figures 2.4 and 2.5) [22]. Alterations due to PLD-inducing drugs might be attributed to acute effects, or due to indirect effects, which would be present only after chronic administration. Following acute administration of each PLD-inducing drug, no significant changes were observed in TC or RSV total accumulation, cellular accumulation, BEI or $CL_{biliary}$ (Figure 2.4, Table 2.1). However, following chronic administration, all drugs that induced PLD decreased $CL_{biliary}$ of TC and RSV, while cellular accumulation was reduced only for RSV. Reduced total accumulation, BEI and $CL_{biliary}$ of TC with no change in cellular accumulation (in other words, reduced excretion of TC into the bile compartment) secondary to PLD is consistent with canalicular transporter dysfunction, specifically reduced Bsep-mediated biliary excretion in the case of TC[36]. Decreased RSV total (cells + bile) and cellular accumulation as well as $CL_{biliary}$, but no change in BEI, is consistent with decreased Oatp-mediated uptake[36]. Importantly, following chronic GTM administration, PLD was not observed in rat SCH, and no differences in TC or RSV disposition were noted (Figure 2.5 and Table 2.1). Taken together, results from the acute- and chronic- exposure experiments indicated that PLD leads to functional changes in hepatic Oatp- and Bsep-mediated uptake

and excretion, respectively. Results also suggest that Ntcp function is maintained and that RSV biliary excretion, mediated by both Mrp2 and Bcrp, does not appear to be altered by PLD. Lysosomal-associated alterations in the disposition and toxicity of drugs have been reported previously. For example, the impact of lysosomal pH-dependent entrapment on the cytotoxicity of chemotherapeutics with and without susceptibility to lysosomal sequestration was examined[29]. When pH-dependent lysosomal sequestration was inhibited by CHQ, cellular toxicity of the lysosomotropic chemotherapeutic agent was enhanced, whereas no effect on toxicity was observed for the non-lysosomotropic chemotherapeutic agent. Additionally, exacerbation of the PLD phenotype with sucrose increased the uptake and lysosomal sequestration of CHQ, which was not observed when PLD induction was inhibited by bafilomycin A1[37]. Therefore, lysosomal enlargement and sequestration appear to alter active anionic transport processes based on the present results, as well as the intracellular disposition of lysosomotropic drugs[8,37].

Some limitations are associated with this work. First, compared to many published studies using immortalized cell lines to screen PLD potential, fewer drugs have been studied in rat SCH. Although this model is lower throughput than typical immortalized cell line screens, development of hepatic-specific PLD with drugs that exhibited a range of hepatic induction potency was demonstrated (AMD and CHQ are strong inducers while DES and AZI are weaker hepatic PLD inducers). Additionally, the PLD-inducing drugs investigated in this study affect different organ systems *in vivo* and have diverse postulated induction mechanisms *in vivo* (i.e. inhibition of phospholipid metabolism with AMD, inhibition of H^+-ATPase with CHQ). The present data indicate that rat SCH are both a sensitive and specific model for identification of drugs that cause hepatic PLD. All drugs tested, including GTM, caused mild to moderate toxicity based on the MTT assay (Figure 2.1). Although drug-induced PLD has not been associated directly with cellular toxicity, the altered anionic transport observed may be related to toxicity. Interestingly, moderate toxicity was observed with GTM although no PLD or change in TC or RSV transport was apparent. This supports the hypothesis that altered TC and RSV transport secondary to PLD are not likely caused solely by the mild to moderate toxicity observed. Additionally, preliminary

data indicate that streptomycin, an aminoglycoside included in the feeding medium that is structurally similar to GTM, did not induce PLD at the low concentrations utilized (172nM).

Drug-induced PLD leads to impaired phospholipid storage, metabolism, and excretion[1]. Several model systems have been evaluated to identify PLD-inducing drugs as early as possible during drug development. As such, PLD potential often is identified during early preclinical development and is handled on a case-by-case basis depending on the severity and target organ(s) affected[38]. This case-based assessment poses challenges due to a limited understanding of the (presumed) association between PLD and organ toxicity. Consequently, increasing attention has been placed on developing sensitive and specific models to predict drug-induced PLD, thereby avoiding late-stage failures due to unanticipated toxicities. A report by leading investigators encourages selection of lead drug candidates based on *in silico* and/or *in vitro* screening for PLD potential[38]. Multiple *in silico* quantitative structure-activity relationship (QSAR) and *in vitro* non-cell-based and cell-based models have been developed[2,14-16,39-41]. These screening methods have identified primarily cationic amphiphilic drugs as causal agents, with a few notable exceptions (i.e., GTM). Although invaluable for initial risk-benefit analyses, these models have limitations. *In vitro* (and by inference *in silico*) models that lack metabolic and transport processes may underestimate PLD potential, as evidenced by the observation that isolated, metabolically active murine macrophages exhibited greater sensitivity and specificity to predict PLD *in vivo* than immortalized cell lines[41]. Additionally, organ-specific transporters and metabolizing enzymes are germane to assess PLD potential *in vitro* as well as facilitate accurate *in vivo* extrapolation to target organs. SCH are a well-established system expressing hepatic-relevant metabolizing enzymes and transport proteins, which may aid in increasing assay sensitivity to identify drugs that require metabolism or transport to induce hepatic PLD[22].

In conclusion, rat SCH are a viable system to evaluate drug-induced hepatic PLD. Initial screening with LysoTracker Red® localization would increase throughput. PLD screening should be evaluated in a metabolically-capable cell-based model such as SCH, which provide the additional benefit that transport processes can be evaluated concurrently. The present data reveal for the first time that drug-

induced hepatic lysosomal dysfunction may be associated with altered Oatp- and Bsep-mediated anionic transport. Clearly, PLD-inducing drugs may exhibit many toxicologic endpoints that require further preclinical evaluation.

REFERENCES

1. Reasor, M. J., Ogle, C. L.Kacew, S. 1989. Amiodarone-induced pulmonary toxicity in rats: biochemical and pharmacological characteristics. Toxicology and applied pharmacology 97(1);124-33.

2. Shahane, S. A., Huang, R., Gerhold, D., Baxa, U., Austin, C. P.Xia, M. 2013. Detection of Phospholipidosis Induction: A Cell-Based Assay in High-Throughput and High-Content Format. Journal of biomolecular screening.

3. Reasor, M. J.Kacew, S. 1996. An evaluation of possible mechanisms underlying amiodarone-induced pulmonary toxicity. Proceedings of the Society for Experimental Biology and Medicine. Society for Experimental Biology and Medicine (New York, N.Y.) 212(4);297-304.

4. Ruben, Z., Dodd, D. C., Rorig, K. J.Anderson, S. N. 1989. Disobutamide: a model agent for investigating intracellular drug storage. Toxicology and applied pharmacology 97(1);57-71.

5. Oikawa, H., Maesawa, C., Sato, R., Oikawa, K., Yamada, H., Oriso, S., Ono, S., Yashima-Abo, A., Kotani, K., Suzuki, K.Masuda, T. 2005. Liver cirrhosis induced by long-term administration of a daily low dose of amiodarone: a case report. World journal of gastroenterology : WJG 11(34);5394-7.

6. Kaloyanides, G. J.Pastoriza-Munoz, E. 1980. Aminoglycoside nephrotoxicity. Kidney international 18(5);571-82.

7. Logan, R., Kong, A.Krise, J. P. 2013. Evaluating the Roles of Autophagy and Lysosomal Trafficking Defects in Intracellular Distribution-Based Drug-Drug Interactions Involving Lysosomes. Journal of pharmaceutical sciences.

8. Ndolo, R. A., Jacobs, D. T., Forrest, M. L.Krise, J. P. 2010. Intracellular Distribution-based Anticancer Drug Targeting: Exploiting a Lysosomal Acidification Defect Associated with Cancer Cells. Molecular and cellular pharmacology 2(4);131-136.

9. Reasor, M. J., Hastings, K. L.Ulrich, R. G. 2006. Drug-induced phospholipidosis: issues and future directions. Expert opinion on drug safety 5(4);567-83.

10. Joshi, U. M., Rao, P., Kodavanti, S., Lockard, V. G.Mehendale, H. M. 1989. Fluorescence studies on binding of amphiphilic drugs to isolated lamellar bodies: relevance to phospholipidosis. Biochimica et biophysica acta 1004(3);309-20.

11. Agoston, M., Orsi, F., Feher, E., Hagymasi, K., Orosz, Z., Blazovics, A., Feher, J.Vereckei, A. 2003. Silymarin and vitamin E reduce amiodarone-induced lysosomal phospholipidosis in rats. Toxicology 190(3);231-41.

12. Sun, H., Xia, M., Shahane, S. A., Jadhav, A., Austin, C. P.Huang, R. 2013. Are hERG channel blockers also phospholipidosis inducers? Bioorganic & medicinal chemistry letters 23(16);4587-90.

13. Xia, M., Shahane, S. A., Huang, R., Titus, S. A., Shum, E., Zhao, Y., Southall, N., Zheng, W., Witt, K. L., Tice, R. R.Austin, C. P. 2011. Identification of quaternary ammonium compounds as potent inhibitors of hERG potassium channels. Toxicology and applied pharmacology 252(3);250-8.

14. Pelletier, D. J., Gehlhaar, D., Tilloy-Ellul, A., Johnson, T. O.Greene, N. 2007. Evaluation of a published in silico model and construction of a novel Bayesian model for predicting phospholipidosis inducing potential. Journal of chemical information and modeling 47(3);1196-205.

15. Ploemen, J. P., Kelder, J., Hafmans, T., van de Sandt, H., van Burgsteden, J. A., Saleminki, P. J.van Esch, E. 2004. Use of physicochemical calculation of pKa and CLogP to predict phospholipidosis-inducing potential: a case study with structurally related piperazines. Experimental and toxicologic pathology : official journal of the Gesellschaft fur Toxikologische Pathologie 55(5);347-55.

16. Kazmi, F., Hensley, T., Pope, C., Funk, R. S., Loewen, G. J., Buckley, D. B.Parkinson, A. 2013. Lysosomal sequestration (trapping) of lipophilic amine (cationic amphiphilic) drugs in immortalized human hepatocytes (Fa2N-4 cells). Drug metabolism and disposition: the biological fate of chemicals 41(4);897-905.

17. Atienzar, F., Gerets, H., Dufrane, S., Tilmant, K., Cornet, M., Dhalluin, S., Ruty, B., Rose, G.Canning, M. 2007. Determination of phospholipidosis potential based on gene expression analysis in HepG2 cells. Toxicological sciences : an official journal of the Society of Toxicology 96(1);101-14.

18. Chandra, P., Lecluyse, E. L.Brouwer, K. L. 2001. Optimization of culture conditions for determining hepatobiliary disposition of taurocholate in sandwich-cultured rat hepatocytes. In vitro cellular & developmental biology. Animal 37(6);380-5.

19. LeCluyse, E. L., Bullock, P. L., Parkinson, A.Hochman, J. H. 1996. Cultured rat hepatocytes. Pharmaceutical biotechnology 8;121-59.

20. Liu, X., LeCluyse, E. L., Brouwer, K. R., Lightfoot, R. M., Lee, J. I.Brouwer, K. L. 1999. Use of Ca2+ modulation to evaluate biliary excretion in sandwich-cultured rat hepatocytes. The Journal of pharmacology and experimental therapeutics 289(3);1592-9.

21. Li, A. P. 1997. Primary hepatocyte cultures as an in vitro experimental model for the evaluation of pharmacokinetic drug-drug interactions. Advances in pharmacology (San Diego, Calif.) 43;103-30.

22. Swift, B., Pfeifer, N. D.Brouwer, K. L. 2010. Sandwich-cultured hepatocytes: an in vitro model to evaluate hepatobiliary transporter-based drug interactions and hepatotoxicity. Drug metabolism reviews 42(3);446-71.

23. Micromedex. 2014. Micromedex.

24. Abe, K., Bridges, A. S.Brouwer, K. L. 2009. Use of sandwich-cultured human hepatocytes to predict biliary clearance of angiotensin II receptor blockers and HMG-CoA reductase inhibitors. Drug metabolism and disposition: the biological fate of chemicals 37(3);447-52.

25. Schwarz, L. R., Burr, R., Schwenk, M., Pfaff, E.Greim, H. 1975. Uptake of taurocholic acid into isolated rat-liver cells. European journal of biochemistry / FEBS 55(3);617-23.

26. Pfeifer, N. D., Yang, K.Brouwer, K. L. 2013. Hepatic basolateral efflux contributes significantly to rosuvastatin disposition I: characterization of basolateral versus biliary clearance using a novel

protocol in sandwich-cultured hepatocytes. The Journal of pharmacology and experimental therapeutics 347(3);727-36.

27. Davies, B.Morris, T. 1993. Physiological parameters in laboratory animals and humans. Pharmaceutical research 10(7);1093-5.

28. Pfeifer, N. D., Bridges, A. S., Ferslew, B. C., Hardwick, R. N.Brouwer, K. L. 2013. Hepatic basolateral efflux contributes significantly to rosuvastatin disposition II: characterization of hepatic elimination by basolateral, biliary, and metabolic clearance pathways in rat isolated perfused liver. The Journal of pharmacology and experimental therapeutics 347(3);737-45.

29. Ndolo, R. A., Forrest, M. L.Krise, J. P. 2010. The role of lysosomes in limiting drug toxicity in mice. The Journal of pharmacology and experimental therapeutics 333(1);120-8.

30. Goldman, S. D., Funk, R. S., Rajewski, R. A.Krise, J. P. 2009. Mechanisms of amine accumulation in, and egress from, lysosomes. Bioanalysis 1(8);1445-59.

31. Kitamura, S., Maeda, K., Wang, Y.Sugiyama, Y. 2008. Involvement of multiple transporters in the hepatobiliary transport of rosuvastatin. Drug metabolism and disposition: the biological fate of chemicals 36(10);2014-23.

32. Huang, L., Wang, Y.Grimm, S. 2006. ATP-dependent transport of rosuvastatin in membrane vesicles expressing breast cancer resistance protein. Drug metabolism and disposition: the biological fate of chemicals 34(5);738-42.

33. Jemnitz, K., Veres, Z., Tugyi, R.Vereczkey, L. 2010. Biliary efflux transporters involved in the clearance of rosuvastatin in sandwich culture of primary rat hepatocytes. Toxicology in vitro : an international journal published in association with BIBRA 24(2);605-10.

34. Byrne, J. A., Strautnieks, S. S., Mieli-Vergani, G., Higgins, C. F., Linton, K. J.Thompson, R. J. 2002. The human bile salt export pump: characterization of substrate specificity and identification of inhibitors. Gastroenterology 123(5);1649-58.

35. Trauner, M.Boyer, J. L. 2003. Bile salt transporters: molecular characterization, function, and regulation. Physiological reviews 83(2);633-71.

36. Annaert, P. P.Brouwer, K. L. 2005. Assessment of drug interactions in hepatobiliary transport using rhodamine 123 in sandwich-cultured rat hepatocytes. Drug metabolism and disposition: the biological fate of chemicals 33(3);388-94.

37. Zheng, N., Zhang, X.Rosania, G. R. 2011. Effect of phospholipidosis on the cellular pharmacokinetics of chloroquine. The Journal of pharmacology and experimental therapeutics 336(3);661-71.

38. Chatman, L. A., Morton, D., Johnson, T. O.Anway, S. D. 2009. A strategy for risk management of drug-induced phospholipidosis. Toxicologic pathology 37(7);997-1005.

39. Zhou, L., Geraci, G., Hess, S., Yang, L., Wang, J.Argikar, U. 2011. Predicting phospholipidosis: a fluorescence noncell based in vitro assay for the determination of drug-phospholipid complex formation in early drug discovery. Analytical chemistry 83(18);6980-7.

40. Vitovic, P., Alakoskela, J. M.Kinnunen, P. K. 2008. Assessment of drug-lipid complex formation by a high-throughput Langmuir-balance and correlation to phospholipidosis. Journal of medicinal chemistry 51(6);1842-8.

41. LeCureux, L., Cheng, C. S., Herbst, J., Reilly, T. P., Lehman-McKeeman, L.Otieno, M. 2011. Evaluation and validation of multiple cell lines and primary mouse macrophages to predict phospholipidosis potential. Toxicology in vitro : an international journal published in association with BIBRA 25(8);1934-43.

Table 2.1: BEI and *In Vitro* $CL_{biliary}$ of Taurocholate (TC) and Rosuvastatin (RSV) Based on Data Presented in Figure 3.5 in Day 4 Rat SCH Following a 10-min Incubation With 1µM [^{3}H]TC or [^{3}H]RSV

		Control	AMD		CHQ		DES			AZI			GTM
			10 µM	50 µM	1 µM	10 µM	1 µM	10 µM	50 µM	1 µM	10 µM	50 µM	1 mM
TC	**BEI (%)**	88.3 (1.2)	87.2 (0.8)	52.9 * (3.7)	86.5 (1.9)	73.4 (4.0)	84.5 (1.5)	87.0 (1.7)	62.0 * (3.2)	75.3 (10.5)	72.8 (4.7)	34.8 * (13.0)	87.8 (1.5)
	$CL_{biliary}$ (mL/min/ kg)	31.7 (5.0)	20.8 (6.3)	3.3 * (1.2)	26.3 (8.4)	9.0 * (2.9)	25.7 (7.9)	16.9 (2.1)	4.7 * (0.7)	16.1 (7.4)	8.0 * (2.6)	2.5 * (1.0)	40.4 (3.2)
RSV	**BEI (%)**	56.7 (3.6)	62.8 (4.2)	50.1 (9.3)	53.2 (4.4)	62.7 (7.8)	46.0 (5.7)	55.6 (3.7)	41.3 (0.9)	59.4 (2.9)	64.9 (3.7)	50.6 (6.7)	50.3 (5.4)
	$CL_{biliary}$ (mL/min/ kg)	78.5 (13.5)	41.4 (8.6)	7.7 * (3.7)	51.5 (10.5)	27.6 * (6.2)	66.8 (13.8)	69.2 (12.5)	10.3 * (1.6)	73.4 (9.8)	38.8 (5.4)	19.6 * (2.3)	61.9 (6.0)

Notes: SCH were treated for 48 h (“chronic exposure”) with vehicle control (0.1% DMSO) or PLD-inducing drugs. Data represent the mean (SEM) of triplicate measurements (n = 3–7 hepatocyte preparations).

*$p < 0.05$, control versus treated

Figure 2.1: Toxicity of AMD, CHQ, DES, AZI, and GTM (incubation for 48 hr) evaluated in day 4 rat SCH measured as percent inhibition of MTT formazan formation. SCH treated with chloroquine at 100 µM and 0.1% DMSO (vehicle) were used as the positive and negative controls, respectively. Data are presented as mean ± SEM, n=3-7 replicates measured in triplicate.

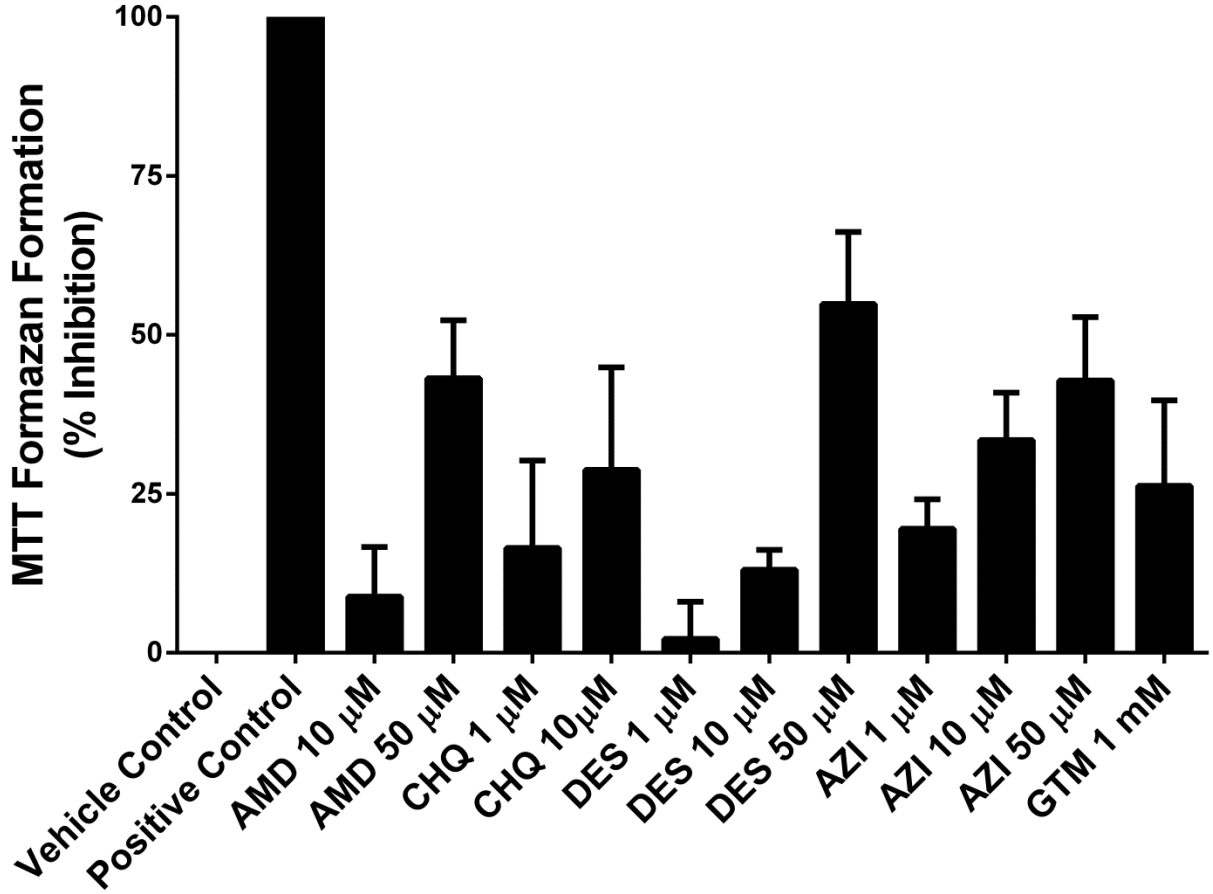

Figure 2.2: Representative images of day 4 rat SCH incubated for 30 min with 100 nM LysoTracker Red® following culture with PLD-inducing drugs or vehicle control (0.1% DMSO) for 48 h; only the highest incubation concentration is shown for clarity. Upper panel: light microscopy image; middle panel: LysoTracker Red® fluorescence; lower panel: overlaid light and fluorescent images filtered to appear blue and green, respectively, for contrast (inset in upper right is enlarged image). Scale bar in upper left corner of each image represents 20 µm.

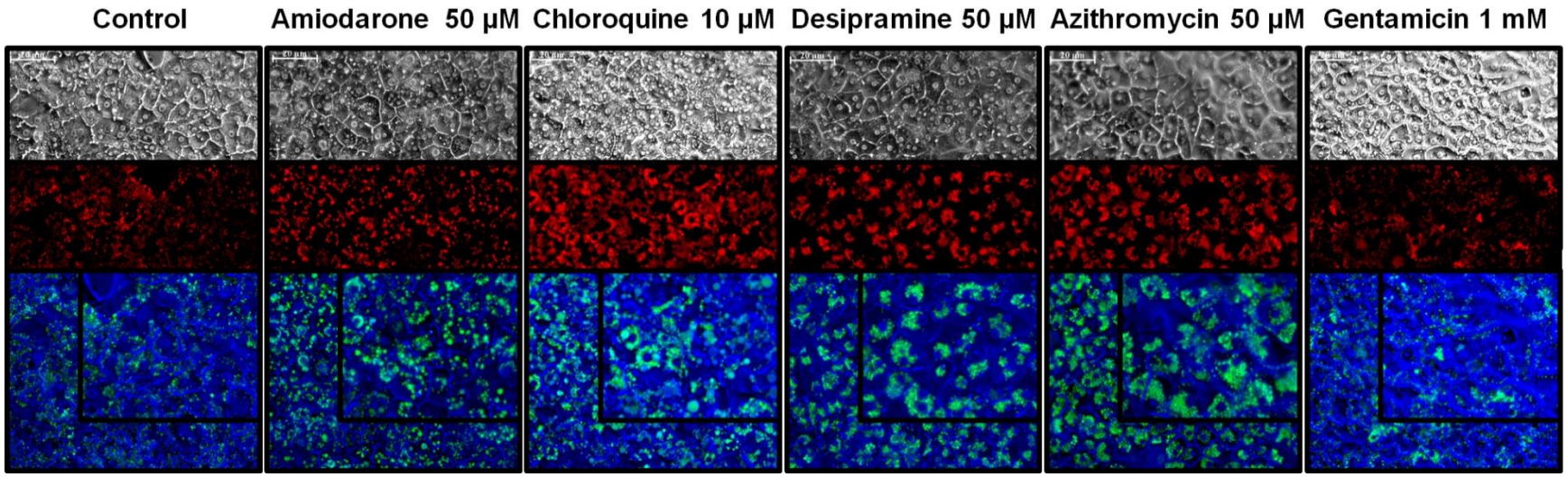

Figure 2.3: Representative electron micrographs of day 4 rat SCH after 48 h culture with PLD-inducing drugs or vehicle control (0.1% DMSO). Arrows indicate normal or enlarged laminar body-containing lysosomes. Scale bar represents 0.5 µm for all phospholipidosis-inducing drugs except control and gentamicin, for which the scale bar represents 2 and 1 µm, respectively.

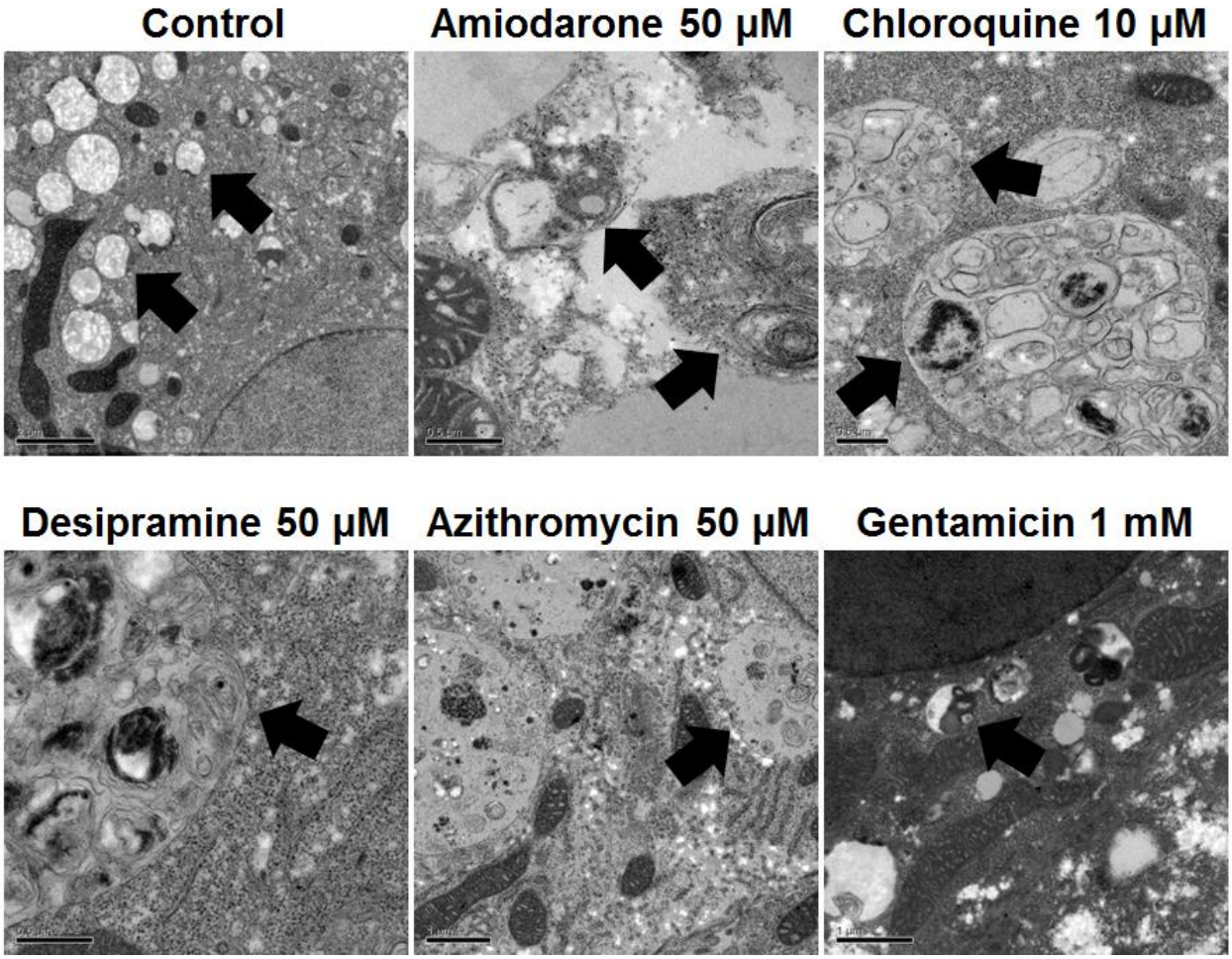

Figure 2.4: Accumulation of TC (left panel) and RSV(right panel) in cells + bile (black bars) and cells (white bars) of day 4 rat SCH following a 10-min co-incubation ("acute exposure") with 1 μM [^{3}H]TC or [^{3}H]RSV in the presence of vehicle control (0.1% DMSO) or PLD-inducing drugs: AMD, CHQ, DES, AZI, and GTM. Data represent the mean ± SEM of triplicate measurements in n=3 hepatocyte preparations. No statistically significant differences were observed between control vs. treated for total (cell + bile) accumulation or cellular accumulation.

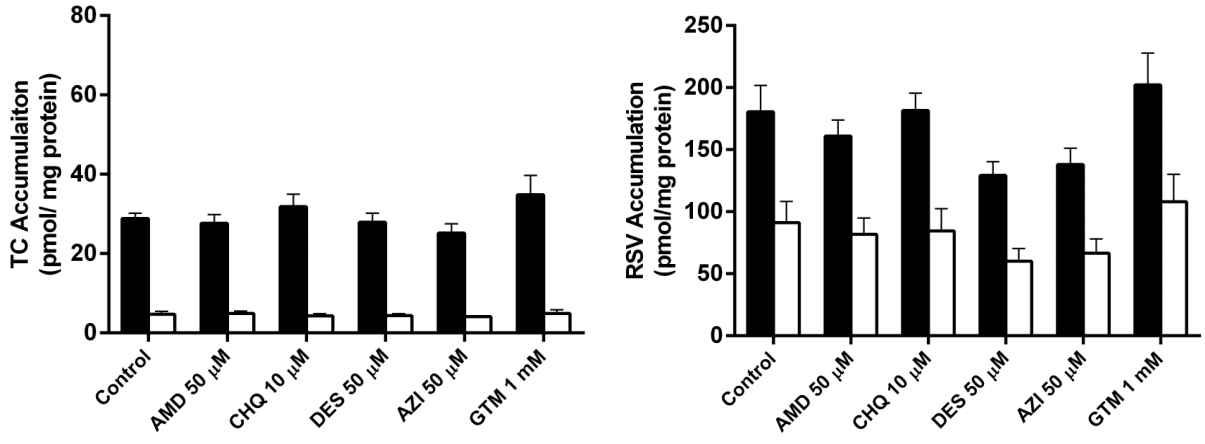

Figure 2.5: Accumulation of TC (left panel) and RSV (right panel) in cells + bile (black bars) and cells (white bars) of day 4 rat SCH following a 10-min incubation with 1 µM [^{3}H]TC or [^{3}H]RSV. SCH were treated for 48 h ("chronic exposure") with vehicle control (0.1% DMSO) or PLD-inducing drugs: AMD, CHQ, DES, AZI, and GTM. Data represent the mean ± SEM of triplicate measurements (n=3-7 hepatocyte preparations); *p<0.05, control vs. treated.

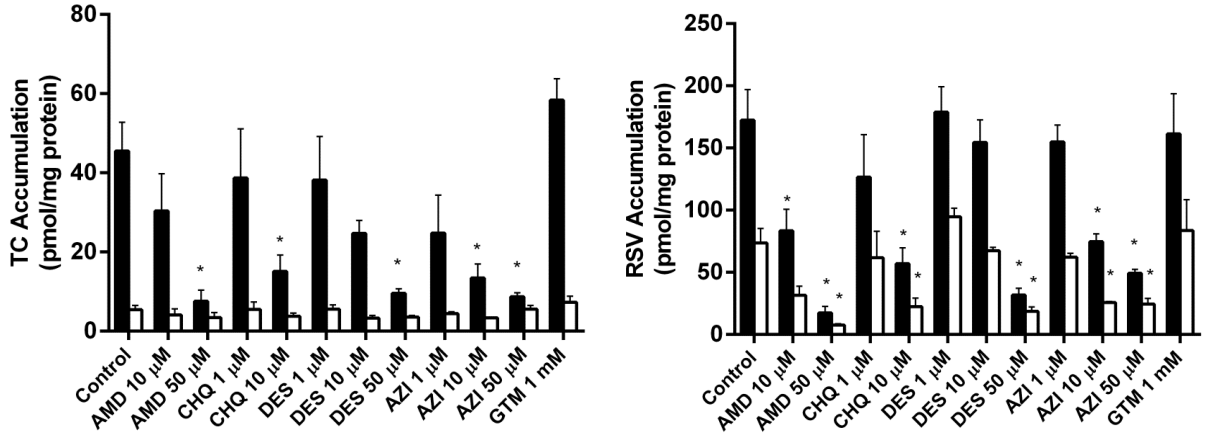

Chapter 3. Role of Multidrug Resistance-Associated Protein 4 in the Basolateral Efflux of Hepatically-Derived Enalaprilat

Introduction

The liver plays a central role in the metabolism, detoxification and elimination of endogenous and exogenous compounds. Following uptake across the basolateral membrane from the blood to the hepatocyte, metabolism typically results in formation of a more hydrophilic, charged molecule that can be eliminated either via the bile, or across the basolateral membrane into the systemic circulation for renal excretion. Importantly, following hydrophilic transformation, active efflux processes typically are required for the metabolite to exit the liver. In contrast to biliary excretion, changes in active basolateral efflux processes (either due to drug-drug interactions [DDIs] or disease-mediated changes in efflux transporter function) are under appreciated[1-3]. Changes in basolateral efflux of active metabolites may alter systemic concentrations and thus, systemic efficacy/toxicity, and potentially warrant detailed evaluation during drug development[3,4].

Enalapril is a prodrug transformed in the liver by carboxylesterases to the active moiety, enalaprilat. Transformation removes the ethylester from enalapril, adding a negative charge, and increasing the potency to inhibit angiotensin converting enzyme, thereby lowering blood pressure and preventing cardiac remodeling and renal dysfunction[5]. Due to the inherent negative charge on the parent drug and added polarity after metabolism, enalapril and enalaprilat require active transport processes to cross membranes. Interestingly, the presence of a diffusional barrier for enalapril and enalaprilat

---

This work has been presented, in part, at the ISSX Annual Meeting, Dallas, TX, October 14-18, 2012 and has been published in *Drug Metabolism and Disposition* and is presented in the style of that journal.

disposition helped lay the foundation for the identification of transporter-mediated disposition and clearance mechanisms of charged molecules[6-9]. Rat organic anion transporting polypeptide (OATP)1a1 and human OATP1B1 are responsible for the uptake of enalapril into the hepatocyte.

Enalaprilat derived in the liver can be excreted into the bile or translocated across the basolateral membrane into the systemic circulation[8,10,11]. Although multidrug resistance-associated protein (MRP)2 is capable of excreting enalaprilat from the hepatocyte into bile, the majority of the absorbed dose of enalapril is excreted in the urine as enalaprilat, which suggests that basolateral efflux of enalaprilat into the systemic circulation predominates since enalaprilat appears to be formed only in the hepatocyte[11-13]. As the site of action for enalaprilat is in the systemic circulation (inhibition of angiotensin converting enzyme), hepatic basolateral efflux is germane in regulating enalaprilat's beneficial effects on blood pressure, cardiac remodeling and kidney protection. Two proteins that may be able to transport enalaprilat from the hepatocyte into sinusoidal blood are MRP3 and MRP4. The localization of MRP3 and MRP4 on the basolateral membrane, and substrate specificity profiles, make them prime candidates to mediate enalaprilat transport[14-16].

Although, enalapril is prescribed extensively in many chronic diseases, including diabetes, non-alcoholic fatty liver disease, and renal failure, little is known about how co-administered medications or disease-associated changes in MRP expression affect enalaprilat disposition. In addition to specific disease states, disease severity also can alter basolateral efflux transporter expression[17-21]. For example, inflammation associated with non-alcoholic fatty liver disease increases protein expression of MRPs (e.g., MRP3, MRP4, MRP6) on the basolateral membrane[17]. Without knowledge of the basolateral transport process(es) involved in enalaprilat disposition, it is difficult to accurately predict how disease state alterations and DDIs may impact systemic concentrations and pharmacological effects.

This study was designed to determine whether MRP3 and/or MRP4 are involved in the hepatic basolateral efflux of enalaprilat, and to demonstrate the impact of MRP inhibition on the hepatic basolateral efflux clearance of enalaprilat. Enalapril and enalaprilat transport were evaluated in membrane vesicles prepared from cells expressing either MRP3 or MRP4. Additionally, a novel

experimental protocol was developed in human sandwich-cultured hepatocytes (SCH) to assess the potential impact of coadministered medications on enalaprilat basolateral efflux.

Materials and Methods

Materials

Enalapril maleate, d_5-enalapril, enalaprilat, d_5-enalaprilat, taurocholate, Hanks' balanced salt solution (HBSS), and Ca^{2+}/Mg^{2+}-free HBSS (Ca^{2+}-free HBSS) were purchased from Sigma-Aldrich (St. Louis, MO). MK-571 was purchased from Cayman Chemical Company (Ann Arbor, MI). Rosuvastatin was purchased from Toronto Research Chemicals (Toronto, Ontario, Canada). [^{3}H]Taurocholate (1 mCi/mL; >97% purity) and [^{3}H]rosuvastatin (1 mCi/mL; >97% purity) were purchased from PerkinElmer (Waltham, MA) and American Radiolabeled Chemicals (St. Louis, MO), respectively. All other chemicals were commercially available and of the highest grade available.

Human Embryonic Kidney Cell Culture and Overexpression of MRP3 and MRP4

Human MRP3 plasmid [pcDNA3.1(-)-MRP3] and MRP4 plasmid [pcDNA3.1(+)-MRP4] were kindly provided by Dr. Susan Cole (Queen's University, Kingston, Canada) and Dr. Dietrich Keppler (German Cancer Research Center, Heidelberg, Germany), respectively. Human embryonic kidney (HEK293T) cells were cultured in Dulbecco's Modified Eagle Medium (DMEM) supplemented with 10% fetal bovine serum in a humidified incubator.

For MRP4, a stable transfected cell line was developed as previously described[18]. For MRP3, transient transfection of HEK293T cells with X-tremeGENE 9 DNA Transfection Reagent (Roche Diagnostics, Mannheim, Germany) was performed according to the manufacturer's instructions. Seventy-two hours after transfection, the cells were harvested. Non-transfected and mock-transfected cells were used to generate control membrane vesicles for the MRP3 and MRP4 assays, respectively. Cells were harvested by trypsinizing and centrifuging the transporter overexpressing cells and the respective control cell lines. The cell pellets were washed in Tris-Sucrose-buffer (TSB; 250 mM sucrose/50 mM Tris, pH 7.4) containing 0.25 mM $CaCl_2$. The final cell pellet was overlaid with 10 ml TSB containing 0.25 mM

$CaCl_2$ and protease inhibitors (complete Mini EDTA-free, Roche Diagnostics, Mannheim, Germany), snap-frozen in liquid nitrogen, and stored at -80°C.

Membrane Vesicle Preparation

Membrane vesicles were prepared for MRP4, MRP3 and respective controls as described previously[22]. Briefly, frozen cell pellets were thawed, resuspended in TSB, and exploded by N_2 cavitation (300 psi, 5 min). After addition of EDTA (1mM), the suspension was centrifuged (800 x g, 10 min, 4°C) and the supernatant was collected. The pellet was resuspended in TSB with 0.5 mM EDTA, and centrifuged (800 x g, 10 min, 4°C). The resulting supernatants were overlaid over 35% (w/w) sucrose/50 mM Tris buffer in a high speed centrifuge tube. After centrifugation (100,000 x g, 90 min, 4°C), the interphase was collected and added to a new high-speed centrifuge tube with 25 mM sucrose/50 mM Tris buffer. After additional centrifugation (100,000 x g, 45 min, 4°C), the pellet was resuspended in 1 ml TSB. The suspension was added to a high-speed centrifuge tube and centrifuged (100,000 x g, 20 min, 4°C). The supernatant was discarded and the pellet was resuspended in TSB. Subsequently, the suspension was homogenized using a 27-gauge needle (15 strokes). The membrane vesicle suspension was divided into aliquots, snap-frozen in liquid nitrogen, and stored at -80°C until use. Successful transfection was confirmed via Western blotting and transport of radiolabeled prototypic probes as described previously[18].

Membrane Vesicle Assay

Membrane vesicles (10 μg) were incubated at 37°C with enalapril or enalaprilat (100 μM) with and without MK-571 (50 μM) in TSB containing $MgCl_2$ (10 mM), creatine phosphate (10 mM), creatine kinase (100 μg/mL), and ATP (4 mM) in a final volume of 50 μL. Enalapril, enalaprilat, and MK-571 stock solutions were prepared in TSB or 100% dimethylsulfoxide (DMSO) with a resulting DMSO final concentration of less than 1% in the total incubation volume. ATP was replaced by AMP (4 mM) for control reactions. At least three separate experiments in triplicate were performed for all incubations, unless otherwise noted. After incubation for 5 min, the reactions were stopped by addition of 800 μL of ice-cold TSB and immediately filtered through glass fiber filters (Pall Life Sciences, Port Washington,

NY) presoaked in 3 mM reduced glutathione/10mM dithiothreitol in TSB overnight. Filters were washed three times with ice-cold TSB. Filters were air dried and dissolved in 1 mL of pure HPLC methanol containing d_5-enalapril and d_5-enalaprilat for LC-MS/MS analysis. ATP-dependent uptake was calculated as the difference in uptake in the presence of AMP and ATP. MRP-dependent substrate transport was calculated by subtracting ATP-dependent uptake in control membrane vesicles from uptake in membrane vesicles prepared from MRP3- or MRP4-expressing cells.

Sandwich-Cultured Hepatocyte (SCH) Isolation and Culture

Human hepatocytes from three donors were kindly provided by Life Technologies (Research Triangle Park, NC) and Triangle Research Labs (Research Triangle Park, NC), and cultured as previously described[23]. Hepatocyte donors included three Caucasian men ranging in age from 20 to 48 years with a body mass index of 19 to 31 kg/m^2. Briefly, freshly isolated human hepatocytes were seeded in 6-well BioCoat® plates (BD Biosciences, San Jose, CA) at a density of 1.5×10^6 cells/well. Hepatocytes were overlaid with Matrigel® basement membrane matrix (BD Biosciences) and maintained as described previously[23].

Sandwich-Cultured Hepatocyte Uptake and Biliary Excretion Studies

Determination of the uptake and biliary excretion of probe substrates in human SCH has been described previously[24]. Slight modifications were made to allow determination of enalapril and enalaprilat uptake, formation and excretion. Briefly, human SCH were washed twice with 2 ml of warm Ca^{2+}-containing standard HBSS (cells + bile) or Ca^{2+}-free HBSS (cells) and incubated with 1.5 mL of the same buffer for 10 min at 37°C containing either [^{3}H]taurocholate (1 µM; 100 nCi/ml), [^{3}H]rosuvastatin (1 µM; 100 nCi/ml), or enalapril (5 µM). After 10 min, cells were washed 3 times with ice-cold standard HBSS and lysed with either 0.5% Triton X-100 in phosphate-buffered saline (for [^{3}H]taurocholate and [^{3}H]rosuvastatin analysis) or pure HPLC grade methanol containing internal standards (for enalapril and enalaprilat analysis). Radioactivity in cell lysates was quantified by liquid scintillation spectroscopy (Packard Tricarb; PerkinElmer, Waltham, MA). Enalapril and enalaprilat were quantified in cell lysates using LC-MS/MS. Accumulation of taurocholate, rosuvastatin, enalapril and enalaprilat in cells and cells

+ bile was normalized to protein determined using a BCA protein assay (Pierce Chemical, Rockford, IL). The biliary excretion index (BEI, %) and *in vitro* biliary clearance ($CL_{biliary}$; ml/min/kg) were calculated using B-CLEAR® technology (Qualyst Transporter Solutions, LCC, Durham, NC) based on the following equations:

$$BEI = \frac{Accumulation_{cells+bile} - Accumulation_{cells}}{Accumulation_{cells+bile}}$$

$$CL_{biliary} = \frac{Accumulation_{cells+bile} - Accumulation_{cells}}{AUC_{medium\ 0\text{-}T}}$$

where the area under the curve in the medium from time 0 to T ($AUC_{medium\ 0\text{-}T}$) represents the product of the incubation time (T) and the initial, taurocholate, rosuvastatin or enalapril concentration in the medium. $CL_{biliary}$ units were converted to ml/min/kg body weight based on previously reported values for human protein content in liver tissue (90 mg/g liver weight) and liver weight (25.7 g/kg body weight)[25].

Sandwich-Cultured Hepatocyte Basolateral Efflux Studies

On day 6 of culture, human SCH were loaded with enalapril for 60 min at 37°C with 2 mL/well of standard HBSS containing 5 µM enalapril with and without 25 µM MK-571. The buffer was removed and the cells were washed two times with warm, standard HBSS. At this point, 1 mL of methanol containing internal standards was added to one set of each SCH preparation (designated as "Pre-Efflux SCH") to assess intracellular accumulation of enalapril and derived enalaprilat. Enalaprilat efflux was initiated in the other set of SCH by adding 2 mL of fresh warm standard HBSS without enalapril followed by incubation for 30 min at 37°C. Aliquots (100 µL) of efflux buffer were taken at 5, 10 and 30 min to determine the amount of enalaprilat translocated into the efflux buffer. At 30 min, the buffer was aspirated and the cells were washed three times with ice-cold buffer. "Post-Efflux SCH" were lysed in 1 mL of ice-cold methanol containing internal standards. Enalapril and enalaprilat were quantified in efflux buffer, and pre- and post-efflux SCH lysates, by LC-MS/MS (Figure 3.1; Table 3.1). Intracellular

enalaprilat concentrations pre- and post-efflux were calculated by dividing the total mass present in the cell lysate by the estimated hepatocyte volume reported previously as 7.69 µL/mg protein, assuming 1 mg cellular protein per well[26]. Intrinsic basolateral efflux clearance of enalaprilat, $CL_{int,\ basolateral}$, was calculated according to the following equation,

$$CL_{int,\ basolateral} = \frac{X_{Efflux\ Buffer\ t1 \rightarrow t2}}{AUC_{Cell\ t1 \rightarrow t2}}$$

where $X_{Efflux\ Buffer}$ was the cumulative amount of enalaprilat excreted from the cell over the efflux period (t1→t2), assuming that biliary excretion and flux from the bile compartment into the efflux buffer were negligible; AUC_{Cell} represented the log-trapezoidal exposure of intracellular enalaprilat over the efflux period.

LC-MS/MS Analysis

Enalapril and enalaprilat were quantified by LC-MS/MS using an Applied Biosystems (Foster City, CA) API 4000 triple quadrupole mass spectrometer equipped with a TurboV® ion source (Applied Biosystems, Foster City, CA), a Shimadzu solvent delivery system (Columbia, MD), and a thermostatted CTC PAL autosampler (Leap Technologies, Carborro, NC). Tuning, operation, integration, and data analysis were carried out in positive mode using multiple reaction monitoring (Analyst® software v.1.4.1, Applied Biosystems). Following an 8 µL injection onto a Varian Pursuit 3 PFP column (50 x 2mm, 3 µm particle size; Santa Clara, CA), analytes were eluted via reverse phase gradient at 0.30 mL/min. Mobile phase A consisted of water and 0.1% formic acid; mobile phase B consisted of methanol with 0.1% formic acid. The initial condition was 80% aqueous, reaching 50% methanol at 1 min, and 97% methanol at 4 min. After a 0.4 min hold at 97% methanol, the mobile phase returned to initial conditions at 4.5 min. The total run time, including re-equilibration, was 5 min. The specific analytes were monitored as follows; enalapril (377.0 → 234.0), d_5-enalapril (internal standard, 382.0 → 239.0), enalaprilat (349.0 → 206.0), and d_5-enalaprilat (internal standard, 354.0 → 211.0)). Duplicate eight-point calibration curves for both enalapril and enalaprilat (0.075-375 nM) were constructed using the peak area ratio of analyte to

deuterated internal standard. In an attempt to mimic the various matrix components (lipids, salts, proteins), separate calibration curves were constructed with blank matrix from each of the different samples types (*i.e.*, vesicles, cell lysate and buffer).

Data Analysis

Data are presented as mean ± SD unless otherwise noted. A two-sided Student's *t*-test was used to determine significant differences; in all cases, $p<0.05$ was considered significant.

Results

ATP-Dependent Transport of Enalapril and Enalaprilat by Membrane Vesicles Prepared from MRP3- and MRP4-Expressing Cells

Prior to enalapril and enalaprilat uptake studies, each batch of membrane vesicles was characterized for protein expression and transport activity of probe substrates as described previously[18]. ATP-dependent uptake of enalapril and enalaprilat by membrane vesicles prepared from MRP3- and MRP4-expressing cells was determined in vesicles incubated with enalapril or enalaprilat (Figure 3.2). ATP-dependent uptake of enalapril was not significantly different in membrane vesicles prepared from MRP3- or MRP4-expressing cells compared to the respective control (Figure 3.2A). Although, ATP-dependent enalaprilat uptake was not significantly different between control and MRP3-expressing vesicles, statistically significant MRP4-dependent uptake was observed (277 ± 194 pmol/mg protein/min); the uptake rate of enalaprilat was 382 ± 133% greater in vesicles from MRP4-expressing cells compared to mock-transfected control cells. MRP4-mediated enalaprilat transport was investigated in the presence of the prototypical MRP inhibitor MK-571, at a concentration of 50 μM. MK-571 significantly inhibited enalaprilat transport by 83 ± 30% (Figure 3.3). MRP4-mediated enalaprilat transport was modestly inhibited by rosuvastatin, but differences were not statistically significant (data not shown).

Human Sandwich-Cultured Hepatocyte (SCH) Uptake and Biliary Excretion Studies

Studies were conducted in human SCH to determine the total and cellular accumulation, biliary excretion index, and $CL_{biliary}$ of the positive controls, taurocholate and rosuvastatin. Following a 10-min incubation of human SCH with 1 μM [^{3}H]taurocholate or 1 μM [^{3}H]rosuvastatin, total accumulation (cells + bile), cellular accumulation (cells) and BEI of taurocholate and rosuvastatin were determined (Figure 3.4A)[24]. BEI and $CL_{biliary}$ values for taurocholate and rosuvastatin were 81 ± 9% and 22.4 ± 4.6 mL/min/kg body weight, and 39 ± 7% and 6.4 ± 1.3 mL/min/kg body weight, respectively, indicating robust biliary clearance of these compounds[24]. Additionally, total accumulation, cellular accumulation, and the BEI of enalapril were measured. Following a 10-min incubation of human SCH with enalapril, a

higher total accumulation and cellular accumulation of derived enalaprilat compared to enalapril was observed (Figure 3.4B) suggesting rapid and extensive conversion of enalapril to enalaprilat. $CL_{biliary}$ of parent enalapril was negligible in human SCH (0.02 ± 0.01 mL/min/kg body weight; mean ± SD, n=2 in triplicate). Biliary excretion of derived enalaprilat was not quantifiable in human SCH after a 10-min incubation period.

Human Sandwich-Cultured Hepatocyte Basolateral Efflux Studies

Basolateral efflux clearance of enalaprilat was assessed in human SCH. Following the 60-min loading phase with and without MK-571, accumulation of enalapril within the hepatocytes was negligible due to rapid conversion to enalaprilat. Pre-efflux cellular accumulation of derived enalaprilat was decreased when MK-571 was co-incubated with enalapril during the loading phase, suggesting inhibition of enalapril uptake processes (Table 3.1). Correspondingly, with decreased intracellular concentrations over the entire efflux period, the total mass available for efflux across the basolateral membrane in human SCH co-incubated with MK-571 also decreased compared to control. Therefore, intrinsic basolateral efflux clearance was calculated by dividing the total mass effluxed across the basolateral membrane by the calculated enalaprilat area under the cellular concentration-time curve (Table 3.1). MK-571 significantly decreased intrinsic basolateral efflux clearance (Table 3.1, Figure 3.5). Enalaprilat intrinsic basolateral efflux clearance was modestly inhibited by rosuvastatin, but differences were not statistically significant (data not shown).

Discussion

The present study was designed to determine the involvement of MRP3 and/or MRP4 in the basolateral efflux of enalapril and enalaprilat. Using membrane vesicles, MRP3 did not appear to transport either enalapril or enalaprilat. Enalaprilat, but not enalapril, was actively transported by MRP4. To confirm MRP4-mediated transport of enalaprilat, inhibition of uptake by the pan-MRP prototypical inhibitor, MK-571, was evaluated[18,27]. Indeed, potent inhibition by MK-571 (83%) was observed.

Studies were conducted in human SCH to assess the basolateral efflux of derived enalaprilat in intact hepatocytes. First, the accumulation and biliary excretion of taurocholate and rosuvastatin, two prototypical positive controls that are excreted into bile, was measured to confirm the functionality of the basolateral uptake and canalicular transport processes in the SCH used in this study. Indeed, human SCH exhibited extensive hepatic uptake and biliary clearance of both taurocholate and rosuvastatin. Biliary excretion of enalaprilat was negligible following a 10-min incubation with enalapril in human SCH (Figure 3.4A). Cellular accumulation of preformed enalaprilat in rat SCH was negligible (data not shown), consistent with previously published data demonstrating a diffusional barrier for hepatic uptake of enalaprilat[11]. Taken together, these data suggest that the basolateral translocation of enalaprilat into the efflux buffer appears to be the only route of excretion of derived enalaprilat in SCH, and that reuptake of enalaprilat does not occur to any measureable extent. Therefore, basolateral excretion of derived enalaprilat was determined in human SCH in the presence and absence of MK-571 to assess the impact of MRP-mediated inhibition of basolateral efflux. Interestingly, the relative extent of inhibition of basolateral efflux clearance of enalaprilat in human SCH was similar to that observed in membrane vesicles prepared from HEK293T cells expressing MRP4 (Figures 3.3 and 3.5); MK-571 inhibition of uptake into membrane vesicles and intrinsic basolateral efflux clearance in human SCH was 83% and 67%, respectively. This finding should be interpreted cautiously because MK-571 is a non-selective MRP inhibitor and other MRP transporters in addition to MRP4 could contribute to the basolateral efflux of enalaprilat in human hepatocytes.

Following intestinal absorption of enalapril, the predominant route of excretion is presumed to be hepatic metabolism to enalaprilat followed by basolateral efflux of enalaprilat into the systemic circulation and subsequent renal excretion[28]. In isolated perfused rat livers, the magnitude of the basolateral efflux clearance of derived enalaprilat was at least 2-fold greater than biliary clearance[11]. This preclinical data is consistent with human data indicating that >90% of orally absorbed enalapril is recovered in the urine as enalaprilat[28,29]. Given this disposition profile, where enalaprilat is excreted preferentially from the liver into the systemic circulation followed by renal excretion, inhibition of MRP4 transport would be expected to decrease systemic enalaprilat concentrations *in vivo* and the resulting pharmacodynamic effect. The converse also may be true, where increased MRP4 protein expression due to disease (e.g. nonalcoholic steatohepatitis[17]) would be expected to increase systemic concentrations.

In the present study, a novel basolateral efflux protocol was developed in human SCH to elucidate the impact of basolateral efflux transporter inhibition (e.g. MRP4) on enalaprilat disposition. Following confirmation of MRP4's role in enalaprilat transport, basolateral efflux clearance was calculated by dividing the amount of enalaprilat translocated from the hepatocyte into the efflux buffer by the estimated exposure of intracellular enalaprilat. Accurate determination of basolateral efflux using this method assumes that: 1) biliary excretion of the compound is negligible, 2) the compound, once effluxed from the hepatocyte, does not reenter the hepatocyte (i.e. the metabolite must be hepatically-derived), and 3) any further conversion from parent to metabolite after the loading phase is insignificant. Data presented in this manuscript suggest that these assumptions are true in the SCH model under the described study conditions. Enalapril and enalaprilat biliary excretion was minimal in human SCH (Figure 3.4); thus, potential flux during the efflux phase from the bile canaliculi of SCH into the medium would be negligible. Pilot studies in rat SCH indicated that preformed enalaprilat does not re-enter the hepatocyte (data not shown), consistent with previous reports that enalaprilat is not transported by rat Oatp1a1[8]. Although rat Oatp1a1 and human OATP1B1 are not completely homologous, pharmacophore modeling indicated that substrates for these transporters have similar structural moieties[30]. Finally, the concentration of enalapril in the hepatocyte was very low compared to enalaprilat following both the

loading phase and the efflux phase in the human SCH protocol, indicating rapid conversion of enalapril to enalaprilat in the hepatocyte. Alternatively, to assess the impact of delayed conversion of parent to metabolite, the relative concentration of parent to metabolite after the loading phase should be assessed. If the amount of parent left in the cell following the loading phase is greater than 10% of the amount of generated metabolite, conversion during the efflux phase may require further investigation or optimization of the loading protocol. If these assumptions are violated, the interplay between uptake, metabolism, basolateral efflux and biliary excretion would need to be deconvoluted using mathematical modeling.

Although inhibition of enalapril uptake would not impact the results of the current study design, it should be noted that enalaprilat cellular concentrations were greatly decreased in human SCH treated concomitantly with MK-571, likely due to inhibition of OATP1B1-mediated uptake of enalapril into hepatocytes. MK-571 is a potent inhibitor (IC_{50} = 0.3 μM) of OATP1B1[31]. Importantly, failing to account for decreased uptake by direct measurement of cellular concentrations prior to initiation of the efflux phase may result in overestimation of basolateral efflux inhibition.

Results suggest that altered MRP4 function may modulate systemic enalaprilat concentrations and thus enalapril efficacy *in vivo*. Our group recently identified many drugs as potent MRP4 inhibitors that are commonly co-administered in patients with metabolic disease or hypertension[18]. In addition to co-medications, concomitant genetic variation or disease states may further influence enalapril and enalaprilat pharmacokinetics and pharmacodynamics. Interestingly, genetic variation resulting in reduced OATP1B1 function increased enalapril and decreased enalaprilat systemic concentrations, which may lead to decreased systemic pharmacologic activity[32]. Similarly, patients with inflammatory liver disease (e.g. nonalcoholic steatohepatitis) have decreased OATP and increased MRP4 expression[33,34]. These changes in transporter expression together with frequent coadministration of potent MRP4 inhibitors (i.e. glyburide, fluoxetine, furosemide, simvastatin[18,35]) may unpredictably alter hepatic and systemic concentrations of drugs/metabolites that are transported in a manner similar to enalapril/enalaprilat, potentially leading to therapeutic failure or unexpected toxicity. Depending on the culture conditions,

MRP4 has been shown to be up-regulated in SCH from various species over the culture period[36,37]. Although this does not affect the inhibition profile of MK-571, careful evaluation of factors that alter protein expression *in vitro* should be considered before data are extrapolated from SCH to *in vivo*.

Human SCH have been utilized to mechanistically evaluate hepatocyte vectorial transport and reveal the relative contribution of basolateral versus biliary efflux to overall clearance. Recently, Pfeifer et al. and Matsunaga et al. demonstrated the importance of the interplay between basolateral and canalicular efflux in the systemic and hepatic disposition of rosuvastatin and mycophenolic acid glucuronide, respectively[27,38,39]. Extensive biliary excretion of rosuvastatin and mycophenolic acid glucuronide required mathematical modeling to deconvolute the contribution of basolateral versus canalicular transport. In contrast, enalapril/enalaprilat exhibited minimal biliary excretion, allowing direct measurement of basolateral efflux in the present studies. These reports demonstrate that altered hepatic transport may result in modulation of both hepatic and systemic concentrations of drugs and derived metabolites. In fact, inhibition of hepatic uptake and biliary excretion of mycophenolic acid glucuronide, which disrupts enterohepatic recirculation of the parent mycophenolic acid, is postulated as the mechanism behind decreased systemic exposure to mycophenolic acid during coadministration with cyclosporine in transplant patients[38,40]. Additionally, investigation of rosuvastatin disposition in human SCH and isolated perfused rat livers revealed that basolateral and canalicular efflux clearances were approximately equal[27,39]. This finding demonstrates that although rosuvastatin is excreted primarily as unchanged drug in the feces, basolateral efflux in concert with canalicular efflux are key determinants of rosuvastatin overall disposition, and may impact pharmacologic efficacy and/or toxicity. These examples, together with the present study, illustrate the importance of hepatic basolateral and canalicular efflux processes in determining both the pharmacokinetic and pharmaco-/toxico-dynamic profile of drugs and their metabolites.

In summary, enalaprilat, the active metabolite of enalapril, is effluxed across the basolateral membrane of hepatocytes by MRP4. MRP4 transport may be inhibited by concomitantly administered drugs[41-43]. This work highlights the significance of active basolateral efflux in the therapeutic efficacy of

active metabolites derived in the liver and excreted into the systemic circulation. SCH represent a robust model to study the interplay between basolateral and canalicular efflux. Further studies are required to understand the mechanistic basis for preferential basolateral or biliary efflux of compounds, and fully appreciate the consequences on the systemic and hepatic action of active/toxic metabolites.

REFERENCES

1. Konig, J., Muller, F.Fromm, M. F. 2013. Transporters and drug-drug interactions: important determinants of drug disposition and effects. Pharmacological reviews 65(3);944-66.

2. Pfeifer, N. D., Hardwick, R. N.Brouwer, K. L. 2014. Role of hepatic efflux transporters in regulating systemic and hepatocyte exposure to xenobiotics. Annual review of pharmacology and toxicology 54;509-35.

3. Kock, K.Brouwer, K. L. 2012. A perspective on efflux transport proteins in the liver. Clinical pharmacology and therapeutics 92(5);599-612.

4. Zamek-Gliszczynski, M. J., Chu, X., Polli, J. W., Paine, M. F.Galetin, A. 2013. Understanding the Transport Properties of Metabolites: Case Studies and Considerations for Drug Development. Drug metabolism and disposition: the biological fate of chemicals.

5. Patchett, A. A., Harris, E., Tristram, E. W., Wyvratt, M. J., Wu, M. T., Taub, D., Peterson, E. R., Ikeler, T. J., ten Broeke, J., Payne, L. G., Ondeyka, D. L., Thorsett, E. D., Greenlee, W. J., Lohr, N. S., Hoffsommer, R. D., Joshua, H., Ruyle, W. V., Rothrock, J. W., Aster, S. D., Maycock, A. L., Robinson, F. M., Hirschmann, R., Sweet, C. S., Ulm, E. H., Gross, D. M., Vassil, T. C.Stone, C. A. 1980. A new class of angiotensin-converting enzyme inhibitors. Nature 288(5788);280-3.

6. Schwab, A. J., Barker, F., 3rd, Goresky, C. A.Pang, K. S. 1990. Transfer of enalaprilat across rat liver cell membranes is barrier limited. The American journal of physiology 258(3 Pt 1);G461-75.

7. de Lannoy, I. A.Pang, K. S. 1986. Presence of a diffusional barrier on metabolite kinetics: enalaprilat as a generated versus preformed metabolite. Drug metabolism and disposition: the biological fate of chemicals 14(5);513-20.

8. Pang, K. S., Wang, P. J., Chung, A. Y.Wolkoff, A. W. 1998. The modified dipeptide, enalapril, an angiotensin-converting enzyme inhibitor, is transported by the rat liver organic anion transport protein. Hepatology (Baltimore, Md.) 28(5);1341-6.

9. Pang, K. S., Cherry, W. F., Terrell, J. A.Ulm, E. H. 1984. Disposition of enalapril and its diacid metabolite, enalaprilat, in a perfused rat liver preparation. Presence of a diffusional barrier for enalaprilat into hepatocytes. Drug metabolism and disposition: the biological fate of chemicals 12(3);309-13.

10. Liu, L., Cui, Y., Chung, A. Y., Shitara, Y., Sugiyama, Y., Keppler, D.Pang, K. S. 2006. Vectorial transport of enalapril by Oatp1a1/Mrp2 and OATP1B1 and OATP1B3/MRP2 in rat and human livers. The Journal of pharmacology and experimental therapeutics 318(1);395-402.

11. de Lannoy, I. A., Barker, F., 3rdPang, K. S. 1993. Formed and preformed metabolite excretion clearances in liver, a metabolite formation organ: studies on enalapril and enalaprilat in the single-pass and recirculating perfused rat liver. Journal of pharmacokinetics and biopharmaceutics 21(4);395-422.

12. Tocco, D. J., deLuna, F. A., Duncan, A. E., Vassil, T. C.Ulm, E. H. 1982. The physiological disposition and metabolism of enalapril maleate in laboratory animals. Drug metabolism and disposition: the biological fate of chemicals 10(1);15-9.

13. Ulm, E. H., Hichens, M., Gomez, H. J., Till, A. E., Hand, E., Vassil, T. C., Biollaz, J., Brunner, H. R.Schelling, J. L. 1982. Enalapril maleate and a lysine analogue (MK-521): disposition in man. British journal of clinical pharmacology 14(3);357-62.

14. Gradhand, U., Lang, T., Schaeffeler, E., Glaeser, H., Tegude, H., Klein, K., Fritz, P., Jedlitschky, G., Kroemer, H. K., Bachmakov, I., Anwald, B., Kerb, R., Zanger, U. M., Eichelbaum, M., Schwab, M.Fromm, M. F. 2008. Variability in human hepatic MRP4 expression: influence of cholestasis and genotype. The pharmacogenomics journal 8(1);42-52.

15. Chai, J., He, Y., Cai, S. Y., Jiang, Z., Wang, H., Li, Q., Chen, L., Peng, Z., He, X., Wu, X., Xiao, T., Wang, R., Boyer, J. L.Chen, W. 2012. Elevated hepatic multidrug resistance-associated protein 3/ATP-binding cassette subfamily C 3 expression in human obstructive cholestasis is mediated through tumor necrosis factor alpha and c-Jun NH2-terminal kinase/stress-activated protein kinase-signaling pathway. Hepatology (Baltimore, Md.) 55(5);1485-94.

16. Klaassen, C. D.Aleksunes, L. M. 2010. Xenobiotic, bile acid, and cholesterol transporters: function and regulation. Pharmacological reviews 62(1);1-96.

17. Hardwick, R. N., Fisher, C. D., Canet, M. J., Scheffer, G. L.Cherrington, N. J. 2011. Variations in ATP-binding cassette transporter regulation during the progression of human nonalcoholic fatty liver disease. Drug metabolism and disposition: the biological fate of chemicals 39(12);2395-402.

18. Kock, K., Ferslew, B. C., Netterberg, I., Yang, K., Urban, T. J., Swaan, P. W., Stewart, P. W.Brouwer, K. L. 2013. Risk Factors for Development of Cholestatic Drug-induced Liver Injury: Inhibition of Hepatic Basolateral Bile Acid Transporters MRP3 and MRP4. Drug metabolism and disposition: the biological fate of chemicals.

19. Tsujimoto, M., Hatozaki, D., Shima, D., Yokota, H., Furukubo, T., Izumi, S., Yamakawa, T., Minegaki, T.Nishiguchi, K. 2012. Influence of serum in hemodialysis patients on the expression of intestinal and hepatic transporters for the excretion of pravastatin. Therapeutic apheresis and dialysis : official peer-reviewed journal of the International Society for Apheresis, the Japanese Society for Apheresis, the Japanese Society for Dialysis Therapy 16(6);580-7.

20. Yeung, C. K., Shen, D. D., Thummel, K. E.Himmelfarb, J. 2013. Effects of chronic kidney disease and uremia on hepatic drug metabolism and transport. Kidney international.

21. Hanada, K., Nakai, K., Tanaka, H., Suzuki, F., Kumada, H., Ohno, Y., Ozawa, S.Ogata, H. 2012. Effect of nuclear receptor downregulation on hepatic expression of cytochrome P450 and transporters in chronic hepatitis C in association with fibrosis development. Drug metabolism and pharmacokinetics 27(3);301-6.

22. Ghibellini, G., Leslie, E. M., Pollack, G. M.Brouwer, K. L. 2008. Use of tc-99m mebrofenin as a clinical probe to assess altered hepatobiliary transport: integration of in vitro, pharmacokinetic modeling, and simulation studies. Pharmaceutical research 25(8);1851-60.

23. Swift, B., Pfeifer, N. D.Brouwer, K. L. 2010. Sandwich-cultured hepatocytes: an in vitro model to evaluate hepatobiliary transporter-based drug interactions and hepatotoxicity. Drug metabolism reviews 42(3);446-71.

24. Abe, K., Bridges, A. S.Brouwer, K. L. 2009. Use of sandwich-cultured human hepatocytes to predict biliary clearance of angiotensin II receptor blockers and HMG-CoA reductase inhibitors. Drug metabolism and disposition: the biological fate of chemicals 37(3);447-52.

25. Davies, B.Morris, T. 1993. Physiological parameters in laboratory animals and humans. Pharmaceutical research 10(7);1093-5.

26. Lee, J. K.Brouwer, K. R. 2010. Determination of Intracellular Volume of Rat and Human Sandwich-Cultured Hepatocytes (Abstract ID 1595). The Toxicologist, Supplement to Toxicological Sciences 114;339.

27. Pfeifer, N. D., Yang, K.Brouwer, K. L. 2013. Hepatic basolateral efflux contributes significantly to rosuvastatin disposition I: characterization of basolateral versus biliary clearance using a novel protocol in sandwich-cultured hepatocytes. The Journal of pharmacology and experimental therapeutics 347(3);727-36.

28. Ulm, E. H. 1983. Enalapril maleate (MK-421), a potent, nonsulfhydryl angiotensin-converting enzyme inhibitor: absorption, disposition, and metabolism in man. Drug metabolism reviews 14(1);99-110.

29. 2011. Enalaprilat for Injection Package Insert.

30. Chang, C., Pang, K. S., Swaan, P. W.Ekins, S. 2005. Comparative pharmacophore modeling of organic anion transporting polypeptides: a meta-analysis of rat Oatp1a1 and human OATP1B1. The Journal of pharmacology and experimental therapeutics 314(2);533-41.

31. Yamazaki, M., Li, B., Louie, S. W., Pudvah, N. T., Stocco, R., Wong, W., Abramovitz, M., Demartis, A., Laufer, R., Hochman, J. H., Prueksaritanont, T.Lin, J. H. 2005. Effects of fibrates on human organic anion-transporting polypeptide 1B1-, multidrug resistance protein 2- and P-glycoprotein-mediated transport. Xenobiotica; the fate of foreign compounds in biological systems 35(7);737-53.

32. Tian, L., Liu, H., Xie, S., Jiang, J., Han, L., Huang, Y.Li, Y. 2011. Effect of organic anion-transporting polypeptide 1B1 (OATP1B1) polymorphism on the single- and multiple-dose pharmacokinetics of enalapril in healthy Chinese adult men. Clinical therapeutics 33(5);655-63.

33. Lake, A. D., Novak, P., Fisher, C. D., Jackson, J. P., Hardwick, R. N., Billheimer, D. D., Klimecki, W. T.Cherrington, N. J. 2011. Analysis of global and absorption, distribution, metabolism, and elimination gene expression in the progressive stages of human nonalcoholic fatty liver disease. Drug metabolism and disposition: the biological fate of chemicals 39(10);1954-60.

34. Fisher, C. D., Lickteig, A. J., Augustine, L. M., Oude Elferink, R. P., Besselsen, D. G., Erickson, R. P.Cherrington, N. J. 2009. Experimental non-alcoholic fatty liver disease results in decreased hepatic uptake transporter expression and function in rats. European journal of pharmacology 613(1-3);119-27.

35. Morgan, R. E., van Staden, C. J., Chen, Y., Kalyanaraman, N., Kalanzi, J., Dunn, R. T., 2nd, Afshari, C. A.Hamadeh, H. K. 2013. A multifactorial approach to hepatobiliary transporter assessment enables improved therapeutic compound development. Toxicological sciences : an official journal of the Society of Toxicology 136(1);216-41.

36. Tchaparian, E. H., Houghton, J. S., Uyeda, C., Grillo, M. P.Jin, L. 2011. Effect of culture time on the basal expression levels of drug transporters in sandwich-cultured primary rat hepatocytes. Drug metabolism and disposition: the biological fate of chemicals 39(12);2387-94.

37. Noel, G., Le Vee, M., Moreau, A., Stieger, B., Parmentier, Y.Fardel, O. 2013. Functional expression and regulation of drug transporters in monolayer- and sandwich-cultured mouse hepatocytes. European journal of pharmaceutical sciences : official journal of the European Federation for Pharmaceutical Sciences 49(1);39-50.

38. Matsunaga, N., Wada, S., Nakanishi, T., Ikenaga, M., Ogawa, M.Tamai, I. 2013. Mathematical Modeling of the in Vitro Hepatic Disposition of Mycophenolic Acid and Its Glucuronide in Sandwich-Cultured Human Hepatocytes. Molecular pharmaceutics.

39. Pfeifer, N. D., Bridges, A. S., Ferslew, B. C., Hardwick, R. N.Brouwer, K. L. 2013. Hepatic basolateral efflux contributes significantly to rosuvastatin disposition II: characterization of hepatic elimination by basolateral, biliary, and metabolic clearance pathways in rat isolated perfused liver. The Journal of pharmacology and experimental therapeutics 347(3);737-45.

40. Pou, L., Brunet, M., Cantarell, C., Vidal, E., Oppenheimer, F., Monforte, V., Vilardell, J., Roman, A., Martorell, J.Capdevila, L. 2001. Mycophenolic acid plasma concentrations: influence of comedication. Therapeutic drug monitoring 23(1);35-8.

41. Hasegawa, M., Kusuhara, H., Adachi, M., Schuetz, J. D., Takeuchi, K.Sugiyama, Y. 2007. Multidrug resistance-associated protein 4 is involved in the urinary excretion of hydrochlorothiazide and furosemide. Journal of the American Society of Nephrology : JASN 18(1);37-45.

42. El-Sheikh, A. A., Greupink, R., Wortelboer, H. M., van den Heuvel, J. J., Schreurs, M., Koenderink, J. B., Masereeuw, R.Russel, F. G. 2013. Interaction of immunosuppressive drugs with human organic anion transporter (OAT) 1 and OAT3, and multidrug resistance-associated protein (MRP) 2 and MRP4. Translational research : the journal of laboratory and clinical medicine 162(6);398-409.

43. Fukuda, Y., Takenaka, K., Sparreboom, A., Cheepala, S. B., Wu, C. P., Ekins, S., Ambudkar, S. V.Schuetz, J. D. 2013. Human immunodeficiency virus protease inhibitors interact with ATP binding cassette transporter 4/multidrug resistance protein 4: a basis for unanticipated enhanced cytotoxicity. Molecular pharmacology 84(3);361-71.

Table 3.1: Parameters describing hepatically-derived enalaprilat disposition in human sandwich-cultured hepatocytes (SCH). Human SCH were incubated with 5 µM enalapril with and without MK-571 (25 µM) for 60 min. Enalapril and enalaprilat concentrations in the post-efflux medium, and in hepatocytes pre- and post-efflux, were quantified as described in the "Materials and Methods".

	Kinetic Parameters		Enalapril (5 µM) Control	Enalapril (5 µM) + MK-571 (25 µM)
Pre-Efflux	**Pre-Efflux Enalaprilat Cellular Concentration (pmol/µL)**	Liver 1	25.5 ± 2.5	6.9 ± 0.6
		Liver 2	5.5 ± 0.3	3.0 ± 0.1
		Liver 3	6.5 ± 0.7	2.0 ± 0.2
		Mean	12.5 ± 11.3	4.0 ± 2.6
Post-Efflux	**Post-Efflux Enalaprilat Cellular Concentration (pmol/µL)**	Liver 1	20.4 ± 1.7	5.2 ± 0.2
		Liver 2	5.2 ± 0.6	3.1 ± 0.2
		Liver 3	6.7 ± 0.8	2.4 ± 0.1
		Mean	10.8 ± 8.4	3.6 ± 1.5
	Mass Enalaprilat Excreted into Efflux Buffer ($X_{\text{Efflux Buffer } 0\rightarrow 30}$, pmol)	Liver 1	16.9 ± 1.5	0.8 ± 1.3
		Liver 2	2.3 †	0.4 ± 0.7
		Liver 3	7.5 ± 0.6	1.3 ± 0.5
		Mean	8.9 ± 7.4	0.8 ± 0.4
	Cellular Enalaprilat Exposure ($AUC_{\text{Cell } 0\rightarrow 30}$, pmol*min/µL)	Liver 1	684 ± 16.9	180 ± 3.2
		Liver 2	160 ± 13.6	91.3 ± 3.4
		Liver 3	199 ± 16.2	65.4 ± 4.3
		Mean	348 ± 293	112 ± 60.4
	Basolateral Enalaprilat Clearance ($CL_{\text{int, basolateral}}$, µL/min)	Liver 1	0.024 ± 0.001	0.004 ± 0.004
		Liver 2	0.014 †	0.004 ± 0.007
		Liver 3	0.037 ± 0.002	0.019 ± 0.008
		Mean	0.026 ± 0.012	0.009 ± 0.009 *

Data are presented as mean ± SD; n= 3 independent hepatocyte preparations performed in triplicate.
† Value imputed due to analytical error as the difference in enalaprilat intracellular concentration pre- vs. post-efflux, assuming a cellular volume of 7.69 µL/mg protein.
*$p<0.05$ vehicle control vs. MK-571.

Figure 3.1: A. Scheme depicting efflux studies in human sandwich-cultured hepatocytes (SCH) describing the loading and efflux phases (see "Materials and Methods" section for a detailed description; HBSS, Hanks' balanced salt solution with calcium). **B.** Average enalaprilat cellular accumulation (red squares) and mass excreted into the efflux buffer (blue diamonds) observed during the efflux phase in a representative human SCH preparation under control conditions according to the scheme depicted in A (mean ± SD of triplicate measurements). The green dotted line indicates the presumed cellular accumulation of enalaprilat during the loading phase. Enalaprilat cellular exposure during the efflux phase ($AUC_{cell\ 0\rightarrow30}$; red trapezoid) was calculated as the log-trapezoidal product of intracellular enalaprilat mass divided by the estimated intracellular volume and time. The mass of enalaprilat excreted into the efflux buffer ($X_{Efflux\ Buffer}$) was determined by multiplying the concentration measured in the buffer by the buffer volume.

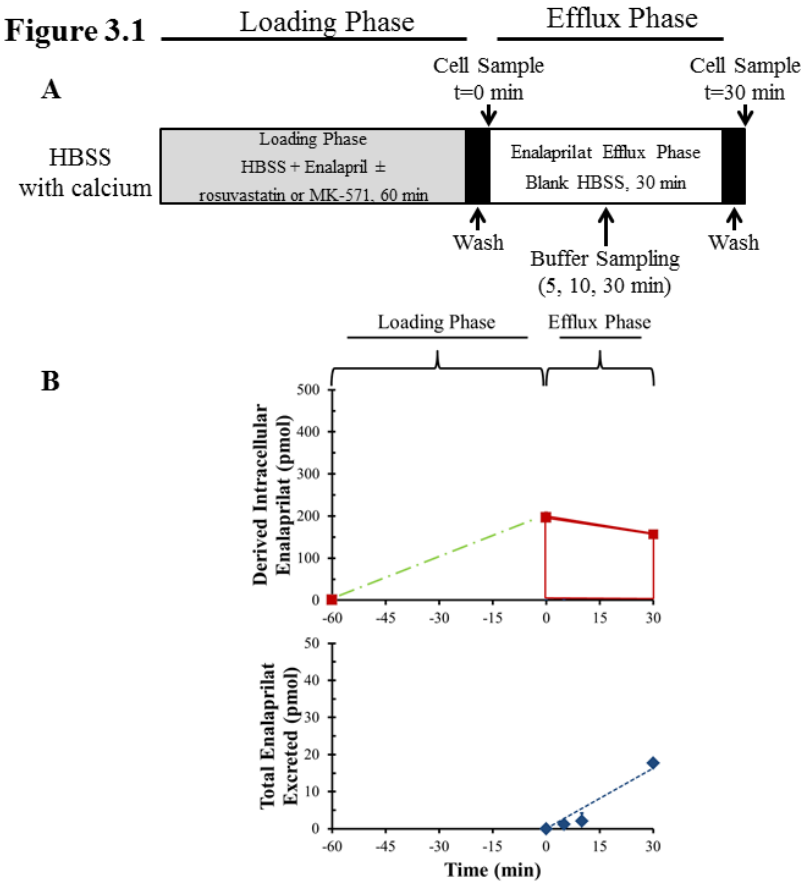

Figure 3.2: Transport of enalapril and enalaprilat by MRP3 and MRP4. Uptake of enalapril (100 µM; **A**) and enalaprilat (100 µM; **B**) into membrane vesicles prepared from HEK293T cells expressing MRP3 or MRP4 (10 µg; solid bars), or mock-transfected controls (10 µg; open bars), was determined after a 5-min incubation in the presence of ATP or AMP. Data are presented as mean ± SD. ATP-dependent uptake into vesicles was determined from three (MRP3) or four (MRP4) independent experiments performed in triplicate; *p<0.05 vs. respective control.

Figure 3.2

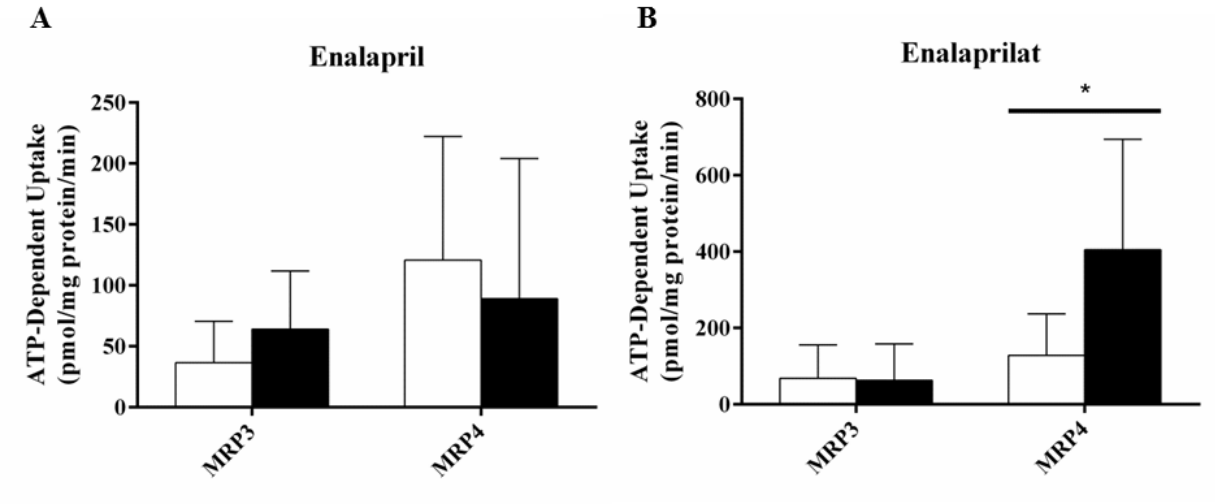

Figure 3.3: Effect of MK-571 on MRP4-mediated enalaprilat transport. Membrane vesicles prepared from MRP4-expressing HEK293T cells were incubated with enalaprilat (100 µM) for 5 min with and without MK-571 (50 µM). MRP4-dependent ATP-dependent uptake was calculated and normalized to transport in MRP4 vesicles in the absence of MK-571. Data are presented as mean ± SD of three independent experiments performed in triplicate; *p<0.05 vehicle control vs. MK-571.

Figure 3.3

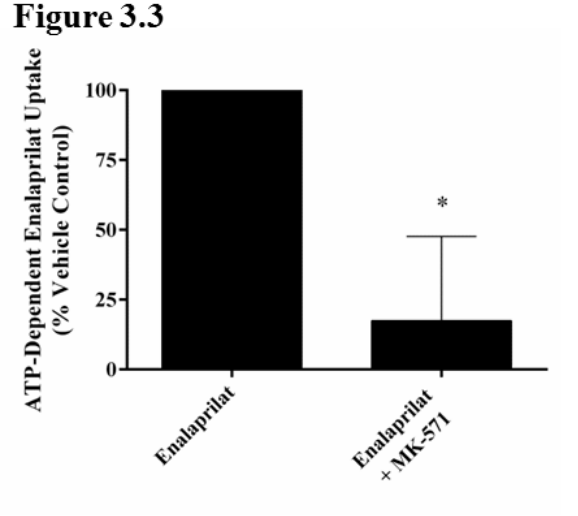

Figure 3.4: Disposition of taurocholate and rosuvastatin (left panel) as well as enalapril and derived enalaprilat (right panel) in human sandwich-cultured hepatocytes (SCH). Accumulation of taurocholate, rosuvastatin, enalapril and enalaprilat in cells + bile (black bars) and cells (white bars) in human SCH was measured following a 10-min incubation with [^{3}H]taurocholate (1 µM), [^{3}H]rosuvastatin (1 µM) or enalapril (5 µM) . The biliary excretion index (BEI) was calculated as detailed in the "Materials and Methods" section; BEI values for enalapril and enalaprilat were negligible. Data represent the mean ± SD of triplicate measurements in three independent hepatocyte preparations for taurocholate and rosuvastatin, or triplicate measurements in two independent hepatocyte preparations for enalapril and enalaprilat.

Figure 3.4

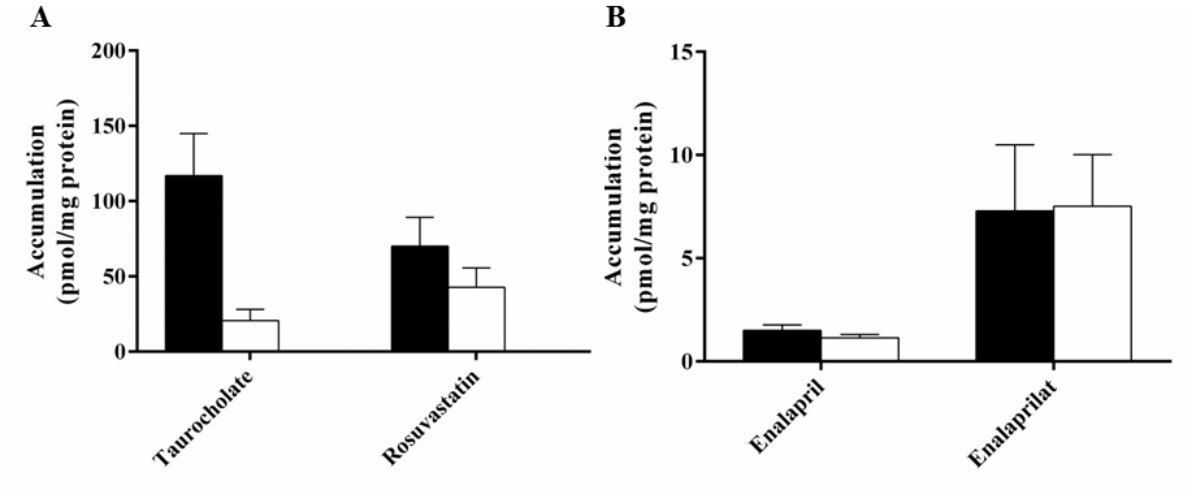

Figure 3.5: Effect of MK-571 on the intrinsic basolateral efflux clearance of enalaprilat in human sandwich-cultured hepatocytes. Intrinsic basolateral efflux clearance ($CL_{int,\ basolateral}$) of enalaprilat was calculated as described in the "Materials and Methods". Clearance values are expressed as a percent of vehicle-treated control. Data are presented as mean ± SD of three independent experiments performed in triplicate; *p<0.05 vehicle control vs. MK-571.

Figure 3.5

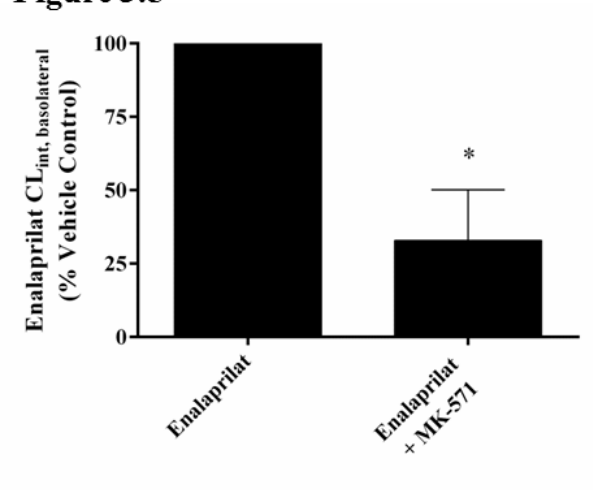

CHAPTER 4. Altered Morphine-Glucuronide and Bile Acid Disposition in Patients with Non-Alcoholic Steatohepatitis

Introduction

Non-alcoholic fatty liver disease (NAFLD) is a progressive liver disease ranging from simple steatosis to cirrhosis of the liver. Non-alcoholic steatohepatitis (NASH) is an intermediate pathologic state on the pathway from simple steatosis to cirrhosis that is characterized by hepatocyte steatosis, ballooning, inflammation and fibrosis.[1] NASH is strongly associated with insulin resistance and metabolic syndrome. NAFLD is believed to be the most common cause of chronic liver disease in the Western world and is recognized as a major public health concern.[2] Equally concerning is the fact that many patients are unaware of their disease until progression to advanced stages has occurred.[3] Left untreated, NAFLD and NASH can progress to advanced fibrosis, cirrhosis and hepatocellular carcinoma, ultimately requiring liver transplantation in some patients.[1] Medications such as metformin, pioglitazone, rosiglitazone and rosuvastatin have been used to improve insulin resistance to reverse the inflammation associated with NAFLD and prevent fibrosis.[4-7] Although modest reductions in serum liver function markers were observed with these medications, histologically, the progression of fibrosis was not reliably prevented or did not regress for any tested pharmacologic intervention. The major site of action of these medications is within hepatocytes; thus, diminished activity may be partially due to decreased hepatocellular concentrations.[8]

The dynamic interplay between hepatic sinusoidal uptake transporters, drug metabolizing enzymes, and basolateral and/or canalicular efflux transporters regulates hepatocellular concentrations

---

This work has been presented, in part, at the ASCPT Annual Meeting, Atlanta, GA, March 18-22, 2014 and has been submitted to *Clinical Pharmacology and Therapeutics* and is presented in the style of that journal.

and exposure to medications and their metabolites.[9,10] Modest changes in one or more of these processes can impact systemic and/or hepatocellular concentrations.[11,12] Bile acid concentrations are regulated by these factors as well as de novo synthesis within hepatocytes; intestinal hydrolysis and transporters, which facilitate reabsorption, also contribute to bile acid exposure.[13] Recently, expression of many uptake and efflux transporters and drug metabolizing enzymes was evaluated in liver samples from patients with NASH compared to healthy subjects. In general, NASH down-regulated transport proteins responsible for hepatic uptake of drugs and bile acids (e.g., organic anion transporting polypeptides [OATPs], sodium-taurocholate cotransporting polypeptide [NTCP]), and up-regulated hepatic excretory proteins (e.g., multidrug resistance-associated protein [MRP]3, MRP4, breast cancer resistance protein [BCRP], MRP2).[14-17] However, the impact of the observed up-regulation in MRP2 protein is difficult to predict due to altered localization of this canalicular protein. In contrast to the predictable nature of the changes observed with transporters (i.e., decreased uptake and increased efflux), cytochrome P450s (CYPs), uridine 5'-diphospho-glucuronosyltransferases (UGTs) and sulfotransferases (SULTs) generally were unchanged with few exceptions.[16] Altered transporter expression in NASH patients is expected to impair hepatic uptake and shift excretion of anionic drugs/hepatically-derived metabolites from bile to sinusoidal blood, resulting in decreased liver exposure and increased systemic concentrations/exposure. These changes may decrease activity or efficacy of highly transported bioactive endogenous substrates, medications and/or hepatically-derived metabolites with an intrahepatic site of action.[4-7]

Despite a general understanding of the impact of decreased transporter-mediated hepatic uptake of medications on systemic and hepatic concentrations[11,18], the importance of altered basolateral efflux is underappreciated. The functional impact of altered uptake and/or efflux transporter expression has not been evaluated in NASH patients.[9,10,19] Therefore, the primary objective of this study was to assess the functional impact of altered hepatic transporter expression in patients with biopsy-confirmed NASH compared to healthy subjects. Hepatically-derived glucuronide conjugates of morphine were selected as a phenotypic probe to evaluate MRP3 function for several reasons: 1) morphine enters the hepatocyte via a combination of passive diffusion and active transport[20] and is unaffected by changes in uptake

transporters known to be altered in NASH[17]; 2) hepatic expression of UGT2B7, which metabolizes morphine to morphine-3- and -6-glucuronide, is not altered in NASH[9,10,16,21]; 3) morphine is eliminated almost exclusively as morphine glucuronide in the urine, suggesting that basolateral efflux is important in the systemic and hepatic disposition; and 4) MRP3 appears to be the only protein that transports hepatically-derived morphine glucuronide into sinusoidal blood.[22,23] Additionally, Mrp3 protein expression positively correlated with basolateral efflux clearance of the Mrp3 substrate acetaminophen glucuronide in rat, and human *UGT2B7* polymorphisms that exhibit decreased function appear to have minimal impact on the systemic concentrations of morphine glucuronide.[24,25] Therefore, systemic morphine glucuronide concentrations should increase in patients with NASH due to MRP3 up-regulation compared to healthy subjects; the pharmacokinetics of parent morphine should be unaffected. Altered transporter expression in patients with NASH could have implications for other MRP3-transported substrates such as endogenous glycocholate and taurocholate.[26] Although bile acids are formed in the liver and generally undergo efficient enterohepatic recirculation[27], increased serum concentrations under fasting conditions would be consistent with decreased hepatic uptake and increased basolateral efflux. Therefore, the secondary objective of this study was to evaluate fasting serum concentrations of total bile acids, glycocholate and taurocholate in patients with NASH compared to healthy subjects.

Results

Study Subjects

Twenty-one volunteers (14 healthy subjects and 7 patients with biopsy-confirmed NASH) were studied (Table 4.1; see Supplementary Figure 4.1 for a summary of volunteer recruitment, enrollment and completion). In selecting healthy subjects, effort was made to recruit a control cohort comparable to the NASH cohort with respect to age, sex, race, and ethnicity. As expected, patients with NASH weighed more and had a higher body mass index (BMI) than the healthy subjects. Serum creatinine was within normal limits for both groups (Table 4.2), resulting in glomerular filtration rates within normal limits for all subjects. Compared to healthy subjects, patients with NASH had higher serum alanine aminotransferase (ALT), alkaline phosphatase (ALP), triglycerides, and insulin resistance as demonstrated by increased fasting glucose and insulin levels, as well as homeostasis model for assessing insulin resistance (HOMA-IR) scores, and decreased HDL (Table 4.2). Biopsy results indicated that all NASH patients had a NAFLD activity score (NAS) of at least 4 with a maximum score of 6 and minimal to moderate (F0 to F3) fibrosis (Table 4.2).

Morphine Pharmacokinetics

The presence of NASH had minimal impact on the pharmacokinetics of intravenously administered morphine (Figure 4.1A and Table 4.3). No statistically significant mean differences were observed between subject groups for maximum serum concentration (C_{max}), area under the serum concentration-time curve to the last measured timepoint ($AUC_{0\text{-}last}$), AUC extrapolated to infinity ($AUC_{0\text{-}\infty}$), total mass of morphine excreted in urine over the 8-hr collection interval (X_{urine}), terminal volume of distribution (V_z), total body clearance (CL), or half-life ($t_{1/2}$). C_{max} for each subject was always at the timepoint immediately following the end of the infusion. The geometric mean C_{max} and $AUC_{0\text{-}last}$ for NASH patients were within 12% and 17%, respectively, of the corresponding values for healthy subjects (Table 4.3).

Morphine Glucuronide Pharmacokinetics

The geometric mean morphine-3-glucuonide $AUC_{0-\infty}$ was approximately 10-fold higher than morphine-6-glucuronide $AUC_{0-\infty}$ in healthy subjects (Figure 4.1), consistent with literature reports.[28,29] The percent difference in C_{max}, time to reach C_{max} (T_{max}), AUC_{0-last}, $AUC_{0-\infty}$, and $t_{1/2}$ for morphine-3-glucuronide in both subject groups (Figure 4.1) exhibited similar trends as morphine-6-glucuronide when evaluated separately. Therefore, for brevity, morphine-3-glucuronide and morphine-6-glucuronide molar concentrations were combined for statistical analysis and reported as "morphine glucuronide".

Morphine glucuronide geometric mean C_{max} and AUC_{0-last} were 52% and 58% higher, respectively, in patients with NASH compared to healthy subjects following intravenous morphine administration ($P = 0.001$ and $P = 0.005$, respectively; Figure 4.1B and Table 4.3). From controls to NASH patients, the median T_{max} shifted by 61% from 38 min to 15 min ($P = 0.427$). The two cohorts were similar with respect to morphine glucuronide X_{urine} ($P = 0.475$) and $t_{1/2}$ ($P = 0.163$) (Table 4.3).

Fasting Serum Bile Acids

Fasting total bile acids, glycocholate and taurocholate serum concentrations in healthy subjects were 1.5±0.6, 0.08±0.06 and 0.02±0.02 μM, similar to previous reports.[30] Total bile acid, glycocholate and taurocholate serum concentrations in patients with NASH were increased 2.5-, 3.1-, and 5.7-fold, respectively, compared to healthy subjects ($P = 0.022$, $P = 0.017$, $P = 0.047$, respectively; Figure 4.2).

Linear Regression

Linear regression models detected an association between the NASH severity score (NAS+Fibrosis scores) and fasting total bile acid, glycocholate and taurocholate serum concentrations (Figure 4.3). Linear regression models also were used to identify clinical predictors of morphine glucuronide disposition. Considered individually, the clinical predictors identified included NASH severity score, waist circumference, waist-to-hip circumference ratio, ALP, fasting glucose, triglycerides, HDL, insulin and HOMA-IR (Table 4.4). When these candidate clinical predictors of morphine

glucuronide were included together in multivariable linear regression models for C_{max} and $AUC_{0\text{-}last}$, only NASH severity remained statistically significantly (Figure 4.3 and Table 4.4).

Discussion

This study is the first designed to assess the impact of a disease-associated increase in hepatic basolateral efflux transporter expression on drug disposition in humans. This study demonstrated that patients with NASH, a liver disease associated with increased protein expression of the hepatic basolateral efflux transporter MRP3, exhibited increased systemic concentrations of morphine glucuronide.[15] The primary endpoint, C_{max} of hepatically-derived morphine glucuronide, which was selected based on the mathematical model developed *a priori*, was higher in patients with NASH compared to healthy subjects (Figure 4.1 and Table 4.3). The increase in morphine glucuronide C_{max} in patients with NASH likely reflected increased hepatic MRP3, which transports glucuronide conjugates from hepatocytes to blood.[15,22] Multivariable linear regression analysis of clinical liver function markers, insulin resistance metrics and biopsy results indicated that only biopsy-determined NASH severity (NAS+Fibrosis) independently predicted the increase in both morphine glucuronide C_{max} and $AUC_{0\text{-last}}$ (Figure 4.3 and Table 4.4). The secondary endpoint, fasting serum bile acid concentrations, was statistically significantly higher in patients with NASH compared to healthy volunteers and positively correlated with NASH severity based on biopsy scores (Figure 4.2). Specifically, serum concentrations of glycocholate and taurocholate, endogenous bile acids that are MRP3 substrates[26], also were increased in NASH patients with varying degrees of disease progression/inflammation. These findings suggest that in the progressive inflammatory states investigated in this study, increasing NASH severity may further increase MRP3 function.

Recently, altered drug metabolizing enzyme and transporter expression was evaluated in liver biopsies from healthy subjects and from patients exhibiting varying degrees of NAFLD, from simple steatosis to steatohepatitis.[14-17] Through what appears to be an adaptive mechanism to prevent further hepatic damage, uptake transporters are generally down-regulated, whereas efflux transporters are up-regulated. Although these changes in expression patterns may protect the hepatocyte from toxins (e.g., increased bile acid concentrations), such alterations may have unanticipated effects on the efficacy of medications that rely on these transporters for hepatic entry and retention. Results from this study and

prior pharmacokinetic modeling of morphine/morphine glucuronide hepatic exposure are consistent with this notion.[31]

Although systematic, comprehensive investigations of altered drug metabolism and/or transport have not been conducted for most hepatic disease states, altered clearance of choline following oral administration to patients with NASH was decreased compared to healthy volunteers.[32] The authors proposed that the increased systemic choline concentrations were due to decreased metabolism secondary to reduced microsomal triglyceride transfer protein function in patients with NASH. Alternatively, increased choline elimination from the blood can be attributed, at least in part, to reduced hepatic uptake and/or increased basolateral efflux.[33] Altered hepatic drug transport was observed in rodent models of NASH.[34] For example, increased systemic and decreased hepatic exposure to simvastatin acid were reported in rats with diet-induced NASH compared to control.[34] Additionally, bile acid concentrations were increased in rodent models of steatosis.[35] Clearly, a growing body of literature demonstrates the importance of altered hepatic uptake and efflux on the systemic and hepatic disposition of many drugs, metabolites, and endogenous substrates.[32,34,35]

Altered hepatic transport due to disease or drug-drug interactions that shifts the predominant excretion pathway of drugs/metabolites can have unexpected consequences on systemic and hepatic disposition and ultimately, therapeutic efficacy and/or toxicity. For example, coadministration of cyclosporine, a potent inhibitor of hepatic transport proteins, with mycophenolate mofetil in transplant patients unexpectedly decreased mycophenolic acid systemic exposure.[36] Further investigation revealed that inhibition of canalicular transport likely shifted the excretion profile of mycophenolic acid glucuronide from predominantly biliary, with subsequent enterohepatic recycling of mycophenolic acid, to hepatic basolateral efflux and ultimately urinary excretion.[37] The recent failure of rosuvastatin to decrease histologic severity or prevent worsening fibrosis in patients with NASH[7] may be an example of altered transporter-mediated pharmacokinetics; decreased hepatic uptake[17,34], with a shift toward basolateral excretion and ultimately terminal urinary elimination[38,39], potentially decreased the hepatic exposure and therapeutic efficacy of rosuvastatin.

Altered hepatic transporter expression may influence the disposition of endogenous compounds (e.g., bile acids) in addition to drugs/metabolites. Bile acids are formed in the liver and undergo efficient enterohepatic recirculation, resulting in low systemic serum concentrations.[30] Fasting serum concentrations of total bile acids, glycocholate, and taurocholate were increased 2.5- to 5.7-fold in patients with NASH compared to healthy controls. These changes correlate with previous reports of intrahepatic bile acid concentrations in liver tissue from patients with NASH compared to healthy subjects.[40] In addition to MRP3 up-regulation, and down-regulation of NTCP and OATPs, taurine conjugation is increased.[40] Further studies are ongoing to investigate the influence of alterations in the bile acid profile in patients with NASH on drug disposition, efficacy and toxicity.

Some limitations are associated with this work. First, this study enrolled a relatively small number of patients with NASH. However, low enrollment was balanced by increased statistical precision obtained by recruiting 2:1 healthy subjects to patients with NASH. Second, to define a homogenous population of healthy subjects, only subjects without insulin resistance and with normal liver enzymes were enrolled in an effort to exclude subjects with prevalent steatosis. Exclusion of patients with probable steatosis was performed for two reasons: 1) since biopsies were not obtained as part of this study and the prevalence of undiagnosed NAFLD/NASH is very high in the overall population, differentiation of non-NAFLD healthy subjects with insulin resistance vs. prevalent simple steatosis or NASH was not possible, and 2) changes in transporter-mediated drug/metabolite disposition are only expected following onset of inflammation (i.e., NAS>3) when efflux transporter expression is up-regulated.[15,17]

In conclusion, patients with NASH exhibited increased morphine glucuronide C_{max} and $AUC_{0\text{-last}}$, as well as fasting serum concentrations of total bile acids, glycocholate, and taurocholate compared to healthy volunteers. These changes are consistent with NASH-associated alterations in expression of hepatic transport proteins reported previously (e.g., increased MRP3). Increased C_{max} and exposure to morphine glucuronide conjugates, as well as bile acids, positively correlated with biopsy-determined NASH severity. Given the increasing incidence of NASH, changes in hepatic transport proteins contributing to altered disposition of drugs/metabolites and bile acids may have a major impact on drug

efficacy and/or toxicity. Understanding the consequences of alterations in transporter-mediated disposition is paramount for new medications that will be administered to patients who may have underlying, undiagnosed liver disease.

Patients and Methods

Patients

Healthy subjects and patients with biopsy-confirmed NASH, between 18 and 65 years of age and of any race and ethnicity who reported drinking less than 20 g/day of alcohol, were enrolled in the study. General inclusion criteria for both groups were normal serum creatinine and total bilirubin levels; nonreactive HIV, hepatitis B antigen and hepatitis C antibody; no history of gastrointestinal surgery, autoimmune disease or other GI/liver disease. Subjects were excluded if they were unable to pass a urine drug screen for opiates, marijuana and barbiturates; female subjects were excluded if they were, or were trying to become, pregnant. Healthy volunteers were eligible if all of the following applied: ALP and ALT levels within normal limits; HOMA-IR score < 2.5; BMI ≤ 30 kg/m^2; not taking any concomitant medications other than birth control or a standard multivitamin. In selecting healthy subjects, effort was made to recruit a control cohort comparable to the NASH cohort with respect to age, sex, race, and ethnicity. Patients with NASH were recruited from the University of North Carolina at Chapel Hill (UNC-CH) hepatology clinic and were eligible for enrollment if all of the following applied: biopsy confirmed non-cirrhotic NASH with non-alcoholic fatty liver disease activity score (NAS) >3 [41]; BMI ≤ 45 kg/m^2; no treatment for type 2 diabetes other than metformin; no milk thistle products or high dose antioxidant treatment during the prior 30 days; absence of prior treatment with NASH-inducing drugs (i.e., tamoxifen, amiodarone, valproate, methotrexate). Written informed consent was obtained from all subjects. This study was approved by the UNC Biomedical Institutional Review Board and published in ClinicalTrials.gov (NCT01766960).

Study Design

This single center, comparative cohort, proof-of-concept study evaluated morphine and morphine glucuronide pharmacokinetics in healthy subjects and patients with NASH. Subjects and patients who met all inclusion/exclusion criteria fasted overnight prior to presenting to the Clinical and Translational Research Center at UNC-CH Hospitals. Following admission, hip and waist circumferences were

measured, vital signs were assessed, and an i.v. catheter was placed in each arm delivering 50 mL/hr of either normal saline or lactated Ringer's solution. Patients ate a standardized breakfast sandwich containing 23.9 g of fat and finished within 30 min. Two hours after completion of the meal, a 5 mg i.v. dose of morphine sulfate was administered as an infusion over 5 min. Blood (5 mL) was collected in glass tubes pre-dose, end of infusion (0), and 5, 10, 15, 30, 45, 60, 90, 120, 180, 240, 300, 360, 420, and 480 min after the end of the infusion; urine was collected at 4-hr intervals after the end of the infusion. Blood samples were allowed to clot for 30 to 60 min, and serum was separated, divided into aliquots and frozen. Serum and urine samples were stored at -80°C until analysis. Following discontinuation of both i.v. lines, patients were administered a safety questionnaire and discharged to a waiting third party to be driven home.

Sample Processing and Analysis

Morphine serum and urine samples were analyzed in batches every three months according to a validated bioanalytical method (see supplementary materials).[42] Briefly, aliquots (100 µL) of serum and urine samples were transferred to a 96-well plate insert; proteins were precipitated with 600 µL acetonitrile containing morphine-d_3, morphine-3-glucuronide-d_3 and morphine-6-glucuronide-d_3 (100 ng/mL) as internal standards (Lipomed, Cambridge, MA). Samples were mixed by vortex for 2.5 min and centrifuged (3,000g for 20 min at 4° C). Supernatant (500 µL) was transferred to a separate 96-well plate insert, dried under nitrogen, and 100 µL of 50:50 water:methanol were added to each insert. Calibration solutions and quality controls containing all three analytes (Lipomed) were prepared similarly using pooled naïve plasma or urine.

Morphine and morphine glucuronide concentrations were measured by high resolution liquid chromatography coupled with an ABSciex 5600 TripleTOF mass spectrometer (LC-MS/MS) as described previously.[42] For morphine analysis, the product of 286.14 with an exact m/z of 286.1200 was monitored. Morphine-3-glucuronide and morphine-6-glucuronide were monitored using an exact m/z of 462.1700. The deuterated internal standards for the glucuronides were monitored using an exact m/z of 465.1900.

Deuterated morphine was monitored at an exact m/z of 289.1600. The two morphine glucuronides were separated chromatographically; insource fragmentation from morphine glucuronide to morphine was negligible.

All 30 bile acid standards were obtained from Steraloids Inc. (Newport, RI), and stable isotope-labeled standards were obtained from C/D/N Isotopes Inc. (Quebec, Canada). The sample preparation followed a published method with modifications.[30] Briefly, 50 µL of serum or standard solution was spiked with 150 µL of internal standard (IS). After centrifugation, the supernatant was transferred to a clean plate and evaporated to dryness. The residue was reconstituted with 20 µL of acetonitrile and 20 µL of water and filtered through a 0.45 µm membrane before injecting 5 µL into the UPLC-MS/MS (ACQUITY UPLC-Xevo TQ-S, Waters Corp., Milford, MA) to quantitate 30 bile acids in serum. The optimized instrument settings are described in the supplementary materials. The sum of all measured bile acids is reported as total bile acids.

Mathematical Modeling and Simulation for Sample Size Calculation

A previously published whole body physiologically-based pharmacokinetic (PBPK) model was used as a base model to describe the disposition of morphine and morphine glucuronide.[43] The model was developed using Phoenix® WinNonlin® (v6.3; Certara, St. Louis, MO) and was parameterized with adult reference values.[43,44] The kinetics of morphine in all the tissues was assumed to be described by a flow-limited, well-mixed model; the distribution of morphine glucuronide was governed by hepatic MRP3-mediated basolateral, and MRP2-mediated canalicular, efflux clearances (CL_{MRP3} and CL_{MRP2}, respectively). Serum morphine-3- and -6-glucuronide were modeled as a single metabolite, morphine glucuronide. Morphine glucuronide metabolites were assumed to be eliminated by the kidney via glomerular filtration. Model optimization was guided by assessing the model output compared to data extracted from published clinical studies.[28,29,45-48] The model was used to simulate altered disposition of morphine and metabolites in virtual patients. Patients with NASH were assumed to have a 3-fold higher morphine glucuronide CL_{MRP3} based on published MRP3 protein expression compared to healthy

patients.[15] Simulations demonstrated a 36% increase in glucuronide C_{max} (data not shown).[31] The difference in mean C_{max} (ΔC_{max}) was selected as the primary endpoint. Based on the modeling output and estimates of variability from two studies using similar analytical techniques[28,47], the number of subjects recruited (14 healthy subjects, 7 NASH patients) was projected to provide sufficient power to reject the null hypothesis of no difference in C_{max} between subject groups.

Pharmacokinetic Data Analysis

Morphine, morphine-3-glucuronide and morphine-6-glucuronide pharmacokinetics were evaluated using non-compartmental analysis (Phoenix® WinNonlin® v6.3). C_{max}, time to reach C_{max} (T_{max}), last measureable concentration (C_{last}), terminal volume of distribution (V_z, for morphine only) and terminal elimination rate constant (λ_z) were estimated from the serum concentration-time profile. The area under the concentration-time curve (AUC) from time zero to the last measurable concentration ($AUC_{0\text{-}last}$) was determined using a linear-up log-trapezoidal-down algorithm. Total AUC ($AUC_{0\text{-}\infty}$) was calculated as the sum of $AUC_{0\text{-}last}$ and C_{last}/λ_z. The terminal half-life ($t_{1/2}$) was calculated as $0.693/\lambda_z$. Total body clearance (CL) of morphine was calculated as the ratio of dose to $AUC_{0\text{-}\infty}$. The total mass of morphine and morphine glucuronide excreted in urine over the 8-hr collection interval (X_{urine}) was calculated as the product of urine concentration and volume of urine collected. Concentrations below the limit of quantification were excluded from the analysis.

Statistical Analysis Strategy

Morphine and morphine glucuronide pharmacokinetic metrics are presented as geometric means and 95% CIs with the exception of T_{max}, which is presented as median and range. Log transformed metrics were compared between groups using a two-tailed *t*-test of size $\alpha = 0.05$; the Wilcoxon Mann-Whitney test was used to detect cohort differences in median T_{max}.

Linear regression models were used to identify clinical predictors of morphine glucuronide $AUC_{0\text{-}last}$ and C_{max}. Candidate clinical predictors included age, BMI, body weight, waist and hip

circumference, waist-to-hip ratio, SCr, ALT, ALP, albumin, total bilirubin, NASH severity score, fasting glucose, triglycerides, HDL and LDL cholesterol, insulin, and HOMA-IR. Separate models for $AUC_{0\text{-last}}$ and C_{max} were fit for each of these predictors. Clinical variables with statistically significant predictive value were included in a multivariable regression model subject to backward elimination. The criterion for retention in the multivariable model was $P \leq 0.10$. NASH severity scores for healthy subjects were assumed to be zero. All statistical computations for the primary analyses were performed using SAS software (v9.3; SAS Institute, Inc., Cary, NC). Unless otherwise stated, data are presented as mean and standard deviation, and a two-tailed *t*-test was used to determine significant differences; $P<0.05$ was considered significant for all tests.

Study Highlights

What is the current knowledge on the topic?

Hepatic transport protein expression is altered in patients with NASH (e.g., MRP3 up-regulation), a prevalent form of liver disease associated with increased mortality. However, functional changes in transporter-mediated drug disposition have not been evaluated in NASH.

What question did the study address?

Hepatically-derived morphine glucuronide and fasting bile acid serum concentrations were evaluated as a phenotypic probe of MRP3 in biopsy-confirmed NASH patients vs. healthy subjects.

What this study adds to our knowledge?

Morphine glucuronide systemic exposure and serum bile acid concentrations were significantly higher in NASH patients vs. healthy subjects. NASH severity was significantly associated with morphine glucuronide and bile acid serum concentrations.

How this might change clinical pharmacology and therapeutics?

NASH patients may exhibit increased systemic exposure to MRP3 substrates (e.g., anionic drugs/metabolites, bile acids). These changes may lead to increased systemic toxicities and decreased hepatic drug efficacy. Understanding the consequences of altered transporter-mediated disposition and hepatic clearance is paramount for medications used in NASH patients. This new knowledge may help guide drug/dose selection in NASH.

REFERENCES

1. Chalasani, N., Younossi, Z., Lavine, J. E., Diehl, A. M., Brunt, E. M., Cusi, K., Charlton, M.Sanyal, A. J. 2012. The diagnosis and management of non-alcoholic fatty liver disease: practice guideline by the American Gastroenterological Association, American Association for the Study of Liver Diseases, and American College of Gastroenterology. Gastroenterology 142(7);1592-609.

2. Browning, J. D., Szczepaniak, L. S., Dobbins, R., Nuremberg, P., Horton, J. D., Cohen, J. C., Grundy, S. M.Hobbs, H. H. 2004. Prevalence of hepatic steatosis in an urban population in the United States: impact of ethnicity. Hepatology 40(6);1387-95.

3. Williams, C. D., Stengel, J., Asike, M. I., Torres, D. M., Shaw, J., Contreras, M., Landt, C. L.Harrison, S. A. 2011. Prevalence of nonalcoholic fatty liver disease and nonalcoholic steatohepatitis among a largely middle-aged population utilizing ultrasound and liver biopsy: a prospective study. Gastroenterology 140(1);124-31.

4. Torres, D. M., Jones, F. J., Shaw, J. C., Williams, C. D., Ward, J. A.Harrison, S. A. 2011. Rosiglitazone versus rosiglitazone and metformin versus rosiglitazone and losartan in the treatment of nonalcoholic steatohepatitis in humans: a 12-month randomized, prospective, open-label trial. Hepatology 54(5);1631-9.

5. Tikkanen, M. J., Fayyad, R., Faergeman, O., Olsson, A. G., Wun, C. C., Laskey, R., Kastelein, J. J., Holme, I.Pedersen, T. R. 2013. Effect of intensive lipid lowering with atorvastatin on cardiovascular outcomes in coronary heart disease patients with mild-to-moderate baseline elevations in alanine aminotransferase levels. International journal of cardiology.

6. Sanyal, A. J., Chalasani, N., Kowdley, K. V., McCullough, A., Diehl, A. M., Bass, N. M., Neuschwander-Tetri, B. A., Lavine, J. E., Tonascia, J., Unalp, A., Van Natta, M., Clark, J., Brunt, E. M., Kleiner, D. E., Hoofnagle, J. H.Robuck, P. R. 2010. Pioglitazone, vitamin E, or placebo for nonalcoholic steatohepatitis. The New England journal of medicine 362(18);1675-85.

7. Nakahara, T., Hyogo, H., Kimura, Y., Ishitobi, T., Arihiro, K., Aikata, H., Takahashi, S.Chayama, K. 2012. Efficacy of rosuvastatin for the treatment of non-alcoholic steatohepatitis with dyslipidemia: An open-label, pilot study. Hepatology research : the official journal of the Japan Society of Hepatology 42(11);1065-72.

8. Chu, X., Korzekwa, K., Elsby, R., Fenner, K., Galetin, A., Lai, Y., Matsson, P., Moss, A., Nagar, S., Rosania, G. R., Bai, J. P., Polli, J. W., Sugiyama, Y.Brouwer, K. L. 2013. Intracellular drug concentrations and transporters: measurement, modeling, and implications for the liver. Clinical pharmacology and therapeutics 94(1);126-41.

9. Kock, K.Brouwer, K. L. 2012. A perspective on efflux transport proteins in the liver. Clinical pharmacology and therapeutics 92(5);599-612.

10. Zamek-Gliszczynski, M. J., Chu, X., Polli, J. W., Paine, M. F.Galetin, A. 2013. Understanding the Transport Properties of Metabolites: Case Studies and Considerations for Drug Development. Drug metabolism and disposition: the biological fate of chemicals.

11. Pfeifer, N. D., Goss, S. L., Swift, B., Ghibellini, G., Ivanovic, M., Heizer, W. D., Gangarosa, L. M.Brouwer, K. L. 2013. Effect of Ritonavir on (99m)Technetium-Mebrofenin Disposition in

Humans: A Semi-PBPK Modeling and In Vitro Approach to Predict Transporter-Mediated DDIs. CPT: pharmacometrics & systems pharmacology 2;e20.

12. Filppula, A. M., Tornio, A., Niemi, M., Neuvonen, P. J.Backman, J. T. 2013. Gemfibrozil impairs imatinib absorption and inhibits the CYP2C8-mediated formation of its main metabolite. Clinical pharmacology and therapeutics 94(3);383-93.

13. Jonker, J. W., Liddle, C.Downes, M. 2012. FXR and PXR: potential therapeutic targets in cholestasis. The Journal of steroid biochemistry and molecular biology 130(3-5);147-58.

14. Fisher, C. D., Lickteig, A. J., Augustine, L. M., Ranger-Moore, J., Jackson, J. P., Ferguson, S. S.Cherrington, N. J. 2009. Hepatic cytochrome P450 enzyme alterations in humans with progressive stages of nonalcoholic fatty liver disease. Drug metabolism and disposition: the biological fate of chemicals 37(10);2087-94.

15. Hardwick, R. N., Fisher, C. D., Canet, M. J., Scheffer, G. L.Cherrington, N. J. 2011. Variations in ATP-binding cassette transporter regulation during the progression of human nonalcoholic fatty liver disease. Drug metabolism and disposition: the biological fate of chemicals 39(12);2395-402.

16. Hardwick, R. N., Ferreira, D. W., More, V. R., Lake, A. D., Lu, Z., Manautou, J. E., Slitt, A. L.Cherrington, N. J. 2013. Altered UDP-glucuronosyltransferase and sulfotransferase expression and function during progressive stages of human nonalcoholic fatty liver disease. Drug metabolism and disposition: the biological fate of chemicals 41(3);554-61.

17. Lake, A. D., Novak, P., Fisher, C. D., Jackson, J. P., Hardwick, R. N., Billheimer, D. D., Klimecki, W. T.Cherrington, N. J. 2011. Analysis of global and absorption, distribution, metabolism, and elimination gene expression in the progressive stages of human nonalcoholic fatty liver disease. Drug metabolism and disposition: the biological fate of chemicals 39(10);1954-60.

18. Watanabe, T., Kusuhara, H., Maeda, K., Shitara, Y.Sugiyama, Y. 2009. Physiologically based pharmacokinetic modeling to predict transporter-mediated clearance and distribution of pravastatin in humans. The Journal of pharmacology and experimental therapeutics 328(2);652-62.

19. Pfeifer, N. D., Hardwick, R. N.Brouwer, K. L. 2014. Role of hepatic efflux transporters in regulating systemic and hepatocyte exposure to xenobiotics. Annual review of pharmacology and toxicology 54;509-35.

20. Tzvetkov, M. V., dos Santos Pereira, J. N., Meineke, I., Saadatmand, A. R., Stingl, J. C.Brockmoller, J. 2013. Morphine is a substrate of the organic cation transporter OCT1 and polymorphisms in OCT1 gene affect morphine pharmacokinetics after codeine administration. Biochemical pharmacology 86(5);666-78.

21. Bodenham, A., Quinn, K.Park, G. R. 1989. Extrahepatic morphine metabolism in man during the anhepatic phase of orthotopic liver transplantation. British journal of anaesthesia 63(4);380-4.

22. Zelcer, N., van de Wetering, K., Hillebrand, M., Sarton, E., Kuil, A., Wielinga, P. R., Tephly, T., Dahan, A., Beijnen, J. H.Borst, P. 2005. Mice lacking multidrug resistance protein 3 show altered morphine pharmacokinetics and morphine-6-glucuronide antinociception. Proc Natl Acad Sci U S A 102(20);7274-9.

23. van de Wetering, K., Zelcer, N., Kuil, A., Feddema, W., Hillebrand, M., Vlaming, M. L., Schinkel, A. H., Beijnen, J. H.Borst, P. 2007. Multidrug resistance proteins 2 and 3 provide alternative routes for hepatic excretion of morphine-glucuronides. Molecular pharmacology 72(2);387-94.

24. Holthe, M., Klepstad, P., Zahlsen, K., Borchgrevink, P. C., Hagen, L., Dale, O., Kaasa, S., Krokan, H. E.Skorpen, F. 2002. Morphine glucuronide-to-morphine plasma ratios are unaffected by the UGT2B7 H268Y and UGT1A1*28 polymorphisms in cancer patients on chronic morphine therapy. European journal of clinical pharmacology 58(5);353-6.

25. Xiong, H., Suzuki, H., Sugiyama, Y., Meier, P. J., Pollack, G. M.Brouwer, K. L. 2002. Mechanisms of impaired biliary excretion of acetaminophen glucuronide after acute phenobarbital treatment or phenobarbital pretreatment. Drug metabolism and disposition: the biological fate of chemicals 30(9);962-9.

26. Yamaguchi, K., Murai, T., Yabuuchi, H.Kurosawa, T. 2010. Measurement of transport activities of bile acids in human multidrug resistance-associated protein 3 using liquid chromatography-tandem mass spectrometry. Analytical sciences : the international journal of the Japan Society for Analytical Chemistry 26(3);317-23.

27. Ahlberg, J., Angelin, B., Bjorkhem, I.Einarsson, K. 1977. Individual bile acids in portal venous and systemic blood serum of fasting man. Gastroenterology 73(6);1377-82.

28. Osborne, R., Joel, S., Trew, D.Slevin, M. 1990. Morphine and metabolite behavior after different routes of morphine administration: demonstration of the importance of the active metabolite morphine-6-glucuronide. Clinical pharmacology and therapeutics 47(1);12-9.

29. Everts, B., Karlson, B. W., Herlitz, J.Hedner, T. 1998. Morphine use and pharmacokinetics in patients with chest pain due to suspected or definite acute myocardial infarction. Eur J Pain 2(2);115-125.

30. Garcia-Canaveras, J. C., Donato, M. T., Castell, J. V.Lahoz, A. 2012. Targeted profiling of circulating and hepatic bile acids in human, mouse, and rat using a UPLC-MRM-MS-validated method. Journal of lipid research 53(10);2231-41.

31. Johnston, C. K., Ferslew, B. C., Barritt, A. S.Brouwer, K. L. R. 2013. Mathematical Modeling of Systemic and Hepatic Disposition of Morphine and Morphine Glucuronides in Nonalcoholic Steatohepatitis to Inform Study Design. AAPS Journal.

32. Imajo, K., Yoneda, M., Fujita, K., Kessoku, T., Tomeno, W., Ogawa, Y., Shinohara, Y., Sekino, Y., Mawatari, H., Nozaki, Y., Kirikoshi, H., Taguri, M., Toshima, G., Takahashi, J., Saito, S., Wada, K.Nakajima, A. 2014. Oral choline tolerance test as a novel noninvasive method for predicting nonalcoholic steatohepatitis. Journal of gastroenterology 49(2);295-304.

33. Lockman, P.Allen, D. 2002. The transport of choline. Drug development and industrial pharmacy 28(7);749-771.

34. Clarke, J. D., Hardwick, R. N., Lake, A. D., Canet, M. J.Cherrington, N. J. 2014. Experimental nonalcoholic steatohepatitis increases exposure to simvastatin hydroxy Acid by decreasing hepatic organic anion transporting polypeptide expression. The Journal of pharmacology and experimental therapeutics 348(3);452-8.

35. Yamazaki, M., Miyake, M., Sato, H., Masutomi, N., Tsutsui, N., Adam, K. P., Alexander, D. C., Lawton, K. A., Milburn, M. V., Ryals, J. A., Wulff, J. E.Guo, L. 2013. Perturbation of bile acid homeostasis is an early pathogenesis event of drug induced liver injury in rats. Toxicology and applied pharmacology 268(1);79-89.

36. Pou, L., Brunet, M., Cantarell, C., Vidal, E., Oppenheimer, F., Monforte, V., Vilardell, J., Roman, A., Martorell, J.Capdevila, L. 2001. Mycophenolic acid plasma concentrations: influence of comedication. Therapeutic drug monitoring 23(1);35-8.

37. Matsunaga, N., Wada, S., Nakanishi, T., Ikenaga, M., Ogawa, M.Tamai, I. 2013. Mathematical Modeling of the in Vitro Hepatic Disposition of Mycophenolic Acid and Its Glucuronide in Sandwich-Cultured Human Hepatocytes. Molecular pharmaceutics.

38. Pfeifer, N. D., Bridges, A. S., Ferslew, B. C., Hardwick, R. N.Brouwer, K. L. 2013. Hepatic basolateral efflux contributes significantly to rosuvastatin disposition II: characterization of hepatic elimination by basolateral, biliary, and metabolic clearance pathways in rat isolated perfused liver. The Journal of pharmacology and experimental therapeutics 347(3);737-45.

39. Pfeifer, N. D., Yang, K.Brouwer, K. L. 2013. Hepatic Basolateral Efflux Contributes Significantly to Rosuvastatin Disposition: Characterization of Basolateral vs. Biliary Clearance Using a Novel Protocol in Sandwich-Cultured Hepatocytes. The Journal of pharmacology and experimental therapeutics.

40. Lake, A. D., Novak, P., Shipkova, P., Aranibar, N., Robertson, D., Reily, M. D., Lu, Z., Lehman-McKeeman, L. D.Cherrington, N. J. 2013. Decreased hepatotoxic bile acid composition and altered synthesis in progressive human nonalcoholic fatty liver disease. Toxicology and applied pharmacology 268(2);132-40.

41. Kleiner, D. E., Brunt, E. M., Van Natta, M., Behling, C., Contos, M. J., Cummings, O. W., Ferrell, L. D., Liu, Y. C., Torbenson, M. S., Unalp-Arida, A., Yeh, M., McCullough, A. J.Sanyal, A. J. 2005. Design and validation of a histological scoring system for nonalcoholic fatty liver disease. Hepatology 41(6);1313-21.

42. Clavijo, C. F., Hoffman, K. L., Thomas, J. J., Carvalho, B., Chu, L. F., Drover, D. R., Hammer, G. B., Christians, U.Galinkin, J. L. 2011. A sensitive assay for the quantification of morphine and its active metabolites in human plasma and dried blood spots using high-performance liquid chromatography-tandem mass spectrometry. Anal Bioanal Chem 400(3);715-28.

43. Chen, S. 2010. Physiologically-Based Pharmacokinetic (PBPK) Models for the Description of Sequential Metabolism of Codeine to Morphine and Morphine 3-Glucuronide (M3G) in Man and Rat. University of Toronto Thesis.

44. Brown, R. P., Delp, M. D., Lindstedt, S. L., Rhomberg, L. R.Beliles, R. P. 1997. Physiological parameter values for physiologically based pharmacokinetic models. Toxicology and industrial health 13(4);407-84.

45. Hanna, M. H., Peat, S. J., Knibb, A. A.Fung, C. 1991. Disposition of morphine-6-glucuronide and morphine in healthy volunteers. British journal of anaesthesia 66(1);103-7.

46. Lotsch, J., Skarke, C., Schmidt, H., Liefhold, J.Geisslinger, G. 2002. Pharmacokinetic modeling to predict morphine and morphine-6-glucuronide plasma concentrations in healthy young volunteers. Clinical pharmacology and therapeutics 72(2);151-62.

47. Skarke, C., Schmidt, H., Geisslinger, G., Darimont, J.Lotsch, J. 2003. Pharmacokinetics of morphine are not altered in subjects with Gilbert's syndrome. British journal of clinical pharmacology 56(2);228-31.

48. Murthy, B. R., Pollack, G. M.Brouwer, K. L. 2002. Contribution of morphine-6-glucuronide to antinociception following intravenous administration of morphine to healthy volunteers. Journal of clinical pharmacology 42(5);569-76.

Table 4.1: Demographic Characteristics of Study Participants

Parameter		Healthy (n=14)	NASH (n=7)
Sex			
	Men	7	3
	Women	7	4
Ethnicity			
	Hispanic	1	1
	Non-Hispanic	13	6
Race			
	White	12	7
	Black	2	0
Age (years)		42 (13)	48 (10)
Body weight (kg)		76 (14)	93 * (17)
Body mass index (kg/m^2)		26 (2.7)	32 * (5.2)
Waist circumference (cm)		90 (7.8)	118 * (23.5)
Hip circumference (cm)		103 (6.4)	117 * (16.4)
Waist-to-hip ratio	All subjects	0.87 (0.05)	1.03 * (0.26)
	Men	0.90 (0.03)	0.96 * (0.01)
	Women	0.84 (0.06)	1.08 (0.36)

Data presented as mean (SD)

* $P<0.05$ Student's two-tailed *t*-test comparing healthy subjects to patients with NASH

Table 4.2: Serum chemistries, insulin resistance and liver biopsy grade.

Clinical Parameter	Healthy	NASH
Creatinine (mg/dL)	0.82 (0.14)	0.80 (0.22)
ALT (U/L)	33 (11)	75 * (36)
ALP (U/L)	63 (13)	80 * (14)
Albumin (g/dL)	4.3 (0.3)	4.5 (0.4)
Total Bilirubin (mg/dL)	0.64 (0.22)	0.81 (0.29)
Cholesterol (mg/dL)	189 (40)	190 (48)
Triglycerides (mg/dL)	91 (46)	253 * (98)
HDL Cholesterol (mg/dL)	68 (26)	37 * (5)
LDL, calculated (mg/dL)	102 (34)	101 (47)
Fasting glucose (mg/dL)	86 (8)	124 * (16)
Serum Insulin (μIU/mL)	8 (3)	40 * (27)
HOMA-IR	2 (1)	12 * (9)
Total NAS Score	N/A	5 (4-6)
Steatosis	N/A	2 (1-3)
Hepatocyte Ballooning	N/A	2 (1-3)
Inflammation	N/A	1 (0-2)
Fibrosis	N/A	1 (0-3)
NAS + Fibrosis	N/A	7 (4-8)

Data presented as mean (SD); biopsy scoring presented as median (range)
ALT; alanine aminotransferase
ALP; alkaline phosphatase
HDL; high-density lipoprotein cholesterol
LDL; low-density lipoprotein cholesterol
NAS: non-alcoholic fatty liver disease activity score
HOMA-IR; homeostasis model for assessing insulin resistance
N/A; not applicable
* $P<0.05$ Student's two-tailed *t*-test comparing healthy subjects to patients with NASH

Table 4.3: Pharmacokinetic parameters for morphine and morphine glucuronide determined by non-compartmental analysis in healthy subjects and patients with NASH

	Morphine		Morphine Glucuronide	
Parameter	Healthy	NASH	Healthy	NASH
C_{max} (nM)	296 (237-369)	332 (200-551)	225 (194-261)	343 * (284-413)
T_{max} [a] (min)	0 (0-0)	0 (0-0)	38 (5-240)	15 (5-90)
$AUC_{0\text{-last}}$ (µM*min)	4.1 (3.1-5.3)	3.5 (2.4-5.0)	37.2 (31.6-43.7)	58.8 * (41.6-83.0)
$AUC_{0\text{-}\infty}$ (µM*min)	5.5 (4.3-6.9)	5.2 (3.7-7.4)	45.2 (37.5-54.5)	67.8 * (46.7-98.5)
V_z (L)	153 (125-188)	173 (113-264)	N/D	N/D
CL (L/min)	1.2 (1.0-1.5)	1.3 (0.9-1.8)	N/D	N/D
Half-life (min)	88 (66-117)	95 (49-182)	187 (153-229)	146 (104-205)
X_{urine} [b] (µmole)	0.89 (0.73-1.16)	0.64 (0.52-0.78)	5.38 (4.52-7.01)	6.23 (3.89-9.59)

Geometric mean (95% CI)
[a] Sum of molar concentrations of morphine-3- and morphine-6-glucuronide
[b] Median (range)
[c] Total mass excreted over 8-hr collection interval
* $P<0.05$ Student's two-tailed *t*-test of natural log transformed data comparing healthy subjects to patients with NASH
N/D: not determined

Table 4.4: Clinical predictors of morphine glucuronide C_{max} and $AUC_{0\text{-last}}$.

	Morphine Glucuronide[a]			
	C_{max}		$AUC_{0\text{-last}}$	
Parameter	β	*P*-value	β	*P*-value
NASH Severity Score[b]	18.51 (4.72)	0.001	4.11 (1.02)	0.001
Waist	1.96 (0.87)	0.036	0.40 (0.19)	0.051
Waist-to-Hip Ratio	157 (110)	0.170	48.86 (22.62)	0.044
ALP	3.14 (1.07)	0.008	0.59 (0.25)	0.027
Fasting Glucose	2.27 (0.75)	0.007	0.45 (0.17)	0.017
Triglycerides	0.42 (0.17)	0.019	0.09 (0.04)	0.024
HDL	-1.75 (0.62)	0.011	-0.20 (0.16)	0.216
Insulin	2.05 (0.78)	0.017	0.38 (0.18)	0.049
HOMA-IR	6.20 (2.35)	0.016	1.15 (0.54)	0.046

Data are presented as the regression parameter estimate (β) (standard error [SE] of the parameter estimate).
[a] Sum of molar concentrations of morphine-3- and morphine-6-glucuronide
[b] Only NASH severity score remained statistically significant when all nine clinical predictors were included in a multivariable regression model subject to backward elimination
ALP; alkaline phosphatase
NAS+Fibrosis; sum of non-alcoholic fatty liver disease activity and fibrosis scores
HOMA-IR; homeostasis model for assessing insulin resistance
N/S; not statistically significant

Figure Legends:

Figure 4.1: Serum morphine (circles, A), morphine-3-glucuronide (triangles, B), and morphine-6-glucuronide (squares, B) concentration vs. time profiles in healthy subjects (blue) and patients with NASH (red). Data are presented as geometric mean and 95% confidence intervals.

Figure 4.1

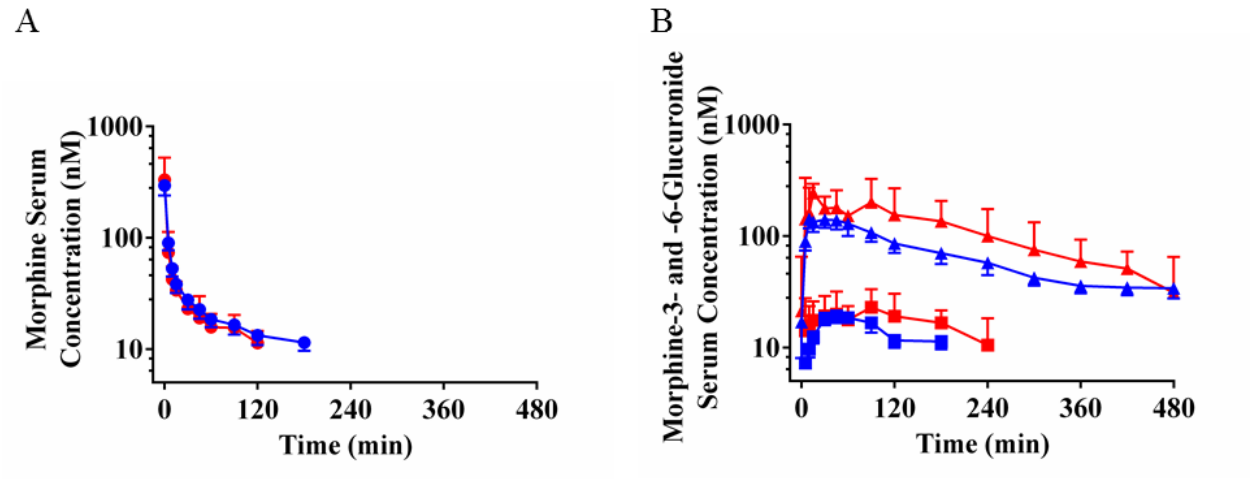

Figure 4.2: Fasting total bile acids, glycocholate and taurocholate serum concentrations in healthy subjects (black bars) and patients with NASH (grey bars). Data are presented as mean ± SE; * $P<0.05$. Results of univariate linear regression analysis of NASH severity (NAS+Fibrosis; sum of non-alcoholic fatty liver disease activity and fibrosis scores) with serum bile acid concentrations are included. Data are presented as the regression parameter estimate (β) and SE of the parameter estimate.

Figure 4.2

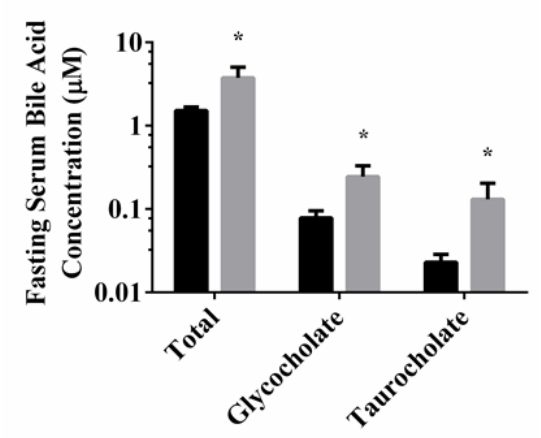

	Total Bile Acids		Glycocholate		Taurocholate	
Parameter	β	P-value	β	P-value	β	P-value
NAS+Fibrosis	0.43 (0.10)	0.004	0.03 (0.01)	0.001	0.02 (0.01)	0.006

Figure 4.3: Association of the NASH severity score (NAS+Fibrosis severity scores) with morphine glucuronide C_{max} (A) and $AUC_{0\text{-}last}$ (B). Values for patients with NASH (red triangles) and values for healthy subjects (blue circles) are shown with the linear regression and its 95% confidence limits (shaded area). The NASH severity score is the sum of the NAS and fibrosis biopsy scores; for healthy subjects, an imputed value of zero was assumed.

Figure 4.3

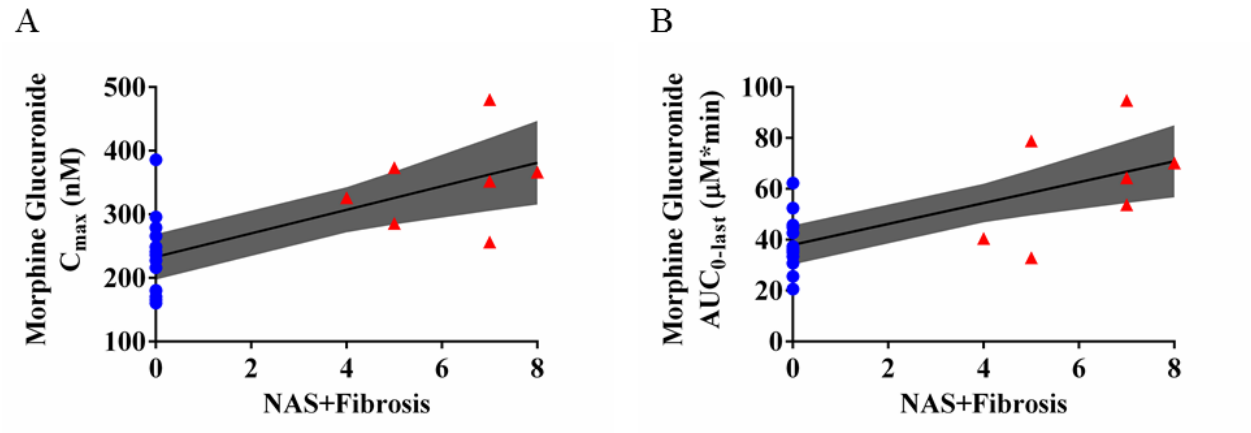

Supplement

Supplementary Methods: Morphine Serum and Urine Sample Processing and Analysis

Morphine and morphine glucuronide metabolites were analyzed using liquid chromatography coupled with tandem mass spectrometry (LC-MS/MS) as described previously.[1] A solvent delivery system (Shimadzu, Columbia, MD) and a Leap HTC Pal thermostated autosampler (LEAP Technologies, Carrboro, NC) connected to an AB Sciex 5600 TripleTOF (Framingham, MA) were used for analysis. Analyte separation was accomplished using an Aquasil C18, 150- 2.1-mm column, with a 5-µm particle size (Keystone Scientific, now Thermo Fisher Scientific, Waltham, MA). Analysis required 5 µl of sample and a solvent flow of 0.4 ml/min. The mass spectrometer was operated in positive ion time-of-flight- (TOF)-high resolution mode. Morphine 3-glucuronide and morphine 6-glucuronide were monitored using an exact m/z of 462.1700. The internal standards for the glucuronides were monitored using an exact m/z of 465.1900. Deuterated morphine was monitored at an exact m/z of 289.1600. However, interference precluded simple TOF monitoring of morphine. Thus, the product of 286.14 with an exact mass of 286.1200 was monitored. Calibration solutions (2.5-500 ng/mL and 25-5000 ng/mL for serum and urine, respectively) and quality controls (2.5, 8, 200 ng/mL and 25, 75, 250, 375, 1000, 4000 ng/mL for serum and urine, respectively) containing all three analytes (Lipomed) were prepared similarly using pooled naïve plasma or urine. Calibration curves were generated using peak area ratios of analyte to internal standard, samples were analyzed with matrix-matched standards and controls, care was taken to chromatographically separate the two morphine glucuronide metabolites, and there was negligible insource fragmentation from morphine glucuronide to morphine.

Quantitative Bile Acid Sample Preparation and Analysis

All 30 bile acid standards were obtained from Steraloids Inc. (Newport, RI), and stable isotope-labeled standards were obtained from C/D/N Isotopes Inc. (Quebec, Canada). The sample preparation followed a published method with modifications.[2] Briefly, 50 µL of serum or standard solution was spiked with 150 µL of internal standards (50 nM d_4-cholic acid, d_4-ursodeoxycholic acid, and d_4-lithocholic acids) The

extraction of bile acids was conducted over 15 min at 1,500 rpm. After centrifugation, the supernatant was transferred to a centrifuge tube for evaporation to dryness. The residue was reconstituted in 20 µL of acetonitrile and 20 µL of water, and filtered through a 0.45 µm membrane before injection. The injection volume was 5 µL. A UPLC-MS/MS system (ACQUITY UPLC-Xevo TQ-S, Waters Corp., Milford, MA) with VanGuard pre-column (2.1×5 mm) and ACQUITY BEH C18 1.7 µM (2.1×100 mm) heated to 45°C was used to quantitate 30 bile acids in the human serum. The aqueous phase, A, was 0.1% formic acid in LC-MS grade water. The mobile phase, B, was 0.1% formic acid in LC-MS grade acetonitrile. The flow rate was 0.45 mL/min with the following mobile phase gradient: 0-1 min (5% B), 1-5 min (5-25% B), 5-15.5 min (25-40% B), 15.5-17.5 min (40-95% B), 17.5-19 min (95% B), 19-19.5 min (95-5% B), 19.6-21 min (5% B). The mass spectrometer was operated in negative ion mode with a 1.2 kV capillary voltage. The source and desolvation gas temperature was 150 and 550 °C, respectively. The cone and collision energy for each bile acid used the optimized settings from QuanOptimize application manager (Waters Corp., Milford, MA). The data were collected with multiple reaction monitoring (MRM). Calibration solutions containing all 30 analytes were prepared at a series of concentrations of 1, 2, 5, 10, 50, 100, 500, 1000, and 5000 nM in pooled naïve plasma depleted of bile acids using activated charcoal. Bile acid concentrations in unknown samples were back-calculated from the generated calibrations curves of standards using the TargetLynx application manager (Waters Corp., Milford, MA).

Supplementary Data: Adverse Effects

Four subjects experienced nausea and vomiting following morphine administration. These subjects received one or two doses of ondansetron. Ondansetron was chosen as the antiemetic because it does not affect the disposition of morphine or morphine glucuronide metabolites in humans.[3] One healthy subject experienced prolonged nausea and intractable vomiting with ondansetron. This subject was not included in the analysis due to non-protocol administration of metoclopramide and possibility of viral infection the day of the pharmacokinetic study. No other adverse effects associated with morphine administration were noted.

Supplementary Figure 1: Study Subject Disposition

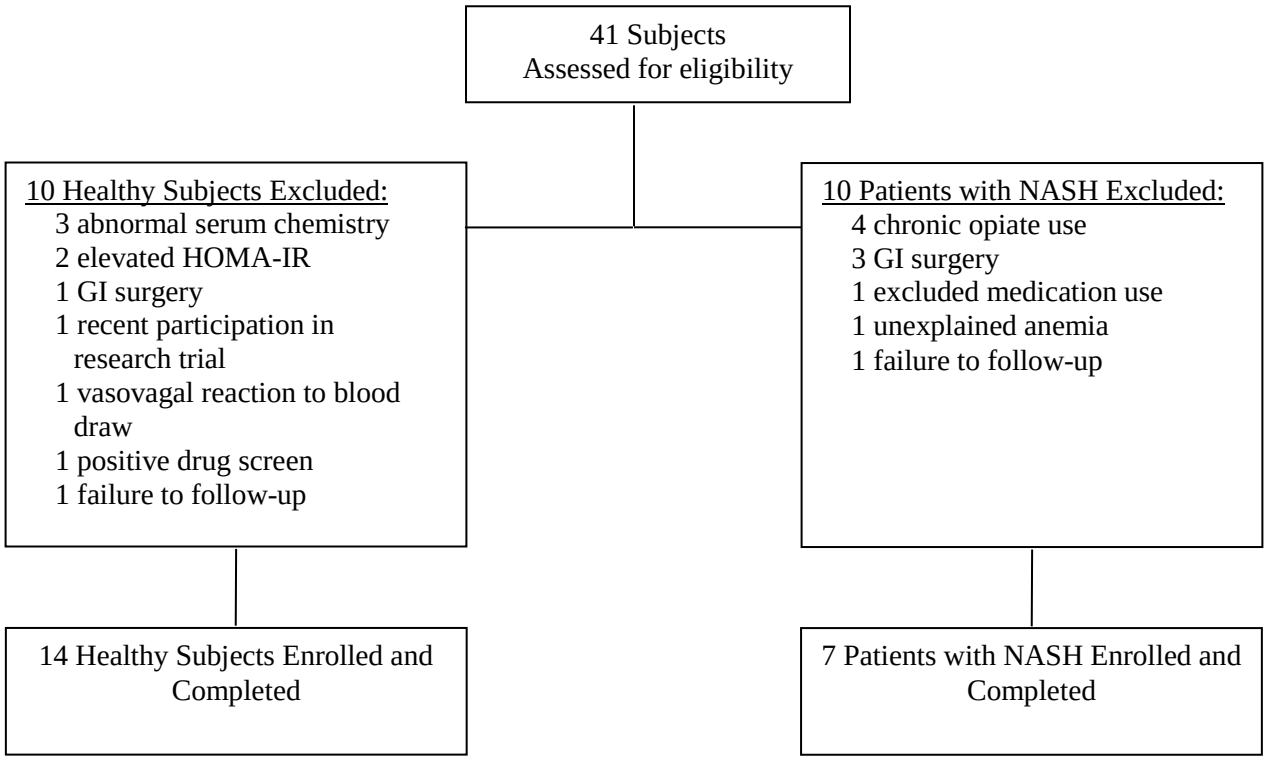

REFERENCES

1. Clavijo, C. F., Hoffman, K. L., Thomas, J. J., Carvalho, B., Chu, L. F., Drover, D. R., Hammer, G. B., Christians, U.Galinkin, J. L. 2011. A sensitive assay for the quantification of morphine and its active metabolites in human plasma and dried blood spots using high-performance liquid chromatography-tandem mass spectrometry. Anal Bioanal Chem 400(3);715-28.

2. Garcia-Canaveras, J. C., Donato, M. T., Castell, J. V.Lahoz, A. 2012. Targeted profiling of circulating and hepatic bile acids in human, mouse, and rat using a UPLC-MRM-MS-validated method. Journal of lipid research 53(10);2231-41.

3. Crews, K. R., Murthy, B. P., Hussey, E. K., Passannante, A. N., Palmer, J. L., Maixner, W.Brouwer, K. L. 2001. Lack of effect of ondansetron on the pharmacokinetics and analgesic effects of morphine and metabolites after single-dose morphine administration in healthy volunteers. British journal of clinical pharmacology 51(4);309-16.

Chapter 5. Summary and Future Directions

This dissertation research has focused on developing preclinical and clinical tools to assess the impact of liver pathology on transporter-mediated systemic and hepatic exposure to medications. Despite a general understanding of the impact of alterations in transporter-mediated hepatic uptake of medications on systemic and hepatic exposure[1-3], the importance of basolateral efflux transporters is underappreciated. For example, altered expression of hepatic transporters (e.g., OATPs, BSEP, MRP2, MRP3, or MRP4) may change both hepatic and systemic concentrations of a drug/metabolite substrate if the affected transport represents a primary clearance route into or from the liver. Furthermore, the functional impact of altered hepatic transporter expression has not been investigated in many hepatic diseases such as NASH. To address this knowledge gap, a translational approach was designed and conducted ranging from identification of altered hepatic transport in response to drug-induced liver pathology (i.e., PLD), to identification of hepatic transport proteins involved in the disposition of hepatically-derived active metabolites *in vitro* (i.e., enalaprilat), to developing *in vivo* methods to assess the impact of altered expression of basolateral efflux transporters secondary to liver disease (i.e., NASH). This research focused primarily on four compounds and their metabolites: taurocholate, rosuvastatin, enalapril, and morphine.

Taurocholate and rosuvastatin are model probe substrates for both hepatic uptake and canalicular efflux transporters. Taurocholate is a metabolically stable bile acid that is transported efficiently into the hepatocyte via NTCP/Ntcp, and excreted into bile via BSEP/Bsep; rosuvastatin is taken up by OATPs/Oatps and reportedly Ntcp, and excreted into bile by MRP2/Mrp2 and BCRP/Bcrp[4-9]. Examination of these probe substrates in tandem allows simultaneous functional evaluation of the major basolateral uptake and canalicular efflux proteins. Enalapril is a prodrug transformed in the liver by

carboxylesterases to the active moiety, enalaprilat. Transformation removes the ethylester from enalapril, adding a negative charge, increasing the potency to inhibit angiotensin converting enzyme, and thereby lowering blood pressure and preventing cardiac remodeling and renal dysfunction[10]. The presence of a diffusional barrier for enalapril and enalaprilat disposition helped lay the foundation for the identification of transporter-mediated hepatic disposition and clearance mechanisms of charged molecules[11-14]. Rat Oatp1a1 and human OATP1B1 are responsible for the hepatic uptake of enalapril following oral absorption. Once inside the hepatocyte, enalapril and hepatically-derived enalaprilat can be excreted into the bile via Mrp2[15] or fluxed across the basolateral membrane. Enalapril currently is being evaluated for its anti-fibrotic effect in patients with NASH[16]. Thus, knowledge of the efflux transporters involved in enalaprilat hepatobiliary disposition may help to inform study design in patients with NASH, where transporter-mediated efflux may be altered. The pharmacokinetics of hepatically-derived morphine glucuronides, MRP3 substrates[17,18], were evaluated in patients with NASH compared to healthy controls to investigate the impact of the reported NASH-associated change in MRP3 expression. Morphine has been reported to enter the hepatocyte via a combination of passive diffusion and active transport[19] where it is metabolized almost exclusively to morphine-3- and -6-glucuronide by UGT2B7[20,21]. The glucuronide metabolites are transported predominantly across the hepatic basolateral membrane into the systemic circulation by MRP3[17,18]. Given that Mrp3 protein expression positively correlated with the efflux of acetaminophen glucuronide[22], and assuming that MRP3 represents the predominant excretion pathway of morphine glucuronides from the hepatocyte, systemic concentrations may be expected to increase in patients with NASH due to up-regulation of MRP3.

Although this translational research project has answered many questions, additional studies are required to fully understand the impact of altered hepatic transport across a greater spectrum of liver pathologies. An overview of the experimental findings and future directions for this work are discussed in the following section.

Identification of Hepatic Phospholipidosis Inducers in Sandwich-Cultured Rat Hepatocytes, a Physiologically Relevant Model, Reveals Altered Basolateral Uptake and Biliary Excretion of Anionic Probe Substrates (Chapter 2)

Phospholipidosis (PLD) is a lysosomal storage disorder where phospholipids accumulate, resulting in concentric lamellar bodies within the lysosome. Drug-induced PLD can occur in any tissue typically following administration of drugs with weakly basic and lipophilic structural moieties. Although PLD has not been linked directly to toxicity[23], certain adverse or undesired effects (i.e. hepatic fibrosis, hERG channel inhibition and renal tubular toxicity) positively associate with known PLD inducers[24-28]. These effects could be direct effects of the drugs within the affected organ or secondary to altered lysosomal function and cellular signaling cascades[27]. The FDA sponsored a working group to further investigate the impact of PLD on organ function and draft a guidance for evaluating these issues in drug development. As part of this ongoing work, model systems that are sensitive and selective for PLD, and capable of determining organ-specific involvement, are needed. Therefore, the current work describes the development of a protocol in rat SCH to screen compounds for hepatic PLD liability. The SCH model also enables the evaluation of transporter-mediated vectorial transport of probe substrates. The disposition of the probe substrates, taurocholate and rosuvastatin, was investigated in SCH cultured under normal conditions compared to hepatocytes pre-incubated with PLD-inducing drugs. Importantly, the current work indicates that PLD results in altered OATP-mediated uptake and BSEP-mediated biliary excretion processes.

Five prototypical PLD-inducing drugs were chosen for initial investigation: amiodarone, chloroquine, desipramine, azithromycin and gentamicin. These drugs were selected because they exhibit varying potencies to induce hepatic PLD as well as distinct postulated induction mechanisms[29,30]. Gentamicin was included because it is only known to induce renal PLD at physiologically-relevant concentrations, thus acting as a negative control for hepatic PLD. Although the number of drugs evaluated was relatively small, the sensitivity and specificity of the rat SCH model to detect drug-induced PLD was evaluated. Lysosomal size was evaluated with LysoTracker Red and PLD was confirmed using

the gold-standard, transmission electron microscopy. The presence of enlarged lysosomes visualized with LysoTracker Red positively correlated with induction of PLD, similar to previous reports[31,32]. This finding suggested that LysoTracker Red localization may be used as an initial screening tool to quickly assess the PLD liability of a compound. Although electron microscopy confirmation should be performed once a lead compound is identified, initially screening compounds with LysoTracker Red in SCH would increase throughput[31,32].

The current work suggests that following PLD induction, the function of both basolateral and canalicular transport proteins is disturbed in rat hepatocytes. Specifically, following PLD induction in rat SCH, altered vectorial transport of rosuvastatin and taurocholate suggested decreased function of Oatps and Bsep. These findings should be confirmed initially in human SCH. If translation to human SCH reveals similar results, evaluation of the disposition of OATP and/or BSEP probes in patients with biopsy-confirmed PLD should be compared to age-, sex-, and comorbid disease-matched patients without PLD. Initially, the mechanism for altered transporter function could be investigated using immunohistochemistry. The localization of transport proteins should be compared in hepatocytes treated with both negative control and PLD-inducing drugs. The observed decrease in Oatp and Bsep function may be due to altered protein trafficking or decreased protein and/or mRNA expression. In addition to these *in vitro* studies, confirmation of these changes *in vivo* would be informative. Care should be taken prior to *in vivo* assessment of transporter probe substrate disposition to adequately characterize the hepatic induction of PLD and transporter localization in the liver. Additionally, PLD itself can alter the lysosomal sequestration and systemic pharmacokinetics of drugs[30,33], so careful consideration of the transporter probes should be undertaken to eliminate confounding variables due to lysosomal sequestration or vesicular elimination pathways[34,35].

This work demonstrates the utility of SCH as a viable screening tool for drug-induced PLD. The studies performed include only two incubation time periods with PLD-inducing drugs: 10 minutes and 48 hours. Although these time points were ideal for evaluation of the impact of PLD on vectorial transport of taurocholate and rosuvastatin, a comprehensive evaluation of onset and offset would provide useful

information. The time course for PLD induction could be established by utilizing serial LysoTracker Red imaging or measurement of a validated biomarker for PLD in the medium[36,37]. For example, PLD-inducing drugs could be added into the feeding medium of SCH for 48 hours and then removed from the feeding medium for another 48 hours. Serial imaging of the cells or medium biomarker measurements every 24 hours in combination with a non-destructive measure of cell viability (e.g. LDH assay) may help provide a link between hepatic PLD and toxicity in addition to characterizing the drug-specific time course for lysosomal dysfunction onset and washout. Intuitively, combination of these time course experiments with standard probe disposition studies (taurocholate and rosuvastatin) *in vitro* would aid in drug development by suggesting whether a change in hepatic transporter-mediated disposition is likely for a compound in development based on the proposed administration schedule in the clinic.

Role of Multidrug Resistance-Associated Protein 4 (MRP4) in the Basolateral Efflux of Hepatically-Derived Enalaprilat (Chapter 3)

The transport proteins responsible for the hepatic uptake and biliary excretion of enalapril and enalaprilat have been well described[11-14], but the processes involved in basolateral efflux of enalaprilat have not been well-characterized. Importantly, enalapril is hydrolyzed to the active form, enalaprilat, by hepatic carboxylesterases and must be fluxed across the basolateral membrane to exert its systemic pharmacologic effect[38]. Additionally, enalapril is being investigated as an anti-fibrotic agent in patients with NASH[16]. Enalaprilat is thought to exert its anti-fibrotic properties through direct inhibition of procollagen proteases, resulting in decreased collagen deposition and fibrosis formation[39]. Therefore, understanding the mechanisms responsible for the hepatic disposition of enalaprilat following transformation may have important therapeutic implications in liver disease where alterations in efflux function may impact both systemic (blood pressure lowering effect) as well as hepatic (inhibition of intracellular proteases involved in fibrosis formation) efficacy. Transport of enalapril and enalaprilat by MRP3 and MRP4 was assessed in membrane vesicles prepared from HEK293 cells transfected to express MRP3 or MRP4. Enalaprilat was transported by MRP4; a modest trend towards inhibition of transport

was observed with rosuvastatin co-incubation whereas co-incubation with the potent pan-MRP inhibitor, MK-571, resulted in significant inhibition. A novel protocol was developed to assess the basolateral efflux of enalaprilat from human SCH. Since enalaprilat was not excreted into the bile compartment, enalaprilat intrinsic basolateral clearance ($CL_{int, basolateral}$) was calculated as the product of the amount excreted across the basolateral membrane into the medium and the reciprocal of the hepatocyte cellular exposure over the incubation time. Since the amount effluxed is corrected by the cellular exposure, inhibition of uptake by concomitantly administered MRP inhibitors does not affect the calculation of clearance. Inhibition of enalaprilat $CL_{int, basolateral}$ in human SCH co-incubated with rosuvastatin or MK-571 was similar to inhibition of enalaprilat MRP4-mediated transport observed in MRP4-expressing membrane vesicles co-incubated with rosuvastatin or MK-571; rosuvastatin resulted in a modest non-significant inhibitory trend, whereas MK-571 resulted in statistically significant potent inhibition. Further studies are required to determine whether changes in MRP4 hepatic expression or function, due to disease or drug-drug interactions, may alter both the hepatic and systemic exposure and pharmacodynamic effect of enalaprilat.

Several strategies using the SCH model have been proposed to assess the basolateral efflux clearance of drugs and/or their derived metabolites[4,40-42]. Unfortunately, when competing mechanisms for clearance exist (e.g. basolateral vs canalicular transport) simple calculation of clearance as mass excreted divided by cellular exposure is not accurate due to flux of the bile canalicular contents into the medium. Although mathematical modeling has been used successfully to deconvolute the net contributions of basolateral vs biliary efflux[40,42-44], this approach requires a significant amount of data to optimize the model. One distinct advantage with enalaprilat is the absence of biliary excretion in the model system, which allows for use of this abbreviated protocol to determine $CL_{int, basolateral}$. Further studies should be performed to test this abbreviated protocol for compounds that satisfy the following three criteria: 1) biliary excretion of the compound in SCH is negligible; 2) the compound, once effluxed from the hepatocyte, does not reenter the hepatocyte (i.e. the metabolite must be hepatically-derived); and 3) any further conversion from parent to metabolite after the loading phase is insignificant. If these criteria are

not met, then mathematical modeling would be required to deconvolute the impact of basolateral vs biliary efflux and/or prolonged metabolite formation.

Following oral administration in humans, enalapril is eliminated primarily as enalaprilat in the urine[38], suggesting that hepatic basolateral efflux is the predominant elimination route from the liver with subsequent renal excretion. Therefore, small changes in basolateral efflux function (*e.g.*, MRP4) *in vivo* could have a large impact on hepatic, and potentially systemic, concentrations and exposure to this active metabolite[45,46]. The current work demonstrates that MRP4 inhibition can decrease enalaprilat $CL_{int, basolateral}$, but was not designed to provide evidence for the impact of increased protein function on hepatic exposure or systemic concentrations of enalaprilat. Adaptation of previously developed protocols to induce localization of efflux proteins on the hepatic basolateral membrane may address this knowledge gap[47]. Cyclic adenosine monophosphate (cAMP) is involved in signaling the translocation of many hepatic transport proteins including Ntcp, Mrp2, Mrp3, Bsep, and multidrug resistance protein (Mdr1 p-glycoprotein and Mdr2 p-glycoprotein) from endosomal reserves to the basolateral or canalicular membrane[47-49]. Assuming cAMP will result in increased trafficking of MRP4 to the basolateral plasma membrane, similar to other efflux transporters, treatment of human SCH with glucagon or a membrane permeable cAMP analogue, such as dibutyryl-adenosine 3',5'-cyclic monophosphate, may result in increased MRP4 localization and function on the basolateral membrane[47]. Utilizing this technique, functional MRP4 protein on the basolateral membrane could be acutely modulated. Comparison of hepatocytes that exhibit increased functional MRP4 protein on the basolateral membrane with vehicle-treated hepatocytes would allow both the cellular exposure and basolateral efflux to be calculated and compared. With increased MRP4 protein expression on the basolateral membrane, it would be expected that hepatically-derived enalaprilat cellular exposure would decrease while the rate of basolateral efflux would increase if MRP4 was the predominant route of excretion from the hepatocyte. Although *in vitro* studies should be performed first as a proof of concept, a clinical investigation of enalapril pharmacokinetic and pharmacodynamic response may provide valuable information regarding the impact of increased efflux protein expression in patients with inflammatory liver disease. Two separate study

designs could be incorporated: 1) a simple pharmacokinetic/pharmacodynamic study comparing healthy subjects to patients with inflammatory liver disease (*e.g.* NASH), or 2) a large cohort epidemiologic study to compare the change in blood pressure in individuals with and without probable inflammatory liver disease treated with enalapril at hypertension diagnosis. Notably, inclusion of two healthy subject control cohorts, normal weight and obese, may help to address the potential confounding factor of obesity in patients with NASH in these studies[50]. Since MRP4 protein expression is up-regulated in inflammatory liver disease, these study designs would evaluate the impact of increased MRP4 expression on enalaprilat basolateral efflux and subsequent systemic pharmacodynamic effect. Caution should be taken, however, noting that the results from these studies would reveal changes in the systemic disposition of enalaprilat, but not necessarily hepatic concentrations or effect. Assuming the target for the anti-fibrotic effect of enalaprilat is in the hepatocyte, a combination of *in vitro* and *in vivo* studies, including modeling and simulation, would provide solid evidence to support or refute the hypothesis that increased MRP4-mediated basolateral efflux will decrease hepatic exposure and pharmacodynamic effect of enalaprilat.

Altered Morphine-Glucuronides Disposition in Patients with Non-Alcoholic Steatohepatitis (Chapter 4)

Probe substrates to assess the clinical impact of hepatic transporter function in response to genetic variation or drug-drug interactions have been investigated previously for basolateral uptake and canalicular efflux transporters [51-54]. This work focused primarily on the impact of altered function of basolateral efflux transporters on the systemic disposition of a probe substrate. Until recently, the importance of basolateral efflux in the hepatic and systemic disposition of drugs and hepatically-derived metabolites was underappreciated[40,43]. The objective of using morphine glucuronides as a probe for MRP3 function was to assess whether the known increase in MRP3 protein expression in patients with NASH leads to an increase in function. Utilizing mathematical modeling and simulation informed by protein expression data from human liver biopsies[55], a comparative cohort study was designed and conducted to compare the systemic disposition of morphine glucuronides in healthy controls compared to

patients with NASH. Consistent with increased MRP3 function, the presence of NASH led to a statistically significant increase in both maximum serum concentration (C_{max}) and exposure ($AUC_{0\text{-}last}$) of morphine glucuronides in patients with NASH compared to healthy controls. This finding confirmed the important role of MRP3 in the systemic and hepatic disposition of morphine glucuronides, but future studies are needed to determine the implications for safety and efficacy of other drugs used in patients with NASH.

Morphine and its hepatically-derived glucuronide metabolites were selected as a phenotypic probe of MRP3 function in patients with NASH for several reasons: 1) morphine enters the hepatocyte via a combination of passive diffusion and active transport and should be unaffected by changes in uptake transporters known to be altered in NASH[56], 2) hepatic expression of UGT2B7, which metabolizes morphine to morphine-3- and -6-glucuronide, is not altered in NASH[2,3,57,58], and 3) MRP3 appears to be the only protein that transports the hepatically-derived morphine glucuronides into the blood[17,18]. Therefore, since expression of Mrp3 protein appears to positively correlate with efflux clearance of glucuronide conjugates, and decreased function polymorphisms in UGT2B7 appear to have minimal impact on systemic glucuronide concentrations[22,59], systemic concentrations of morphine glucuronides may increase due to the increased MRP3 protein expression in patients with NASH compared to healthy subjects; the pharmacokinetics of parent morphine should be unaffected due to its ability to passively cross membrane barriers.

A physiologically-based pharmacokinetic model was developed to estimate the expected change in systemic morphine glucuronides pharmacokinetics in healthy subjects compared to patients with NASH. Using a previously published model as the starting point, the model was optimized using data extracted from the literature[60-66]. Morphine was assumed to exhibit flow-limited distribution to all tissues. The sum of both morphine glucuronides (morphine-6-glucuronide and morphine-3-glucuronide, hereafter referred to as morphine glucuronide) was assumed to be limited by a diffusional barrier in the liver compartment described by biliary and basolateral clearance parameters (CL_{MRP2} and CL_{MRP3}, respectively). For simulation purposes, CL_{MRP3} was assumed to be increased by 3-fold in NASH patients

based on published protein expression data[55]. These simulations indicated a 36% increase in morphine glucuronide C_{max} in patients with NASH compared to healthy controls; no difference in morphine glucuronide $AUC_{0-\infty}$ was expected; a corresponding 56% decrease in hepatic exposure was predicted. Therefore, morphine glucuronide C_{max} was chosen as the primary endpoint for the study and the sample size was estimated. This methodology of developing an *a priori* model to inform study design, expected outcomes, primary endpoint selection, and sample size estimation highlights the utility of mathematical modeling and simulation to provide rational study design in drug development. Additionally, *a priori* modeling and simulation revealed that in tandem with increased morphine glucuronide systemic concentrations, a concurrent decrease in hepatic concentrations and exposure would be expected. This approach would be particularly useful in early phase trials (Phase I and II) where *in vitro* data and disease state models could be leveraged to help avoid futile trial designs.

The experimental paradigm followed in this dissertation research could be applied to additional substrates with unique transporter-mediated clearance pathways and pharmacodynamic properties to better characterize the impact of altered transporter expression in NASH. Substrates should be selected to evaluate basolateral and canalicular transporters other than MRP3 that allow either direct or indirect measurement of hepatic concentration or exposure. Contrary to the current study with morphine, radio-ligand labeled probes or magnetic resonance imaging probes would allow direct measurement of systemic and hepatic exposure in healthy subjects and patients with NASH[51,67-70]. Where imaging agents are not available to assess transporter function, an indirect pharmacodynamic measure could be evaluated as a surrogate for hepatic concentrations. Utilizing a surrogate pharmacodynamic marker for intrahepatic cellular concentrations would require three assumptions: 1) the pharmacodynamic effect of the chosen drug would be directly related to intracellular concentration, 2) a biomarker for the intracellular drug effect must be present in the systemic circulation, and 3) the disease process being investigated does not directly affect the pharmacodynamic effect of the chosen drug. If these three assumptions are reasonable for the chosen drug, comparison of the systemic pharmacokinetics of both the drug and the circulating biomarker of intracellular concentration will provide a relative understanding of systemic and hepatic

disposition of the drug in diseased compared to healthy individuals. Additionally, if the relationship between intracellular concentration and pharmacodynamic inhibition/activation profile of the target is well described, a mathematical modeling and simulation approach would provide additional information regarding expected hepatic intracellular concentrations. These studies could provide further insight into the impact of NASH on hepatic transporter-mediated drug disposition and increase our understanding of how altered hepatic pharmacokinetics influences the pharmacodynamics of medications used in this population. Another potential approach would be measurement of naturally occurring endogenous compounds that may be modulated by changes in hepatic and/or intestinal transport processes associated with NASH. This metabolomics approach could provide additional insight into the interplay between altered hepatic homeostasis of endogenous molecules and vectorial transport of exogenous drugs. Taken together, these datasets may increase our understanding of how the hepatic manifestations of NASH impact both transporter-mediated drug disposition and important inflammatory or disease-related signaling cascades.

The objective of this dissertation project was to develop preclinical and clinical tools to assess the impact of liver pathology on transport protein-mediated vectorial transport. Decreased uptake or increased basolateral efflux may alter the systemic and hepatic exposure to drugs/metabolites and, in turn, change the pharmacodynamic profile of medications. This research has made multiple contributions to the field of hepatic transport, which will enhance our ability to investigate future compounds in greater detail with improved efficiency. These novel approaches can be employed to help predict altered drug disposition due to patient-specific factors such as disease, and enhance the design of safe and efficacious medications.

APPENDIX. Data Appendix

Figure 2.1

	Replicate					Mean Toxicity	SEM
Treatment	1	2	3	4	5		
AMD 10 µM	38.7	10.0	0.0	-4.0	-0.4	8.9	7.8
AMD 50 µM	56.7	61.2	27.0	27.8	-	43.2	9.2
CHQ 1 µM	26.4	65.0	0.0	4.8	-13.7	16.5	13.7
CHQ 10 µM	0.0	21.7	89.5	28.9	3.8	28.8	16.1
DES 1 µM	-4.8	-2.5	13.8	-	-	2.2	5.9
DES 10 µM	9.6	10.3	19.3	-	-	13.1	3.1
DES 50 µM	-	-	72.3	33.6	58.7	54.9	11.3
AZI 1 µM	-	-	28.7	13.9	16.0	19.5	4.6
AZI 10 µM	-	-	48.0	23.3	29.0	33.5	7.5
AZI 50 µM	-	-	62.4	36.3	29.8	42.8	10.0
GTM 1 mM	52.2	46.7	1.0	5.2	-	26.3	13.5

Figure 2.4

	[^{3}H] Taurocholate Accumulation									
	Cells + Bile					Cells				
	Replicate			Mean	SEM	Replicate			Mean	SEM
	1	2	3			1	2	3		
Control	31.4	28.0	27.1	28.8	1.3	4.8	5.9	3.5	4.7	0.7
AMD 50 µM	31.9	24.7	26.2	27.6	2.2	5.3	5.7	3.8	4.9	0.6
CHQ 10 µM	37.0	32.3	26.2	31.8	3.1	4.3	5.2	3.4	4.3	0.5
DES 50 µM	31.5	28.4	23.8	27.9	2.3	4.1	5.3	3.6	4.3	0.5
AZI 50 µM	29.8	23.5	22.1	25.2	2.4	4.0	4.5	3.8	4.1	0.2
GTM 1 mM	43.2	34.9	26.5	34.9	4.8	4.5	6.7	3.5	4.9	0.9
	[^{3}H] Rosuvastatin Accumulation									
	Cells + Bile					Cells				
	Replicate			Mean	SEM	Replicate			Mean	SEM
	1	2	3			1	2	3		
Control	197.8	205.6	138.2	180.5	21.3	92.4	120.2	60.9	91.2	17.1
AMD 50 µM	173.8	173.8	135.1	160.9	12.9	84.1	103.4	57.6	81.7	13.3
CHQ 10 µM	194.6	196.5	153.3	181.5	14.1	88.3	113.4	51.7	84.5	17.9
DES 50 µM	135.3	144.6	108.0	129.3	11.0	60.5	77.4	42.6	60.2	10.1
AZI 50 µM	148.6	153.5	112.2	138.1	13.0	69.8	84.5	45.2	66.5	11.5
GTM 1 mM	218.9	235.7	152.2	202.3	25.5	116.3	141.4	66.3	108.0	22.1

Figure 2.5

	[^{3}H] Taurocholate Accumulation																		
	Cells + Bile									Cells									
	Replicate							Mean	SEM	Replicate							Mean	SEM
	1	2	3	4	5	6	7			1	2	3	4	5	6	7		
Control	47.3	34.2	27.9	43.3	24.2	67.6	74.1	45.5	7.3	7.8	5.0	2.5	3.8	2.3	7.0	9.6	5.4	1.1
AMD 10 µM	-	-	-	19.9	12.9	33.4	55.4	30.4	9.4	-	-	-	2.4	1.4	4.5	8.1	4.1	1.5
AMD 50 µM	-	-	-	-	2.5	8.2	12.0	7.6	2.8	-	-	-	-	1.3	3.4	5.6	3.4	1.2
CHQ 1 µM	-	-	-	-	15.2	57.3	43.6	38.7	12.4	-	-	-	-	1.6	7.3	7.5	5.5	1.9
CHQ 10 µM	-	-	-	-	7.4	21.7	16.1	15.1	4.2	-	-	-	-	2.3	4.0	5.0	3.8	0.8
DES 1 µM	59.9	30.3	24.1	-	-	-	-	38.1	11.0	7.5	5.3	4.0	-	-	-	-	5.6	1.0
DES 10 µM	31.0	23.3	19.9	-	-	-	-	24.7	3.3	4.2	3.6	1.9	-	-	-	-	3.3	0.7
DES 50 µM	11.7	9.3	7.8	-	-	-	-	9.6	1.1	4.3	3.1	3.4	-	-	-	-	3.6	0.3
AZI 1 µM	42.8	10.0	21.5	-	-	-	-	24.8	9.6	5.1	4.6	3.6	-	-	-	-	4.4	0.4
AZI 10 µM	20.3	8.8	11.2	-	-	-	-	13.4	3.5	3.8	3.1	3.1	-	-	-	-	3.3	0.2
AZI 50 µM	10.3	7.0	8.9	-	-	-	-	8.7	1.0	6.9	6.1	3.7	-	-	-	-	5.6	0.9
GTM 1 mM	-	-	-	47.6	-	62.0	65.4	58.3	5.4	-	-	-	4.5	-	7.9	9.5	7.3	1.5

	[^{3}H] Rosuvastatin Accumulation																		
	Cells + Bile									Cells									
	Replicate							Mean	SEM	Replicate							Mean	SEM
	1	2	3	4	5	6	7			1	2	3	4	5	6	7		
Control	243.8	182.4	221.3	88.8	94.6	234.1	142.2	172.5	24.6	94.8	86.1	58.3	33.3	45.7	123.0	75.0	73.7	11.6
AMD 10 µM	-	-	-	-	54.4	113.7	82.4	83.5	17.1	-	-	-	-	16.8	40.4	37.2	31.5	7.4
AMD 50 µM	-	-	-	-	9.8	27.4	14.8	17.3	5.2	-	-	-	-	5.9	8.6	8.6	7.7	0.9
CHQ 1 µM	-	-	-	-	78.1	192.8	108.5	126.5	34.3	-	-	-	-	30.0	102.0	53.5	61.8	21.2
CHQ 10 µM	-	-	-	34.4	45.2	93.4	54.6	56.9	12.8	-	-	-	7.3	14.2	35.9	31.9	22.3	6.9
DES 1 µM	212.8	142.3	181.5	-	-	-	-	178.9	20.4	107.5	92.7	84.0	-	-	-	-	94.7	6.9
DES 10 µM	190.1	130.7	142.8	-	-	-	-	154.5	18.1	72.6	66.5	62.9	-	-	-	-	67.3	2.8
DES 50 µM	40.3	33.0	21.8	-	-	-	-	31.7	5.4	24.3	19.1	12.6	-	-	-	-	18.7	3.4
AZI 1 µM	181.6	146.1	136.6	-	-	-	-	154.8	13.7	64.4	66.2	56.1	-	-	-	-	62.3	3.1
AZI 10 µM	86.4	64.6	72.8	-	-	-	-	74.6	6.4	25.5	27.1	24.6	-	-	-	-	25.7	0.8
AZI 50 µM	55.1	44.3	48.1	-	-	-	-	49.2	3.2	33.1	22.7	17.8	-	-	-	-	24.5	4.5
GTM 1 mM	-	-	-	111.3	-	221.6	151.4	161.4	32.2	-	-	-	44.2	-	129.2	77.5	83.6	24.7

Figure 3.2

	ATP-Dependent Uptake (pmol/mg protein)			
	Enalapril			
	MRP3		MRP4	
Replicate	MOCK	MRP3	MOCK	MRP4
1	11.6	19.4	15.2	15.2
2	75.2	114.1	252.1	89.5
3	23.1	58.7	140.8	251.5
4	-	-	75.1	0.0
Mean	36.6	64.1	120.8	89.0
SEM	19.6	27.5	50.7	57.6

	ATP-Dependent Uptake (pmol/mg protein)			
	Enalaprilat			
	MRP3		MRP4	
Replicate	MOCK	MRP3	MOCK	MRP4
1	21.9	11.5	3.9	17.0
2	13.7	173.0	223.5	703.8
3	169.0	5.3	72.0	388.3
4	-	-	214.7	511.3
Mean	68.2	63.3	128.5	405.1
SEM	50.5	54.9	54.1	144.7

Figure 3.3

ATP-Dependent Uptake (% Control)					
	Replicate			Mean	SEM
	1	2	3		
Control	100	100	100	100	
+50 μM MK-571	52.3	0	0	17.4	17.4

Figure 3.4

	Accumulation (pmol/mg protein)									
	Cells + Bile					Cells				
	Replicate			Mean	SEM	Replicate			Mean	SEM
	1	2	3			1	2	3		
[^{3}H] Taurocholate	98.0	103.8	149.0	116.9	16.1	19.0	28.7	14.0	20.6	4.3
[^{3}H] Rosuvastatin	49.0	74.0	87.0	70.0	11.2	32.0	39.0	57.0	42.7	7.4
Enalapril	1.3	1.7	-	1.5	0.2 (SD)	1.0	1.3	-	1.1	0.1 (SD)
Enalaprilat	5.0	9.6	-	7.3	2.3 (SD)	5.8	9.3	-	7.5	1.8 (SD)

Figure 3.5

	$CL_{int,basolateral}$ (% Control)				
	Replicate			Mean	SEM
	1	2	3		
Control	100	100	100	100	
+50 µM MK-571	16.9	30.6	51.1	32.9	9.9

Figure 4.1

	M Healthy			M NASH		
Time	Mean (nM)	Upper 95% CI	Lower 95% CI	Mean (nM)	Upper 95% CI	Lower 95% CI
0	295.6	396.4	239.6	331.9	524.2	217.0
5	89.8	112.1	76.9	73.7	112.8	47.0
10	53.0	68.7	44.8	42.4	54.8	33.1
15	38.1	52.1	31.9	33.8	40.2	28.4
30	27.6	36.7	22.7	23.0	27.4	19.4
45	22.7	29.9	18.7	19.0	29.8	11.8
60	18.6	24.1	15.7	15.7	20.7	11.7
90	16.5	21.3	13.5	15.5	20.2	11.7
120	13.3	16.9	10.9	11.3	14.5	8.7
180	11.4	13.5	9.6			
240						
300						
360						
420						
480						
	M3G Healthy			M6G Healthy		
Time	Mean (nM)	Upper 95% CI	Lower 95% CI	Mean (nM)	Upper 95% CI	Lower 95% CI
0	16.9	33.3	8.1			
5	89.4	118.1	74.0	7.3	35.9	-20.7
10	141.6	193.4	117.4	9.7	12.0	8.1
15	133.6	187.1	108.9	12.5	15.4	10.8
30	140.5	180.1	118.2	18.4	22.7	15.8
45	138.5	191.3	114.5	19.3	24.3	16.6
60	129.4	180.7	99.9	18.5	21.7	16.4
90	107.2	146.1	88.7	16.7	22.4	13.6
120	85.6	118.1	70.5	11.6	14.6	9.9
180	70.2	104.3	56.2	11.3	13.7	9.7
240	57.7	80.8	44.6			
300	42.2	60.1	35.9			
360	35.8	46.2	30.7			
420	34.4	44.3	29.4			
480	34.1	48.0	27.5			
	M3G NASH			M6G NASH		
Time	Mean (nM)	Upper 95% CI	Lower 95% CI	Mean (nM)	Upper 95% CI	Lower 95% CI
0	21.3	65.3	-0.3			
5	142.3	333.1	47.9	14.1	27.6	2.0
10	161.6	271.0	96.3	15.7	23.5	9.7
15	243.5	293.2	202.0	17.5	25.9	12.5
30	177.6	225.8	140.0	19.3	28.9	13.1
45	179.5	257.5	121.6	19.9	31.8	12.2
60	152.3	172.8	134.4	17.7	23.5	13.3
90	200.7	324.5	124.6	23.0	33.3	16.4
120	155.0	267.8	88.6	19.1	30.4	11.9
180	135.4	206.1	86.8	16.7	21.5	12.8
240	100.1	174.7	57.8	10.5	18.3	4.8
300	75.3	132.7	42.0			
360	59.2	92.8	37.7			
420	51.1	72.5	35.5			
480	31.1	64.8	16.3			

Figure 4.1

	M Healthy (nM)													
Time/Subject	1	2	3	4	5	6	7	8	9	10	11	12	13	14
0	242.6	357.3	219.7	364.5	389.0	210.6	385.6	209.5	236.7	177.3	654.0	213.9	283.2	508.8
5	79.7	57.7	138.8	91.1	110.0	94.1	46.7	70.5	69.8	94.3	129.8	145.2	119.5	75.7
10	36.1	40.9	60.3	47.3	77.1	69.3	43.3	23.0	37.4	75.7	93.3	81.0	65.5	44.4
15	31.8	20.4	56.8	19.2	71.8	47.3	34.5	15.3	31.5	57.5	59.9	59.9	43.8	38.2
30	24.5	20.1	27.6	22.1	59.9	36.1	27.9	11.6	21.6	28.1	48.6	26.6	26.8	34.2
45	22.3	11.6	25.3	27.1	45.9	38.7	21.5	13.6	16.6	22.0	34.9	20.9	16.4	23.3
60	14.0	8.4	17.5	14.7	28.2	27.1	17.9	9.9	17.7	25.5	29.9	15.8	22.2	29.6
90	20.5		13.4	13.4	26.1	21.1	14.1		12.1	17.6	30.8	14.0	10.1	15.4
120	9.8				19.7	17.7	8.8		13.5	10.7	20.4	10.5	12.9	14.5
180					11.5	11.2			9.6	9.7	15.8	10.7	12.5	
240						10.4			10.3		11.5			
300									11.4		10.6			
360											8.3			
420														
480														

	M3G Healthy (nM)													
Time/Subject	1	2	3	4	5	6	7	8	9	10	11	12	13	14
0		48.3		8.8	16.1		16.9			9.4	16.1		9.5	40.4
5	58.0	104.0	56.6	149.1	124.2	70.7	55.9	86.0	52.6	90.1	84.1	145.5	97.9	170.0
10	54.4	207.1	170.8	207.8	286.0	114.7	116.5	109.9	71.0	208.2	115.5	224.4	172.1	117.2
15	101.1	150.7	223.2	71.5	221.0	138.1	197.4	102.7	57.8	288.2	73.5	188.8	118.5	139.9
30	132.7	221.4	130.5	164.9	260.0	104.5	119.1	160.2	77.1	208.5	106.4	179.0	82.3	141.8
45	92.0	162.0	244.9	203.0	200.2	202.8	95.0	250.3	55.1	223.2	80.9	116.3	105.1	109.7
60	106.5	140.2	151.9	110.9	195.5	99.3	87.7	150.3	75.2	357.6	99.2	139.7	137.6	112.2
90	71.3	119.0	178.6	160.4	181.2	57.7	84.6	107.9	59.0	202.6	129.3	138.8	53.3	100.1
120	43.2	108.7	47.5	85.2	182.2	65.6	36.0	85.3	73.9	154.7	107.1	105.9	112.2	112.6
180	50.2	76.7	31.4	138.0	107.5	51.5	28.4	61.6	39.1	164.5	101.5	118.2	94.9	59.4
240	36.7	93.2	58.1	70.0	44.0	46.8	35.5	53.2	156.4	54.6	41.2	77.8	52.0	58.4
300	13.3	61.3	43.6	78.2	55.3	42.5	11.2	49.5	66.9	83.6	47.7	44.7	29.9	44.4
360	19.1	56.7	42.9	42.5	39.0	33.9	13.8	31.4	50.0	56.1	49.9	30.4	24.5	47.8
420	39.6	46.2	47.7	36.4	44.0	25.4	12.5	33.3	28.4	59.6	27.4	23.5	37.5	54.7
480	33.0	72.4	28.2	33.4	24.9		9.7	27.6	33.0	68.5	43.3	32.3	43.3	41.3

	M6G Healthy (nM)													
Time/Subject	1	2	3	4	5	6	7	8	9	10	11	12	13	14
0														
5				5.4										9.8
10	6.4	13.8	6.7	8.6	9.8	8.2	9.7			9.1	12.3	16.9	8.3	10.7
15	14.7	12.8	10.8	7.6	15.4	17.4	18.7	8.7	10.7	16.3	8.1	18.2	9.0	15.0
30	27.8	27.3	18.4	13.2	24.3	25.3	19.7	16.3	13.2	14.3	16.1	26.2	9.4	18.3
45	21.4	14.0	20.8	24.5	26.9	33.5	21.0	29.0	7.2	19.9	17.0	20.6	14.5	15.9
60	21.6	14.0	17.6	13.0	25.1	16.6	20.5	15.3	14.4	28.4	18.6	24.9	17.0	19.4
90	21.2	9.9	16.1	16.0	28.2	17.4	14.4	13.7	9.8	16.1	36.3	20.5	8.5	24.0
120	10.9	9.6	7.5	10.5	20.3	15.5	5.6	8.9	15.8	14.6	13.7	16.9	11.0	10.5
180	12.2	6.7		11.4	16.1	10.3			8.9	11.3	13.4	15.4	11.1	
240	6.9		5.7	8.5		14.4			14.1				6.4	
300				8.8		6.1			16.6					
360														
420														
480														

Figure 4.1

	M NASH (nM)						
Time/Subject	1	2	3	4	5	6	7
0	365.6	609.8	472.4	488.5	264.8	274.4	118.6
5	56.6	77.4	54.0	146.5	85.5	98.5	40.6
10	33.3	46.3	44.2	56.8	53.1	50.5	23.6
15	29.4	40.0	26.1	39.2	27.7	41.4	36.4
30	23.7	26.4	18.7	25.7	22.8	29.3	17.0
45	12.3	24.0	17.5	37.0	11.6	29.5	13.7
60		19.2	13.5	17.7	13.8	22.3	10.7
90		20.5	12.7	14.1	14.9	21.5	11.9
120		9.7	8.6	11.5	11.5	16.8	11.4
180		10.2		15.1			
240				9.7			
300							
360							
420							
480							

	M3G NASH (nM)						
Time/Subject	1	2	3	4	5	6	7
0	7.6	10.7	15.2	35.0	41.2	107.3	10.4
5	84.7	44.6	104.3	224.3	324.3	461.6	89.4
10	101.9	60.7	173.8	208.2	351.1	231.9	158.0
15	272.6	182.5	328.5	280.1	211.6	221.0	237.0
30	176.7	115.9	142.5	205.0	244.3	229.7	165.9
45	153.8	127.9	158.0	326.3	149.3	257.9	153.7
60	119.9	172.1	161.3	179.9	150.2	156.7	135.2
90	76.2	294.7	179.2	158.0	261.9	409.6	192.0
120	68.0	78.0	179.0	136.5	236.7	346.7	202.3
180	75.4	99.2	142.2	183.0	103.6	266.5	154.9
240	52.9	52.0	121.8	158.8	182.0	192.2	54.1
300	46.2	34.2	100.4	85.5	146.9	153.4	44.8
360	33.6	33.2	87.7	86.1	108.5	42.9	64.8
420	34.2	34.2	64.5	57.7	91.2	43.8	52.2
480	19.6	6.3	69.8	51.5	73.9	42.7	19.8

	M6G NASH (nM)						
Time/Subject	1	2	3	4	5	6	7
0	0.0	0.0	0.0	0.0	0.0	0.0	0.0
5	0.0	0.0	9.0	0.0	16.7	18.8	0.0
10	0.0	0.0	13.7	17.7	22.3	20.8	8.6
15	13.2	6.3	23.5	28.3	22.0	21.1	19.6
30	17.7	8.1	14.0	30.4	31.5	21.1	24.4
45	10.5	12.8	15.1	40.3	23.2	30.1	22.0
60	13.9	14.2	14.8	25.7	25.6	13.9	20.6
90	9.7	31.4	18.0	24.2	31.9	36.0	22.4
120		7.2	17.5	18.6	29.7	31.0	23.0
180		10.4	14.2	19.3	20.8	21.1	17.0
240		5.2	9.9	19.3		14.4	8.9
300			5.4	8.8		13.0	
360			7.4				
420			5.9483823				
480							

Figure 4.2

	Subject	Total Bile Acids (µM)	Glycocholate (µM)	Taurocholate (µM)
Healthy	1	0.90	0.04	0.01
	2	1.82	0.08	0.01
	3	1.60	0.03	0.00
	4	0.83	0.03	0.01
	5	1.85	0.18	0.03
	6	1.61	0.08	0.01
	7	1.94	0.23	0.05
	8	3.05	0.12	0.06
	9	1.89	0.05	0.01
	10	1.19	0.04	0.02
	11	0.90	0.03	0.02
	12	1.45	0.11	0.07
	13	1.00	0.01	0.00
	14	1.23	0.05	0.01
	Mean	1.52	0.08	0.02
	SD	0.59	0.06	0.02
NASH	1	3.26	0.08	0.03
	2	1.03	0.05	0.02
	3	10.15	0.63	0.26
	4	6.30	0.45	0.52
	5	1.18	0.05	0.01
	6	2.38	0.21	0.06
	7	1.96	0.24	0.02
	Mean	3.75	0.24	0.13
	SD	3.34	0.22	0.19

Figure 4.3

	Maximum Concentration (C_{max}; nM)			Area Under the Concentration-Time Curve (AUC; µM*min)		
NAS+Fibrosis	Predicted MG C_{max}	Predicted MG C_{max} Upper Limit	Predicted MG C_{max} Lower Limit	Predicted MG AUC	Predicted MG AUC Upper Limit	Predicted MG AUC Lower Limit
0	233.3	269.2	197.4	38.0	45.7	30.3
0	233.3	269.2	197.4	38.0	45.7	30.3
0	233.3	269.2	197.4	38.0	45.7	30.3
0	233.3	269.2	197.4	38.0	45.7	30.3
0	233.3	269.2	197.4	38.0	45.7	30.3
0	233.3	269.2	197.4	38.0	45.7	30.3
0	233.3	269.2	197.4	38.0	45.7	30.3
0	233.3	269.2	197.4	38.0	45.7	30.3
0	233.3	269.2	197.4	38.0	45.7	30.3
0	233.3	269.2	197.4	38.0	45.7	30.3
0	233.3	269.2	197.4	38.0	45.7	30.3
0	233.3	269.2	197.4	38.0	45.7	30.3
0	233.3	269.2	197.4	38.0	45.7	30.3
0	233.3	269.2	197.4	38.0	45.7	30.3
4	307.3	342.7	271.9	54.5	62.1	46.9
5	325.8	367.4	284.2	58.6	67.5	49.6
5	325.8	367.4	284.2	58.6	67.5	49.6
7	362.8	420.1	305.6	66.8	79.1	54.5
7	362.8	420.1	305.6	66.8	79.1	54.5
7	362.8	420.1	305.6	66.8	79.1	54.5
8	381.3	447.2	315.4	70.9	85.1	56.7

REFERENCES

1. Konig, J., Muller, F.Fromm, M. F. 2013. Transporters and drug-drug interactions: important determinants of drug disposition and effects. Pharmacological reviews 65(3);944-66.

2. Zamek-Gliszczynski, M. J., Chu, X., Polli, J. W., Paine, M. F.Galetin, A. 2013. Understanding the Transport Properties of Metabolites: Case Studies and Considerations for Drug Development. Drug metabolism and disposition: the biological fate of chemicals.

3. Kock, K.Brouwer, K. L. 2012. A perspective on efflux transport proteins in the liver. Clinical pharmacology and therapeutics 92(5);599-612.

4. Abe, K., Bridges, A. S.Brouwer, K. L. 2009. Use of sandwich-cultured human hepatocytes to predict biliary clearance of angiotensin II receptor blockers and HMG-CoA reductase inhibitors. Drug metabolism and disposition: the biological fate of chemicals 37(3);447-52.

5. Byrne, J. A., Strautnieks, S. S., Mieli-Vergani, G., Higgins, C. F., Linton, K. J.Thompson, R. J. 2002. The human bile salt export pump: characterization of substrate specificity and identification of inhibitors. Gastroenterology 123(5);1649-58.

6. Huang, L., Wang, Y.Grimm, S. 2006. ATP-dependent transport of rosuvastatin in membrane vesicles expressing breast cancer resistance protein. Drug metabolism and disposition: the biological fate of chemicals 34(5);738-42.

7. Jemnitz, K., Veres, Z., Tugyi, R.Vereczkey, L. 2010. Biliary efflux transporters involved in the clearance of rosuvastatin in sandwich culture of primary rat hepatocytes. Toxicology in vitro : an international journal published in association with BIBRA 24(2);605-10.

8. Kitamura, S., Maeda, K., Wang, Y.Sugiyama, Y. 2008. Involvement of multiple transporters in the hepatobiliary transport of rosuvastatin. Drug metabolism and disposition: the biological fate of chemicals 36(10);2014-23.

9. Trauner, M.Boyer, J. L. 2003. Bile salt transporters: molecular characterization, function, and regulation. Physiological reviews 83(2);633-71.

10. Patchett, A. A., Harris, E., Tristram, E. W., Wyvratt, M. J., Wu, M. T., Taub, D., Peterson, E. R., Ikeler, T. J., ten Broeke, J., Payne, L. G., Ondeyka, D. L., Thorsett, E. D., Greenlee, W. J., Lohr, N. S., Hoffsommer, R. D., Joshua, H., Ruyle, W. V., Rothrock, J. W., Aster, S. D., Maycock, A. L., Robinson, F. M., Hirschmann, R., Sweet, C. S., Ulm, E. H., Gross, D. M., Vassil, T. C.Stone, C. A. 1980. A new class of angiotensin-converting enzyme inhibitors. Nature 288(5788);280-3.

11. de Lannoy, I. A.Pang, K. S. 1986. Presence of a diffusional barrier on metabolite kinetics: enalaprilat as a generated versus preformed metabolite. Drug metabolism and disposition: the biological fate of chemicals 14(5);513-20.

12. Pang, K. S., Cherry, W. F., Terrell, J. A.Ulm, E. H. 1984. Disposition of enalapril and its diacid metabolite, enalaprilat, in a perfused rat liver preparation. Presence of a diffusional barrier for enalaprilat into hepatocytes. Drug metabolism and disposition: the biological fate of chemicals 12(3);309-13.

13. Pang, K. S., Wang, P. J., Chung, A. Y.Wolkoff, A. W. 1998. The modified dipeptide, enalapril, an angiotensin-converting enzyme inhibitor, is transported by the rat liver organic anion transport protein. Hepatology (Baltimore, Md.) 28(5);1341-6.

14. Schwab, A. J., Barker, F., 3rd, Goresky, C. A.Pang, K. S. 1990. Transfer of enalaprilat across rat liver cell membranes is barrier limited. The American journal of physiology 258(3 Pt 1);G461-75.

15. Liu, L., Cui, Y., Chung, A. Y., Shitara, Y., Sugiyama, Y., Keppler, D.Pang, K. S. 2006. Vectorial transport of enalapril by Oatp1a1/Mrp2 and OATP1B1 and OATP1B3/MRP2 in rat and human livers. The Journal of pharmacology and experimental therapeutics 318(1);395-402.

16. Sookoian, S., Gianotti, T. F., Rosselli, M. S., Burgueno, A. L., Castano, G. O.Pirola, C. J. 2011. Liver transcriptional profile of atherosclerosis-related genes in human nonalcoholic fatty liver disease. Atherosclerosis 218(2);378-85.

17. van de Wetering, K., Zelcer, N., Kuil, A., Feddema, W., Hillebrand, M., Vlaming, M. L., Schinkel, A. H., Beijnen, J. H.Borst, P. 2007. Multidrug resistance proteins 2 and 3 provide alternative routes for hepatic excretion of morphine-glucuronides. Molecular pharmacology 72(2);387-94.

18. Zelcer, N., van de Wetering, K., Hillebrand, M., Sarton, E., Kuil, A., Wielinga, P. R., Tephly, T., Dahan, A., Beijnen, J. H.Borst, P. 2005. Mice lacking multidrug resistance protein 3 show altered morphine pharmacokinetics and morphine-6-glucuronide antinociception. Proc Natl Acad Sci U S A 102(20);7274-9.

19. Fukuda, T., Chidambaran, V., Mizuno, T., Venkatasubramanian, R., Ngamprasertwong, P., Olbrecht, V., Esslinger, H. R., Vinks, A. A.Sadhasivam, S. 2013. OCT1 genetic variants influence the pharmacokinetics of morphine in children. Pharmacogenomics 14(10);1141-51.

20. Chen, X. Y., Zhao, L. M.Zhong, D. F. 2003. A novel metabolic pathway of morphine: formation of morphine glucosides in cancer patients. British journal of clinical pharmacology 55(6);570-8.

21. Chau, N., Elliot, D. J., Lewis, B. C., Burns, K., Johnston, M. R., Mackenzie, P. I.Miners, J. O. 2014. Morphine glucuronidation and glucosidation represent complementary metabolic pathways that are both catalyzed by UDP-glucuronosyltransferase 2B7: kinetic, inhibition, and molecular modeling studies. The Journal of pharmacology and experimental therapeutics 349(1);126-37.

22. Xiong, H., Suzuki, H., Sugiyama, Y., Meier, P. J., Pollack, G. M.Brouwer, K. L. 2002. Mechanisms of impaired biliary excretion of acetaminophen glucuronide after acute phenobarbital treatment or phenobarbital pretreatment. Drug metabolism and disposition: the biological fate of chemicals 30(9);962-9.

23. Chatman, L. A., Morton, D., Johnson, T. O.Anway, S. D. 2009. A strategy for risk management of drug-induced phospholipidosis. Toxicologic pathology 37(7);997-1005.

24. Agoston, M., Orsi, F., Feher, E., Hagymasi, K., Orosz, Z., Blazovics, A., Feher, J.Vereckei, A. 2003. Silymarin and vitamin E reduce amiodarone-induced lysosomal phospholipidosis in rats. Toxicology 190(3);231-41.

25. Kaloyanides, G. J.Pastoriza-Munoz, E. 1980. Aminoglycoside nephrotoxicity. Kidney international 18(5);571-82.

26. Oikawa, H., Maesawa, C., Sato, R., Oikawa, K., Yamada, H., Oriso, S., Ono, S., Yashima-Abo, A., Kotani, K., Suzuki, K.Masuda, T. 2005. Liver cirrhosis induced by long-term administration of a daily low dose of amiodarone: a case report. World journal of gastroenterology : WJG 11(34);5394-7.

27. Sun, H., Xia, M., Shahane, S. A., Jadhav, A., Austin, C. P.Huang, R. 2013. Are hERG channel blockers also phospholipidosis inducers? Bioorganic & medicinal chemistry letters 23(16);4587-90.

28. Xia, M., Shahane, S. A., Huang, R., Titus, S. A., Shum, E., Zhao, Y., Southall, N., Zheng, W., Witt, K. L., Tice, R. R.Austin, C. P. 2011. Identification of quaternary ammonium compounds as potent inhibitors of hERG potassium channels. Toxicology and applied pharmacology 252(3);250-8.

29. Goldman, S. D., Funk, R. S., Rajewski, R. A.Krise, J. P. 2009. Mechanisms of amine accumulation in, and egress from, lysosomes. Bioanalysis 1(8);1445-59.

30. Ndolo, R. A., Forrest, M. L.Krise, J. P. 2010. The role of lysosomes in limiting drug toxicity in mice. The Journal of pharmacology and experimental therapeutics 333(1);120-8.

31. Kazmi, F., Hensley, T., Pope, C., Funk, R. S., Loewen, G. J., Buckley, D. B.Parkinson, A. 2013. Lysosomal sequestration (trapping) of lipophilic amine (cationic amphiphilic) drugs in immortalized human hepatocytes (Fa2N-4 cells). Drug metabolism and disposition: the biological fate of chemicals 41(4);897-905.

32. Lemieux, B., Percival, M. D.Falgueyret, J. P. 2004. Quantitation of the lysosomotropic character of cationic amphiphilic drugs using the fluorescent basic amine Red DND-99. Analytical biochemistry 327(2);247-51.

33. Ndolo, R. A., Jacobs, D. T., Forrest, M. L.Krise, J. P. 2010. Intracellular Distribution-based Anticancer Drug Targeting: Exploiting a Lysosomal Acidification Defect Associated with Cancer Cells. Molecular and cellular pharmacology 2(4);131-136.

34. Wustner, D., Mukherjee, S., Maxfield, F. R., Muller, P.Herrmann, A. 2001. Vesicular and nonvesicular transport of phosphatidylcholine in polarized HepG2 cells. Traffic (Copenhagen, Denmark) 2(4);277-96.

35. Kipp, H., Pichetshote, N.Arias, I. M. 2001. Transporters on demand: intrahepatic pools of canalicular ATP binding cassette transporters in rat liver. The Journal of biological chemistry 276(10);7218-24.

36. Baronas, E. T., Lee, J. W., Alden, C.Hsieh, F. Y. 2007. Biomarkers to monitor drug-induced phospholipidosis. Toxicology and applied pharmacology 218(1);72-8.

37. Tengstrand, E. A., Miwa, G. T.Hsieh, F. Y. 2010. Bis(monoacylglycerol)phosphate as a non-invasive biomarker to monitor the onset and time-course of phospholipidosis with drug-induced toxicities. Expert opinion on drug metabolism & toxicology 6(5);555-70.

38. Ulm, E. H. 1983. Enalapril maleate (MK-421), a potent, nonsulfhydryl angiotensin-converting enzyme inhibitor: absorption, disposition, and metabolism in man. Drug metabolism reviews 14(1);99-110.

39. Mannisto, T. K., Karvonen, K. E., Kerola, T. V.Ryhanen, L. J. 2001. Inhibitory effect of the angiotensin converting enzyme inhibitors captopril and enalapril on the conversion of procollagen to collagen. Journal of hypertension 19(10);1835-9.

40. Pfeifer, N. D., Yang, K.Brouwer, K. L. 2013. Hepatic basolateral efflux contributes significantly to rosuvastatin disposition I: characterization of basolateral versus biliary clearance using a novel protocol in sandwich-cultured hepatocytes. The Journal of pharmacology and experimental therapeutics 347(3);727-36.

41. Swift, B., Pfeifer, N. D.Brouwer, K. L. 2010. Sandwich-cultured hepatocytes: an in vitro model to evaluate hepatobiliary transporter-based drug interactions and hepatotoxicity. Drug metabolism reviews 42(3);446-71.

42. Matsunaga, N., Wada, S., Nakanishi, T., Ikenaga, M., Ogawa, M.Tamai, I. 2013. Mathematical Modeling of the in Vitro Hepatic Disposition of Mycophenolic Acid and Its Glucuronide in Sandwich-Cultured Human Hepatocytes. Molecular pharmaceutics.

43. Pfeifer, N. D., Bridges, A. S., Ferslew, B. C., Hardwick, R. N.Brouwer, K. L. 2013. Hepatic basolateral efflux contributes significantly to rosuvastatin disposition II: characterization of hepatic elimination by basolateral, biliary, and metabolic clearance pathways in rat isolated perfused liver. The Journal of pharmacology and experimental therapeutics 347(3);737-45.

44. Lee, J. K., Marion, T. L., Abe, K., Lim, C., Pollock, G. M.Brouwer, K. L. 2010. Hepatobiliary disposition of troglitazone and metabolites in rat and human sandwich-cultured hepatocytes: use of Monte Carlo simulations to assess the impact of changes in biliary excretion on troglitazone sulfate accumulation. The Journal of pharmacology and experimental therapeutics 332(1);26-34.

45. Pfeifer, N. D., Hardwick, R. N.Brouwer, K. L. 2014. Role of hepatic efflux transporters in regulating systemic and hepatocyte exposure to xenobiotics. Annual review of pharmacology and toxicology 54;509-35.

46. Zamek-Gliszczynski, M. J., Kalvass, J. C., Pollack, G. M.Brouwer, K. L. 2009. Relationship between drug/metabolite exposure and impairment of excretory transport function. Drug metabolism and disposition: the biological fate of chemicals 37(2);386-90.

47. Chandra, P., Zhang, P.Brouwer, K. L. 2005. Short-term regulation of multidrug resistance-associated protein 3 in rat and human hepatocytes. American journal of physiology. Gastrointestinal and liver physiology 288(6);G1252-8.

48. Webster, C. R. L.Anwer, M. S. 1999. *Role of the PI3K/PKB signaling pathway in cAMP-mediated translocation of rat liver Ntcp*.

49. Roelofsen, H., Soroka, C. J., Keppler, D.Boyer, J. L. 1998. Cyclic AMP stimulates sorting of the canalicular organic anion transporter (Mrp2/cMoat) to the apical domain in hepatocyte couplets. Journal of cell science 111 (Pt 8);1137-45.

50. Nedogoda, S. V., Ledyaeva, A. A., Chumachok, E. V., Tsoma, V. V., Mazina, G., Salasyuk, A. S.Barykina, I. N. 2013. Randomized trial of perindopril, enalapril, losartan and telmisartan in overweight or obese patients with hypertension. Clinical drug investigation 33(8);553-61.

51. Pfeifer, N. D., Goss, S. L., Swift, B., Ghibellini, G., Ivanovic, M., Heizer, W. D., Gangarosa, L. M.Brouwer, K. L. 2013. Effect of Ritonavir on (99m)Technetium-Mebrofenin Disposition in

Humans: A Semi-PBPK Modeling and In Vitro Approach to Predict Transporter-Mediated DDIs. CPT: pharmacometrics & systems pharmacology 2;e20.

52. Giacomini, K. M., Huang, S. M., Tweedie, D. J., Benet, L. Z., Brouwer, K. L., Chu, X., Dahlin, A., Evers, R., Fischer, V., Hillgren, K. M., Hoffmaster, K. A., Ishikawa, T., Keppler, D., Kim, R. B., Lee, C. A., Niemi, M., Polli, J. W., Sugiyama, Y., Swaan, P. W., Ware, J. A., Wright, S. H., Yee, S. W., Zamek-Gliszczynski, M. J.Zhang, L. 2010. Membrane transporters in drug development. Nature reviews. Drug discovery 9(3);215-36.

53. Takashima, T., Kitamura, S., Wada, Y., Tanaka, M., Shigihara, Y., Ishii, H., Ijuin, R., Shiomi, S., Nakae, T., Watanabe, Y., Cui, Y., Doi, H., Suzuki, M., Maeda, K., Kusuhara, H., Sugiyama, Y.Watanabe, Y. 2012. PET imaging-based evaluation of hepatobiliary transport in humans with (15R)-11C-TIC-Me. Journal of nuclear medicine : official publication, Society of Nuclear Medicine 53(5);741-8.

54. Daali, Y., Millet, P., Dayer, P.Pastor, C. M. 2013. Evidence of drug-drug interactions through uptake and efflux transport systems in rat hepatocytes: implications for cellular concentrations of competing drugs. Drug metabolism and disposition: the biological fate of chemicals 41(8);1548-56.

55. Hardwick, R. N., Fisher, C. D., Canet, M. J., Scheffer, G. L.Cherrington, N. J. 2011. Variations in ATP-binding cassette transporter regulation during the progression of human nonalcoholic fatty liver disease. Drug metabolism and disposition: the biological fate of chemicals 39(12);2395-402.

56. Lake, A. D., Novak, P., Fisher, C. D., Jackson, J. P., Hardwick, R. N., Billheimer, D. D., Klimecki, W. T.Cherrington, N. J. 2011. Analysis of global and absorption, distribution, metabolism, and elimination gene expression in the progressive stages of human nonalcoholic fatty liver disease. Drug metabolism and disposition: the biological fate of chemicals 39(10);1954-60.

57. Hardwick, R. N., Ferreira, D. W., More, V. R., Lake, A. D., Lu, Z., Manautou, J. E., Slitt, A. L.Cherrington, N. J. 2013. Altered UDP-glucuronosyltransferase and sulfotransferase expression and function during progressive stages of human nonalcoholic fatty liver disease. Drug metabolism and disposition: the biological fate of chemicals 41(3);554-61.

58. Bodenham, A., Quinn, K.Park, G. R. 1989. Extrahepatic morphine metabolism in man during the anhepatic phase of orthotopic liver transplantation. British journal of anaesthesia 63(4);380-4.

59. Holthe, M., Klepstad, P., Zahlsen, K., Borchgrevink, P. C., Hagen, L., Dale, O., Kaasa, S., Krokan, H. E.Skorpen, F. 2002. Morphine glucuronide-to-morphine plasma ratios are unaffected by the UGT2B7 H268Y and UGT1A1*28 polymorphisms in cancer patients on chronic morphine therapy. European journal of clinical pharmacology 58(5);353-6.

60. Everts, B., Karlson, B. W., Herlitz, J.Hedner, T. 1998. Morphine use and pharmacokinetics in patients with chest pain due to suspected or definite acute myocardial infarction. Eur J Pain 2(2);115-125.

61. Hanna, M. H., Peat, S. J., Knibb, A. A.Fung, C. 1991. Disposition of morphine-6-glucuronide and morphine in healthy volunteers. British journal of anaesthesia 66(1);103-7.

62. Osborne, R., Joel, S., Trew, D.Slevin, M. 1990. Morphine and metabolite behavior after different routes of morphine administration: demonstration of the importance of the active metabolite morphine-6-glucuronide. Clinical pharmacology and therapeutics 47(1);12-9.

63. Lotsch, J., Skarke, C., Schmidt, H., Liefhold, J.Geisslinger, G. 2002. Pharmacokinetic modeling to predict morphine and morphine-6-glucuronide plasma concentrations in healthy young volunteers. Clinical pharmacology and therapeutics 72(2);151-62.

64. Skarke, C., Schmidt, H., Geisslinger, G., Darimont, J.Lotsch, J. 2003. Pharmacokinetics of morphine are not altered in subjects with Gilbert's syndrome. British journal of clinical pharmacology 56(2);228-31.

65. Murthy, B. R., Pollack, G. M.Brouwer, K. L. 2002. Contribution of morphine-6-glucuronide to antinociception following intravenous administration of morphine to healthy volunteers. Journal of clinical pharmacology 42(5);569-76.

66. Chen, S. 2010. Physiologically-Based Pharmacokinetic (PBPK) Models for the Description of Sequential Metabolism of Codeine to Morphine and Morphine 3-Glucuronide (M3G) in Man and Rat. University of Toronto Thesis.

67. Hume, W. E., Shingaki, T., Takashima, T., Hashizume, Y., Okauchi, T., Katayama, Y., Hayashinaka, E., Wada, Y., Kusuhara, H., Sugiyama, Y.Watanabe, Y. 2013. The synthesis and biodistribution of [(11)C]metformin as a PET probe to study hepatobiliary transport mediated by the multi-drug and toxin extrusion transporter 1 (MATE1) in vivo. Bioorganic & medicinal chemistry 21(24);7584-90.

68. Shingaki, T., Takashima, T., Ijuin, R., Zhang, X., Onoue, T., Katayama, Y., Okauchi, T., Hayashinaka, E., Cui, Y., Wada, Y., Suzuki, M., Maeda, K., Kusuhara, H., Sugiyama, Y.Watanabe, Y. 2013. Evaluation of Oatp and Mrp2 activities in hepatobiliary excretion using newly developed positron emission tomography tracer [11C]dehydropravastatin in rats. The Journal of pharmacology and experimental therapeutics 347(1);193-202.

69. Leonhardt, M., Keiser, M., Oswald, S., Kuhn, J., Jia, J., Grube, M., Kroemer, H. K., Siegmund, W.Weitschies, W. 2010. Hepatic uptake of the magnetic resonance imaging contrast agent Gd-EOB-DTPA: role of human organic anion transporters. Drug metabolism and disposition: the biological fate of chemicals 38(7);1024-8.

70. Ulloa, J. L., Stahl, S., Yates, J., Woodhouse, N., Kenna, J. G., Jones, H. B., Waterton, J. C.Hockings, P. D. 2013. Assessment of gadoxetate DCE-MRI as a biomarker of hepatobiliary transporter inhibition. NMR in biomedicine 26(10);1258-70.